Regulation of thermogenic capacity in white and brown adipose tissues by chronic endurance exercise and high-fat diet

Michelle Victoria Wu

A THESIS SUBMITTED TO THE FACULTY OF GRADUATE STUDIES IN PARTIAL FULFILMENT OF THE REQUIREMENTS FOR THE DEGREE OF

MASTER OF SCIENCE

GRADUATE PROGRAM IN KINESIOLOGY AND HEALTH SCIENCE
YORK UNIVERSITY
TORONTO, ONTARIO
AUGUST 2015
© Michelle Victoria Wu, 2015

ABSTRACT

This study investigated the effects of high-fat (HF) diet and chronic endurance exercise (Ex) on the regulation of thermogenic capacity in both brown adipose tissue (BAT) and subcutaneous (SC) white adipose tissue (WAT), and how it affects whole-body energy expenditure (EE). Analysis of tissue mass, PGC-1α and UCP-1 content, presence of multilocular adipocytes and palmitate oxidation revealed that HF diet increased the thermogenic capacity of BAT, while Ex suppressed it. Conversely, Ex induced the browning of the SC WAT, indicated by an increased number of multilocular adipocytes, as well as PGC-1α and UCP-1 content, and palmitate oxidation, whereas HF diet attenuated this effect. Despite reducing thermogenic capacity of BAT, Ex increased whole-body EE during the dark cycle. We propose that exercise-induced browning of SC WAT reduces thermogenic capacity in core body regions to manage the increased heat production of exercise, and increases it in peripheral regions to adjust metabolic rate.

ACKNOWLEDGEMENTS

Dr. Rolando Ceddia- From my very first position as a volunteer to the final draft of this thesis, your guidance and support along the way will never be forgotten. Your passion for science is unsurpassed and it has motivated me to achieve all that I have. You have shown me that hard work pays off and without you, I would still be presenting at a mile a minute. You are an exceptional teacher and learning from the *King of Adipocytes* has been the greatest privilege.

Diane Sepa-Kishi- I am so grateful you have become a part of this lab. When you voluntarily moved from my desk on the very first day we met, I knew we would become great friends. You are the most kind hearted, sincere, and importantly, the most tolerant person I have ever met. I could not have done this without you. Thank you for your perspective and advice throughout this experience. I have learned so much from you not only in the lab but also in life. I could not have wished for a better lab mate to share my snacks and cute animal pictures with, and I will miss seeing your smile and hearing you giggle every day.

Abinas Uthayakumar...the Abinator- I will always cherish the moments in the animal facility watching you play *Spin the Cage*. Your presence in the lab was quiet but meaningful and I hope I will be fortunate enough to be surrounded by more people like you. You always knew when to give me space and helped me keep my sanity. Thank you for always being there when I needed you, whether it was personal- or lab- or gym-related, you have become a great friend and I look forward to seeing where life takes us. P.S...I will never forget the time you developed cardboard. Sincerely, chup sum bong.

Arta Mohasses- Thank you for all the jokes and keeping me entertained in the lab. Without you, I would not have known about all the great food places on campus and life is always better with Miso. You were always very understanding of my OCD-tendencies and I appreciate all the times you allowed me to take up space on your desk even though I never let you touch mine. We have come a long way since volunteering as undergrads and I am glad we have made it to the end without killing each other. I will see you in Dubai.

Lab mates past, present, and extended- Dr. Ricardo Pinho and Dr. George Bikopolous. It has been a pleasure working with you. The knowledge you have shared with me is invaluable and has helped me progress to where I am today. Thank you. Sana and Jon, thank you for all the help in the lab. I wish you both the best.

My loved ones, family and friends- Mom, Dad, Jakka, Daren, Wilson, Bridget, Umar, Bernadette, Elvia, Amy, Hana...Thank you all for your endless support and encouragement throughout the past two years, especially during the times when I felt overwhelmed. I am blessed to have such great people in my life and I would not be here without you. I hope that I can continue to make you proud and that I have made a positive impact in your lives as much as you have in mine.

TABLE OF CONTENTS

LIST OF TABLES

LIST OF FIGURES

LIST OF ACRONYMS

18F-FDG	18-F-fluorodeoxyglucose
aBAT	Aortic brown adipose tissue
AC	Adenylyl cyclise
ACC	Acteyl CoA carboxylase
AMP	Adenosine monophosphate
AMPK	AMP-activated protein kinase
ANP	Atrial natriuretic peptide
Aqp7	Aquaporin-7
Aqp9	Aquaporin-9
AT	Activity thermogenesis
ATGL	Adipose triglyceride lipase
ATP	Adenosine triphosphate
β-AdR	Beta adrenergic receptor
BAT	Brown adipose tissue
Bmp7	Bone morphogenetic protein 7
BMR	Basal metabolic rate
BNP	Brain-type natriuretic peptide
BW	Body weight
C/EBPβ	CCAAT-enhancer-binding protein beta
CAC	Citric acid cycle
cAMP	Cyclic AMP
CGI-58	Comparative gene identification-58
CLAMS	Comprehensive laboratory animal monitoring system
CPT-1	Carnitine palmitoltransferase I
CV	Caloric value
DAG	Diacylglycerol
DIO2	Type II iodothryonine deiodinase
DIO	Diet-induced obesity
DIT	Diet-induced thermogenesis
DNP	Dinitrophenol
EAT	Exercise-related activity thermogenesis
EDL	Extensor digitorum longus
EE	Energy expenditure
EI	Energy intake
Epid	Epididymal
ETC	Electron transport chain
Ex	Endurance exercise trained
FA	Fatty acid
$FADH_2$	Flavin adenine dinucleotide
FI	Food intake

FGF21	Fibroblast growth factor 21
FNDC5	Fibronectin domain-containing protein 5
GAPDH	Glyceradehyde-3-phosphate dehydrogenase
Gi	Inhibitory GPCR
GPCR	G-protein coupled receptor
hASCs	Human adiposederived stem cells
HF	High-fat
HSL	Hormone sensitive lipase
iBAT	Interscapular brown adipose tissue
IRS-1	Insulin receptor substrate 1
LBM	Lean body mass
LCFA	Long chain fatty acid
LF	Low-fat
MAG	Monoacylglycerol
MAPK	Mitogen-activated protein kinase
MGL	Monoacylglycerol Lipase
NADH	Nicotinamide adenine dinucleotide
NE	Norepinephrine
NEAT	Non-exercise activity thermogenesis
PDE3B	Phosphodiesterase 3B
PGC-1α	Peroxisome proliferator-activated receptor gamma coactivator 1-alpha
PI3-k	Phosphoinositide 3-kinase
PKA	Protein Kinase A
PKB	Protein Kinase B
PLIN	Perilipin
PPARγ	Peroxisome proliferator-activated receptor gamma
PRDM16	PR domain containing 16
RER	Respiratory exchange ratio
Retro	Retroperitoneal
Sed	Sedentary
SNS	Sympathetic nervous system
Sol	Soleus
Sc ING	Subcutaneous Inguinal
TDEE	Total daily energy expenditure
TEF	Thermic effect of food
TG	Triglyceride
UCP-1	Uncoupling Protein 1
VCO_2	Carbon dioxide production
VO_2	Oxygen consumption
WAT	White adipose Tissue

1. INTRODUCTION

Throughout the past few decades, the prevalence of obesity has increased at an alarming rate and continues to grow on a worldwide scale[1,2]. A sedentary lifestyle in combination with poor eating habits results in the hypertrophy and hyperplasia of adipocytes, leading to various other metabolic disorders such as type 2 diabetes, coronary heart disease, and cancer[3,4]. In order to prevent these chronic diseases and maintain a stable and healthy body weight, the tight regulation of energy intake (EI) and energy expenditure (EE) is required. The accumulation of adipose tissue results from an imbalance of EI and EE in which the former exceeds the latter, potentially leading to obesity in the long-term. Conversely, weight loss occurs when EE surpasses EI causing an energy deficit that is compensated for by the mobilization of fat stored in the white adipose tissue. Unfortunately, weight loss is often accompanied by the activation of energy-sparing mechanisms that oppose further fat reduction and favour the return to initial body weight by decreasing metabolic rate and whole-body energy expenditure[5]. Therefore, the success rate of this therapeutic approach is low. Current research is focused on gaining a better understanding of the molecular and metabolic mechanisms involved in the development of obesity, and the effective therapies that could improve the outcome of obesity and its associated metabolic disorders.

It is well-established that there are two types of adipose tissue with unique morphology and function identifiable in both human and murine mammals; white adipose tissue (WAT) and brown adipose tissue (BAT). The primary function of WAT is to store energy and secrete hormones, whereas BAT functions to regulate thermogenesis by dissipating energy in the form

of heat[6]. The presence of BAT allows for high rates of fatty acid and glucose uptake and the clearance of plasma lipids, leaving less substrate available for storage in the WAT. Therefore, these two tissues play a major role in adjusting energy storage and dissipation, and are of great interest to the study of metabolic regulation and whole-body energy expenditure.

Importantly, exercise also has profound effects on the regulation of body weight and whole-body EE. It is well known that sympathetic nervous system (SNS) activity increases during exercise when compared before and after training under conditions of same relative intensity[7]. SNS activity and circulating catecholamines strongly stimulate BAT activity through the activation of β3-adrenergic receptors (β3-AR), which leads to an increase in the expression of thermogenic genes as well as lipolysis[8,9]. Since adrenergic receptors in the WAT are also stimulated by exercise to increase lipolysis, it has been proposed that exercise may also induce the expression of thermogenic genes, in the WAT (a process called "browning"). White adipocytes with increased expression of thermogenic genes are called "beige" or "brite" adipocytes and display a brown-like phenotype[10]. Although classical brown adipocytes are located in designated depots and have high thermogenic capacity, beige adipocytes found in WAT are also capable of dissipating energy in the form of heat and could be potentially used as a target for increasing whole-body energy expenditure.

Recent studies have provided evidence that endurance exercise can induce browning of white adipocytes through a myokine called irisin[11]. However, exercise in itself is thermogenic and it would seem counterintuitive to increase BAT activity and heat production when exercise already creates a state of increased body temperature. Although exercise increases SNS activity

and circulating hormones that can potentially activate BAT, it has been reported that endurance training decreases the oxidative capacity of mitochondria isolated from the interscapular BAT (iBAT) of rats[12]. This provides evidence that chronic endurance exercise actually reduces thermogenic activity in classical BAT. Based on these findings, it seems that chronic endurance exercise exerts opposite effects on thermogenic capacity of BAT and WAT; however, limited information is available regarding this effect. Therefore, the aim of this study was to determine the effects of chronic endurance exercise on thermogenesis in classical BAT and WAT and the impact on whole-body energy expenditure.

2. LITERATURE REVIEW

2.1 Energy Balance

Regulation of body weight is controlled by EI and EE. When EI is higher than EE, there is a surplus of energy that leads to an increase in energy stores and weight gain. Conversely, if EE is higher than EI, weight loss occurs. Total daily energy expenditure (TDEE) includes basal metabolic rate (BMR), thermic effect of food (TEF) and activity thermogenesis (AT). Adaptive thermogenesis may also occur in response to overfeeding or to changes of environmental temperature. BMR represents the amount of energy required to sustain vital functions at rest in a post-absorptive state and accounts for ~60% of TDEE [13]. BMR variance is accounted for by body mass and is influenced by the relatively more or less active internal organs and cell type metabolism[14]. The thermic effect of food (TEF) accounts for 10-15% of TDEE and represents the increased EE required to digest, absorb, and store food. Activity thermogenesis accounts for the final 25-30% of TDEE and can be separated into 2 components: exercise-related activity thermogenesis (EAT) and non-exercise activity thermogenesis (NEAT). While EAT represents the amount of energy expended for volitional exercise activities such as sport, NEAT accounts for EE required for daily living activities such as sitting, walking, talking, and shopping. Some people do not take part in any exercise and therefore their EAT can be close to zero. Thus, NEAT is the determining factor of the large variance in activity thermogenesis that contributes to overall TDEE. Although it is difficult to measure, NEAT can be estimated by NEAT=TDEE-(BMR+TEF). Previous studies have shown that NEAT can increase with a positive energy balance and decrease with a negative energy balance. Consequently, NEAT is biologically regulated to adjust TDEE and maintain energy balance[13].

2.1.1. Weight loss and body weight regulation

When an individual loses weight, TDEE decreases. In contrast, if an individual gains weight, TDEE increases. Individuals who lose 10-20% of initial body weight have significantly lower TDEE [15]. Alterations in BMR, DIT and AT contribute to these adaptations and counteract weight loss through biological mechanisms such as enhanced skeletal muscle efficiency, decreased sympathetic nervous system (SNS) tone, and reduced circulating concentrations of fat reducing hormones such as leptin, thyroxine, and triiodothryonine[5,13,15]. Therefore, these energy-sparing mechanisms may be the cause of the low success rate of weight loss and it is of great interest to find ways to decrease metabolic efficiency or increase TDEE through an increased BMR, DIT or AT.

2.2 White Adipose Tissue

White adipose tissue (WAT) is the primary organ for triglyceride (TG) storage for use as metabolic energy and it also acts as a thermal insulator. The quantity of body fat varies widely in mammals and typically accounts for ~20% of body mass in humans and can increase to >50% in obese individuals. Such variability demonstrates the delicate balance of factors controlling the storage and breakdown of triglycerides. WAT is an essential organ for life and transgenic mice without WAT (named A-ZIP/F-1) display adverse physiological consequences such as delayed growth, decreased fecundity, premature death, and enlarged organs[16]. Mice lacking WAT are also diabetic and have elevated insulin, glucose, free fatty acids and triglyceride levels [16]. Although the surplus of WAT is associated with many metabolic disorders such as obesity,

the absence of WAT as demonstrated by A-ZIP/F-1 mice indicates that WAT is required for a healthy life and contributes greatly to energy metabolism, reproductive function and disease susceptibility[16].

WAT is a highly active metabolic and endocrine organ that is regulated by multiple external influences such as autonomic nervous system activity, blood flow, hormones and autocrine and paracrine feedback. WAT possesses the ability to modulate its own metabolic activity through hypertrophy of already existing adipocytes, and hyperplasia or differentiation of new adipocytes. In addition to its role as an energy storage compartment, adipocytes can also secrete endocrine and paracrine factors called adipokines to regulate metabolism in peripheral tissues such as the liver and central nervous system[17]. Ultimately, the amount of TG stored within adipocytes is a reflection of net EI:EE, and the pathways of fat storage (lipogenesis) and breakdown (lipolysis) are carefully regulated to maintain whole-body energy balance [18].

2.2.1. WAT distribution and morphology

White adipocytes are unilocular and contain one large lipid droplet that comprises majority of the cell surrounded by a layer of cytoplasm and an offset nucleus (Figure 1). It looks ivory or yellow in colour and can be found distributed throughout the body. In humans and rodents, white adipose tissue can be found under the skin, termed subcutaneous fat; and it can also be found surrounding internal organs in the intra-abdominal cavity termed visceral fat. Although white fat can be found distributed throughout the body, each depot may have

physiological differences [19]. The capacity for triglyceride storage is large as the lipid droplet can encompass more than 95% of the entire cell and cell size can fluctuate greatly from 25-200µm in diameter [17].

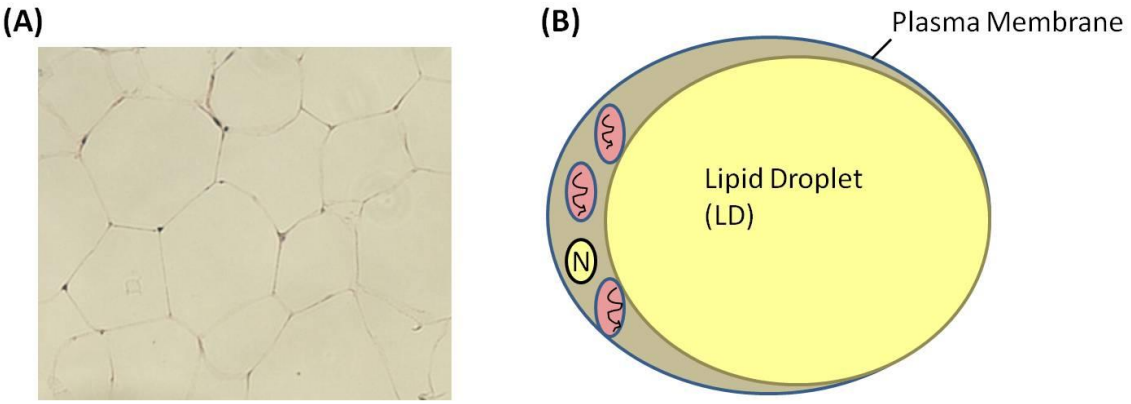

Figure 1: Subcutaneous inguinal fat with H&E staining and microscopic analysis (A). Representation of a white adipocyte (B) with one large lipid droplet (LD) and offset nucleus (N).

2.3. Regulation of lipolysis in adipocytes

The rate of lipolysis is determined by the actual energy requirements of the body and is regulated by hormonal and paracrine and/or autocrine signals. These signals vary in response to different physiological situations such as periods of fasting, or exercise, or when glucose stores are limited. In order to spare glucose for the central nervous system, fatty acids (FA) become the major substrate of energy production for muscles and peripheral tissues and thus, lipolysis occurs[20,21]. In this context, the process of lipolysis is imperative to breakdown the triglycerides stored within adipocytes to release glycerol and FA into the plasma. FAs that exit the adipocyte are bound to albumin which facilitates their transport through the blood to be utilized for oxidation in the skeletal muscle, heart and liver[22]. WAT lipolysis is regulated by the opposing

action of various hormones, mainly catecholamines and insulin and therefore, the net release of FA from WAT is determined by the balance between these hormones that stimulate and suppress lipolysis, respectively.

2.3.1. Lipolytic pathway

In response to fasting or exercise, insulin secretion is decreased and catecholamines such as epinephrine and norepinehphrine are released into the blood stream. WAT lipolysis is stimulated through direct sympathetic innervation and catecholamines bind to the β-adrenergic receptors (β-AdR) located on the surface of adipocytes. On the plasma membrane, β1- and β2-AdRs are expressed in human WAT, and β3-AdRs are found in rodents[19,23]. The β-AdR is coupled to an intracellular G-protein coupled receptor (GPCR) that activates adenylyl cyclase (AC). The effector, AC, then catalyzes the conversion of ATP to cyclic AMP (cAMP). Increased cAMP levels bind to the subunits of cAMP-dependent protein kinase A (PKA) and its activation then initiates two processes; the phosphorylation and activation of hormone-sensitive lipase (HSL), and the phosphorylation, and thus deactivation, of perilipin (PLIN). Normally, PLIN coats the lipid droplet and protects it from lipases in a basal state to maintain lipid content. Once PLIN is deactivated, it undergoes a conformational change which allows HSL (in the cytosol) access to the lipid droplet, and it also releases comparative gene identification-58 (CGI-58) which is an activator of adipose triglyceride lipase (ATGL)[24–26]. Once TG mobilization is initiated, ATGL hydrolyzes TGs to diacylglycerol (DAG) and HSL breaks down DAG to produce monoacylglycerol (MAG) (Figure 2). Finally, MAG lipase (MGL) releases the glycerol backbone and the final FA.

Free FA are then released from adipocytes to the circulatory system and are taken up by peripheral tissues for oxidation or can be re-esterified into TG[9,20,21,27,28].

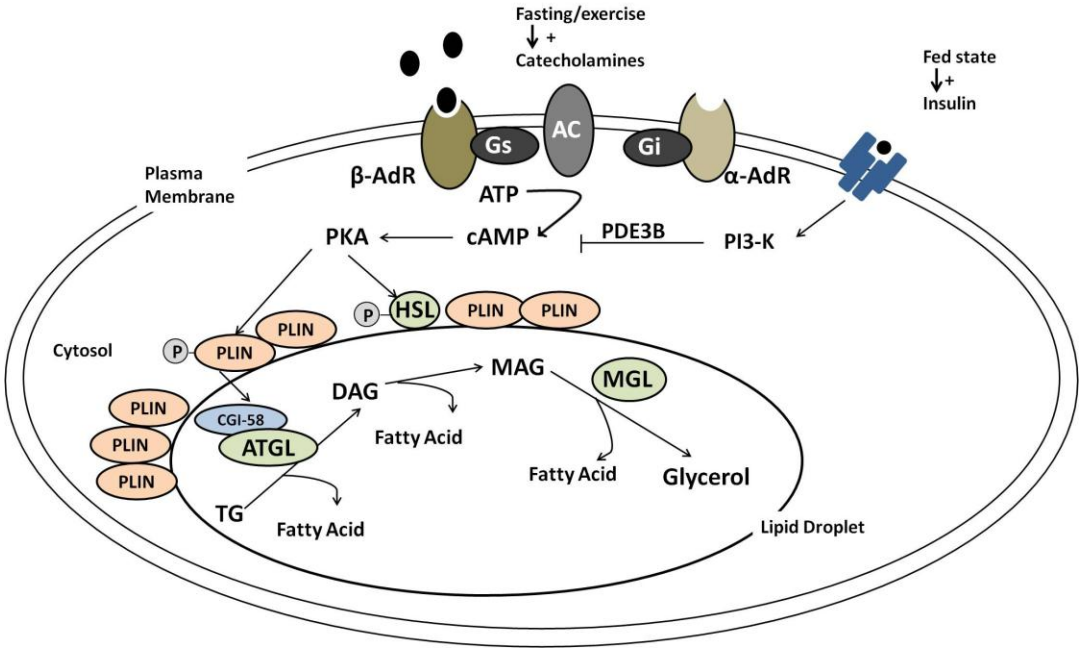

Figure 2: Schematic representation of catecholamine-induced lipolysis in an adipocyte. Catecholamines bind to β-adrenergic receptor (β-AdR) that activates G-protein coupled receptor (GPCR) located on the plasma membrane. GPCR activates adenylyl cyclase (AC) that produces cyclic AMP (cAMP). High levels of cAMP activate protein kinase A (PKA) that phosphorylates hormone sensitive lipase (HSL) and perilipin (PLIN). PLIN releases comparative gene-58 (CGI-58) that activates adipose triglyceride lipase (ATGL) that hydrolyzes triglycerides (TG) to diacylglycerol (DAG), and HSL hydroyzes DAG to monoacylglycerol (MAG) and MAG lipase (MGL) releases the final fatty acid and glycerol. Insulin secretion in a fed state leads to a cascade of events that counteracts cAMP production through phosphoidesterase 3B (PDE3B) activity.

The mobilization of FA and glycerol from TG is facilitated in three successive reactions. ATGL is responsible for the first step and its importance has been demonstrated in ATGL-KO mouse models. Without ATGL, mice displayed substantial TG accumulation throughout the

body, leading to cardiac dysfunction and death[29,30]. In addition, ATGL and CGI-58 gene mutations lead to neutral lipid storage disease characterized by systemic abnormal TG accumulation in tissues such as bone marrow, skin, and muscle[30,31]. In response to chronic endurance exercise, ATGL expression and HSL phosphorylation increase, resulting in an increased lipolytic capacity and higher FA oxidation of the skeletal muscle[30].

2.3.2. Anti-lipolytic Pathway

Lipolysis can be inhibited by catecholamines that bind to the α-AdRs on the cell surface of the adipocyte. The α-receptor signals the inhibitory GPCR (Gi) that blocks the activity of AC which leads to the subsequent decrease in cAMP formation and thus lipolysis is inhibited downstream (Figure 2). This cascade can also be affected by the presence of insulin. In a postprandial state, exogenous energy sources are available and the need for endogenous substrate is reduced, consequently; the breakdown of TG to release FA for fuel is not required. The main hormone mediating the suppression of TG breakdown is insulin[20,24]. Insulin is a potent anti-lipolytic hormone and is released by pancreatic β-cells following a meal. When insulin binds to its plasma membrane receptor, it leads to the phosphoryation of insulin receptor substrate-1 (IRS-1) on the tyrosine residue and the subsequent activation of phosphatidyl inositol 3-kinase (PI3-k). PI3-k then phosphorylates and activates protein kinase B/Akt (PKB/Akt), and PKB/Akt phosphorylates phosphodiesterase 3B (PDE3B) which catalyzes the degradation of intracellular cAMP[28]. Consequently, the degredation of cAMP inhibits the activation of PKA which leads to the de-phosphorylation of HSL and PLIN and thus, the process

of lipolysis is halted[21]. Furthermore, insulin can also stimulate the re-esterification of FA to form TG[18,20,26].

2.4. The fate of substrates derived from lipolysis

Following the hydrolysis of TG, glycerol and FA can be utilized in extra- and intra-adipocyte metabolic pathways. Glycerol is not utilized by the adipocyte and is transported out of the cell to the plasma by an aquaglyceroporin protein known as aquaporin 7 (Aqp7)[32,33]. Without Aqp7, mice displayed impaired glycerol release and severe fasting-induced hypoglycemia[34], thus demonstrating the importance of Aqp7 as a glycerol channel. Glycerol in the circulation is taken up by hepatic aquaporin 9 (Aqp9) to be utilized as a gluconeogenic precursor[32].

As previously mentioned, FA can be released into the blood and circulating FA bound to albumin are taken up FA transporter proteins in peripheral tissues such as skeletal muscle for fuel. Any unused circulating FA will return to the adipocyte to be re-esterified into TG[35]. FAs that stay within the cell are either degraded by peroxisomes or channeled towards the mitochondria for oxidation. FA are transferred into the mitochondria via the carnitine shuttle system and are β-oxidized to yield acetyl CoA for the citric acid cycle (CAC). Following the CAC, nicotinamide adenine dinucleotide (NADH) and flavin adenine dinucleotide ($FADH_2$) enter the electron transport chain (ETC) and electrons released through the ETC results in the pumping of protons from the mitochondrial matrix to the inner membrane space. The electric potential created across the inner membrane drives the movement of protons back into mitochondrial

matrix through the ATP synthase complex and thus, ATP is produced and can be used for energy[9,14].

2.5. Energy status and AMP-activated protein kinase (AMPK)

AMPK is an energy sensing and signalling enzyme that increases ATP production by enhancing glucose uptake and fatty acid oxidation in the skeletal muscle and adipose tissue. AMPK is a key regulator of energy metabolism and constantly monitors the energy status of a cell by sensing changes in intracellular adenosine monophosphate (AMP):ATP ratio brought about by exercise or fasting conditions. A decrease in ATP leads to an increase in AMP generation that competes with ATP on the Bateman domain of AMPK. The binding of AMP induces a conformational change and allows AMPK to be phosphorylated on the threonine residue 172 (Thr-172) and thus AMPK becomes active[36].

2.5.1. AMPK signaling

Due to the variations in energy demands, energy-sensing AMPK plays an important role in regulating mitochondrial oxidation. Once activated, AMPK phosphorylates and inactivates acetyl-CoA carboxylase (ACC) which leads to the suppression of malonyl-coA production. Malonyl coA inhibits inner-mitochondrial membrane protein carnitine palmitoyltransferase 1 (CPT-1), the rate-limiting step that blocks long-chain FA (LCFA) entry into the mitochondria. Thus, when malonyl co-A is reduced, CPT-1 is disinhibited and LCFA can enter the mitochondria

for β-oxidation and subsequently ATP production[30,36–38](Figure 3). This is supported by reports of marked increases in AMPK phosphorylation and decreased muscle malonyl-coA of rats exposed to exercise[14,39]. Furthermore, chronic AMPK activation also induces the expression of perixosome proliferator-activated receptor gamma coactivator 1-alpha (PGC1-α), an important transcription factor for mitochondrial biogenesis[40]. Thus, AMPK up-regulates the oxidative capacity of skeletal muscle by multiple mechanisms. Furthermore, the activation of AMPK and consequently the entry of LCFA to the mitochondria is also important for the function of UCP-1 which will be discussed in further detail in a later section.

In addition to its role in allowing LCFA into the mitochondria for β-oxidation, AMPK also plays an important role in FA oxidation by modulating lipolysis. Some studies have proposed that AMPK exerts a pro-lipolytic effect in adipocytes, while others have suggested an anti-lipolytic effect. AMPK activation has been shown to have an anti-lipolytic effect by phosphorylating HSL on a serine residue that antagonizes the phosphorylation of HSL by PKA. This mechanism has been proposed to be an energy-sparing mechanism that limits the breakdown of TG in WAT to reduce the potential energy cost of re-esterifying FA that are not used[41–44]. Interestingly, prolonged AMPK activation leads to the prevention of TG storage and the promotion of energy dissipation through an increase of ATGL content, decreased lipogenesis and increased FA oxidation despite the inhibition of HSL[41,44]. When chronically activated, AMPK also promotes alterations in gene expression of mitochondrial biogenesis markers such as PGC-1α, PPARγ, and CPT-1. By modulating HSL and ATGL in an antagonistic manner, AMPK demonstrates a time-dependent function as a cellular energy sensor to regulate

the release of FA into the circulation and to upregulate genes that promote lipid utilization rather than storage[41,44].

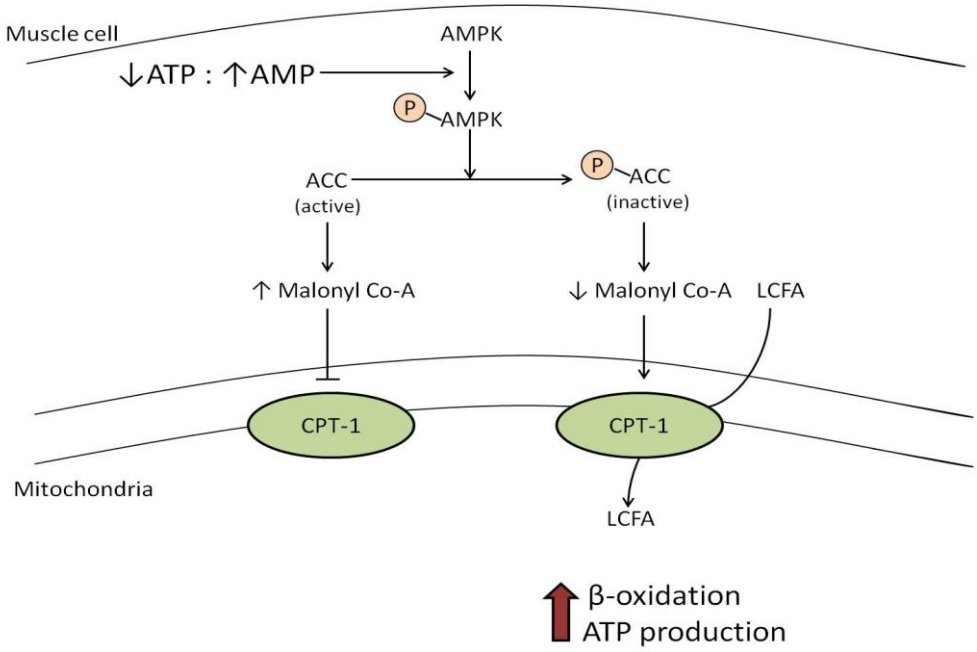

Figure 3: An increase in intracellular adenosine monophosphate (AMP) activates AMPK, which phosphorylates and inactivates actetyl-CoA (ACC) which suppresses malonyl-coA production. Suppressed malonyl co-A production leads to the deinhibition of carnitine palmitoltransferase 1 (CPT-1) and long-chain fatty acids (LCFA) can enter the mitochondria for β-oxidation.

2.6. Brown Adipose Tissue

Throughout history, humans have endured periods of food scarcity and cold weather. Fortunately, we have been able to survive these environmental stressors due to the presence of adipose tissue. As previously described, WAT acts as an insulator and an energy storage organ that allows us to cope with the changing availability of exogenous food sources and varying environmental conditions. Another fat depot that has also aided in our survival as a thermoregulatory organ is the brown adipose tissue (BAT). BAT was first described in small

mammals as a hibernating organ[45] and in contrast to WAT, the function of BAT is to regulate thermogenesis by dissipating energy in the form of heat[6,9,46]. Although it was previously believed that functional BAT was only found in newborns to survive the cold stress of birth, investigators have more recently been able to detect BAT in adult humans using PET/CT scans[46].

A dual role for BAT has been proposed; aside from its role as a thermoregulatory organ in response to cold, it has also been suggested to function as a metaboregulatory organ in response to large caloric loads. The mitochondria of BAT contain a specialized protein called uncoupling protein-1 (UCP-1), which allows for protons to translocate from the intermembrane space to the mitochondrial matrix while bypassing the ATP synthase complex (Figure 4). This process is called non-shivering thermogenesis and results in the generation of heat, rather than ATP[46]. The high rates of fatty acid and glucose uptake in BAT allow for the clearance of plasma lipids leaving less substrate available for storage in the WAT. It has been estimated that basal metabolic rate can increase by up to 20% from just 50 g of fully activated BAT [47]. Previous studies have also shown that there is a negative correlation between the amount of BAT, and body fat or BMI [48,49] and animals with more functional BAT were less likely to develop obesity and type II diabetes[50]. This suggests that metabolically active BAT may be of therapeutic value for obese individuals and therefore, the thermogenic capacity of BAT is not only important for the regulation of body temperature, but also for EE and maintenance of body weight.

Importantly, other uncoupling proteins have been discovered in BAT such as UCP-2 and UCP-3; however, they are not essential for thermogenesis[9,51]. In isolated brown adipocytes from UCP-1 ablated mice, no thermogenesis could be induced with norepinephrine (NE) nor FA

stimulation. In these cells, UCP-2 and UCP-3 were present but did not substitute for UCP-1 as a thermogenic protein. This establishes the importance of UCP-1 as the only physiologically thermogenic uncoupling protein and that no other mechanisms exist for thermogenesis other than the mediation by UCP-1[9,51].

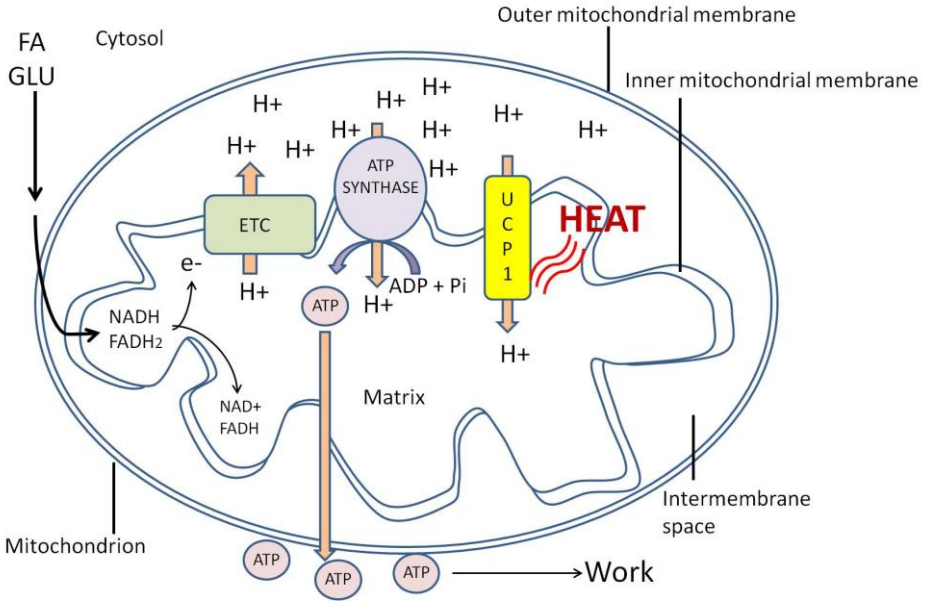

Figure 4: Schematic representation of a mitochondrion in brown adipose tissue (BAT). Fatty acids (FA) and glucose (GLU) undergo β-oxidation and glycolysis respectively, and yield nicotinamide adenine dinucleotide (NADH) and flavin adenine dinucleotide ($FADH_2$). The electron transport chain (ETC) on the inner mitochondrial membrane releases free energy from NADH and $FADH_2$ that is used to pump protons from the mitochondrial matrix to the intermembrane space. The presence of uncoupling protein-1 (UCP1) allows for protons to leak across the inner mitochondrial membrane and uncouples oxidative phosphorylation from adenosine triphosphate (ATP) synthesis. Heat is created instead of ATP.

2.6.1. BAT distribution and morphology

BAT is highly vascularised and is populated with brown adipocytes containing multiple small lipid droplets (multilocular) with a vast number of mitochondria with abundant cristae

(Figure 5)[52]. The tissue appears brown in colour and can be found in various regions throughout the body. In rodents, the largest BAT compartments are found between the scapulae (termed interscapular BAT, iBAT) and surrounding the aorta (termed periaortic BAT, aBAT). Recent research has used 18F-fluorodeoxyglucose (18F-FDG) to trace glucose uptake within the human body. An increase in 18F-FDG uptake indicates the presence of active BAT. Using this method, researchers have found that human BAT is mostly located in the lower neck and paracervical/supraclavicular region[19,53]. It has also been found in a kite-shaped sheet between the scapula of infants[46]. Brown adipocytes express β-AdR on the surface of the cell and the tissue is densely innervated by the sympathetic nervous system (SNS)[52].

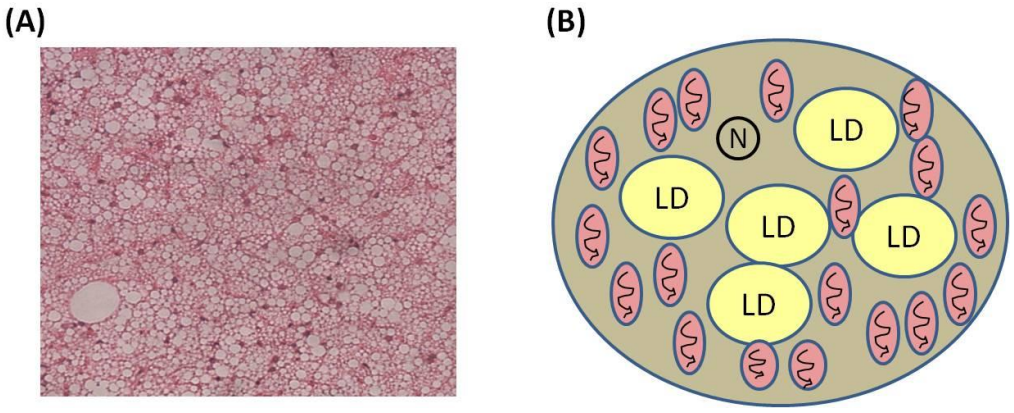

Figure 5: Brown adipose tissue with H&E staining and microscopic analysis (A). Representation of a brown adipocyte (B) with multiple small lipid droplets (LD) and numerous mitochondria. The nucleus (N) is round and centrally located.

2.6.2 .Transcriptional control of BAT

Prolonged cold exposure is a strong activator of BAT recruitment and function. Cold temperatures sensed by thermoreceptors in the skin elicit sympathetic outflow and the growth

of blood vessels to facilitate oxygen delivery and heat exchange. Several transcriptional factors that govern BAT development have been discovered including PR domain-containing protein-16 (PRDM16) and peroxisome proliferator-activated receptor γ-coactivator-1α (PGC-1α)[10,54].

PRDM16 is highly expressed in BAT and acts by binding to transcriptional factors such as CCAT/enhancer binding proteins (C/EBPβ), peroxisome proliferator-activated receptor gamma (PPARγ), and peroxisome proliferator-activated receptor alpha (PPARα), and PGC-1α, that are important for brown fat differentiation. PRDM16 converts myoblasts and white fat precursors into UCP-1 containing thermogenic adipocytes and PRDM16 knockout models show no thermogenic characteristics and have an increased expression of white fat genes[10]. Thus, PRDM16 is a critical determinant of BAT lineage during embryonic development. Several factors have been shown to modulate brown adipocyte differentiation by regulating PRDM16 expression and activity, such as bone morphogenetic protein (Bmp7)[10].

PGC-1α is induced by cold exposure and exercise, and is highly expressed in tissues with abundant mitochondrial content such as BAT, liver, and skeletal muscle. It is a master regulator of mitochondrial biogenesis and oxidative metabolism, and it directly increases the transcription of thermogenic genes such as UCP-1[55–58]. PGC-1α expression and activity is directly regulated by the β-adrenergic/cAMP signalling and is phosphorylated and activated by p38 mitogen-activated protein kinase (MAPK) in response to sympathetic stimulation. Activated PGC-1α regulates the expression of thermogenic genes by interacting with transcription factors such as PPARγ. Retinoblastoma family members (pRb and p107) and nuclear co-repressor Rip140 repress PGC-1α activity and block the expression of BAT specific genes. Cells lacking

PGC-1α can differentiate into mature brown adipocytes, however the induction of thermogenic genes in these cells was impaired, indicating that PGC-1α is indeed essential for thermogenesis[55]. Therefore, thermogenesis is controlled by the positive regulators or repressors of PGC-1α transcriptional activity.

2.6.3. β3-Adrenergic signalling is required for thermogenesis

All three subunits of β-AdR receptors have been identified in BAT, however, the role of β1- and β2-AdRs is not yet well understood. β3-AdRs have the highest expression in BAT and is a key player in cell signalling processes[9]. Transgenic mice that are unable to synthesize catecholamines displayed impaired BAT function[8] and β-AdR-less mice were thermogenically inactive and were unable to maintain body temperature at 4°C. In addition, iBAT taken from these mice were large unilocular adipocytes with no UCP-1 and type II deiodinase DIO2 expression, and oxidation did not increase with pharmacological β-agonist stimulation. Interestingly, although food intake between the β-less and wildtype mice were equal, β-less mice exposed to a HF diet developed obesity[8,59]. These findings confirm the significance of β-AdR for thermogenic function of BAT and the maintenance of body temperature, as well as for the metaboregulatory function of BAT and its defense against diet-induced obesity[8].

2.6.4. Fatty acids are thermogenic substrates

No thermogenesis can occur without first activating lipolysis and all experiments that induce lipolysis in BAT also simultaneously induce thermogenesis[9]. Following the activation of β-AdR, lipolysis occurs as previously outlined and FA are released. Some FA may leave the cell for fuel for peripheral tissues while remaining FA bound by FA binding proteins in the cytosol are channeled towards the mitochondria. Importantly, long chain FAs (LCFAs) are required as substrate for β-oxidation and thermogenesis, and they are also involved in the function of UCP-1. Within the mitochondria, UCP-1 in the resting state is inactive and requires LCFAs to become activated. Although the current understanding of the LCFA-dependent mechanism of UCP-1 still remains elusive, it has been proposed that an allosteric interaction of FA on UCP-1 leads to its activation by overcoming the nucleotide inhibition of UCP-1[9,60,61]. Two other theories of LCFA involvement with UCP-1 include its action as a cofactor, and action as a proton shuttle. In the cofactory theory, LCFA are localized to binding sites within UCP-1 to act as stepping stones for protons as they pass through the membrane. The shuttling theory suggests that protons are not transported through UCP-1, but that protons enter the mitochondria by translocating fatty acid anions through UCP-1[9,60,61]. Despite multiple theories of how LCFAs are involved with UCP-1 activation, it is well-accepted that LCFAs or its derivative are directly involved in the physiological activation of UCP-1.

2.6.5. BAT and diet-induced thermogenesis (DIT)

Aside from its role as a thermoregulatory organ, BAT has also demonstrated a role in DIT in response to high caloric load. Increased heat production during chronic overfeeding is largely mediated by BAT thermogenesis. This has been interpreted as defensive mechanism that allows the organism to adjust metabolic rate according to energy intake and availability. BAT is activated in rodents after overeating to preserve energy balance and limit weight-gain, resulting in DIT[10,62]. BAT has been shown to undergo hypertrophy accompanied by an increased respiration rate[63] and blood flow[64] following a single meal in rats, and an increased glucose uptake after a single meal in humans[65]. In addition, UCP-1 ablated mice demonstrated no diet-induced increase in oxygen consumption (VO_2), showing that DIT is mediated by the presence and activation of UCP-1[50]. Taken together, this data indicates an important role of BAT in the overall thermic effect after a meal.

2.7. WAT and BAT plasticity

Despite major structural and functional differences between WAT and BAT, both types of adipose tissue can acquire features of one another with the appropriate physiological stimulus[66]. Within WAT, clusters of UCP-1 expressing adipocytes with thermogenic capacity can develop (a process called "browning"). White adipocytes with increased expression of thermogenic genes are called "beige" or "brite" cells and display a brown-like phenotype[10]. Although classical brown adipocytes are located in designated depots and have high thermogenic capacity, beige adipocytes found in WAT are also capable of dissipating energy in

the form of heat and consequently, the browning process of WAT has emerged as a potential target for the prevention and treatment of metabolic abnormalities.

Temperatures below thermoneutrality induce the activation of SNS, a strong stimulator for BAT activation. Noradrenaline levels in iBAT were higher in animals exposed to cold environments and lower in warm-acclimatized mice. Brown adipocytes from warm-acclimatized mice were characterized by a unilocular lipid droplet and did not express UCP-1, demonstrating that brown adipocyte function and morphology changes according to physiological stimulus[66]. WAT conversion to BAT has also been suggested by *in vitro* studies using human Sc tissue. PPARγ agonists and PGC-1a transfection induced UCP-1 expression in these Sc adipocytes[66,67]. Taken together, this data demonstrates that the adipose organ is plastic and each depot has the ability to take on features of one another. Interestingly, the capacity of inducing beige adipocytes in WAT varies within each depot. It appears that the Sc Ing fat depot is more susceptible to undergo browning in comparison to visceral fat depots as beige adipocytes are found most abundantly within Sc Ing depot of rats[10,68,69]. In addition, PRDM16, a key driver of brown fat cell development, is highly expressed in Sc Ing fat in comparison to other mouse WAT depots. A reduction in PRDM16 inhibits the induction of the thermogenic gene program in Sc Ing cells resulting in the reduced recruitment of beige adipocytes in WAT. In contrast, transgenic over-expression of PRDM16 led to the development of beige adipocyte formation within WAT[10,68]. Primary human subcutaneous adipocytes showed an enhanced BAT-like phenotype after FNDC5/FGF21 treatment in comparison to visceral adipocytes[70], further demonstrating that the induction of a brown phenotype is depot specific. Additional depot-

specific traits of WAT have also been proposed- it has been suggested that adipocytes have a maximum cell volume in which it cannot further expand by hypertrophy under conditions of positive energy balance. The maximum volume, also known as critical cell size, is genetically determined and adipocytes that have reached this stage will trigger an increase in cell number. It has been reported that visceral fat depots such as the epididymal and mesenteric depots have a higher critical cell size and are more prone to hypertrophy while inguinal fat depots are more prone to hyperplasia[66].

2.7.1. Endocrine factors that induce WAT browning

Several factors have been reported to regulate brown and beige adipocyte formation and differentiation. Notably, bone morphogenic protein 7 (Bmp7) has proven essential for brown fat development. Bone morphogenic proteins are a part of the transforming growth factor-β family and were originally thought to control vital steps of embryonic development such as bone formation. However, it has been discovered that Bmps are multifunctional and also play an important role in adipogenesis. Although most Bmps such as Bmp2 and Bmp4 enhance WAT adipogenesis, Bmp7 is unique in inducing brown and beige adipocytes with functioning thermogenic capacity through the induction of brown fat regulators such as PRDM16 and PGC-1α[10,71]. Treatment with Bmp7 in preadipocytes led to the initiation of a full brown adipocyte transcriptional program marked by significant increases of PPARγ, PRDM16, C/EBPs as well as UCP-1. Bmp7 treatment significantly increased PGC-1α as well as nuclear respiratory factor-1 and cytochrome C, demonstrating signs of increased mitochondrial

biogenesis, an important aspect of brown fat cell development. In addition, there was a 5-fold increase in mitochondrial density in Bmp7 treated cells. Taken together, this data demonstrates that Bmp7 activates brown adipogenesis by inducing factors important for brown fat cell development and mitochondrial biogenesis. Bmp7 has proven to be a physiological necessity for BAT development as demonstrated by Bmp7-knockout mice. At birth, Bmp7-knockout mice had 50-70% less iBAT mass in comparison to wild type littermates. In addition, the expression of UCP-1 was nearly absent in brown fat from Bmp7-null embryos. The role of Bmp7 in energy homeostasis was also studied in C57BL/6 mice. Injection with adenovirus encoding for Bmp7 led to a significant increase in brown fat mass with no changes to WAT mass. Moreover, no changes to physical activity or food intake were reported but an increase in energy expenditure was observed, leading to a significant reduction in weight gain of Bmp injected mice in comparison to controls. This establishes an essential role of Bmp7 in brown fat development *in vivo*[71].

Fibroblast growth factor 21 (FGF21) is a circulating hormone released by the liver to stimulate gluconeogenesis and ketogenesis during conditions of prolonged fasting[72]. In response to FGF21 stimulation, differentiated mouse adipocytes and human primary adipocytes showed stimulated glucose uptake, and the overexpression of FGF21 in transgenic mice led to improved insulin sensitivity and reduced plasma triglyceride concentrations[73–75]. In response to fasting, FGF21 is secreted to increase lipolysis and the release of FA, which are used for oxidation and/or are converted into ketones that can be used by the brain[73,74]. Importantly, FGF21 plays an important role in the regulation of carbohydrate and lipid metabolism, and it also seems to affect thermogenesis in classical BAT and WAT following β-adrenergic

stimulation. In response to cold exposure, circulating FGF21 and FGF21mRNA levels in BAT increased[70,76], and treatment with exogenous FGF21 resulted in the up-regulation of brown fat genes in human adipocytes[70] and promoted thermogenic activity in isolated brown adipocytes[73]. FGF21 administration in *ob/ob* mice resulted in up-regulation of genes involved in lipid metabolism such as UCP-1, PGC-1α, HSL, and ATGL in WAT, and UCP-1 in BAT[69,77]. In addition, these mice showed an increased net energy expenditure, an elevated core body temperature, and a reduced total adiposity with no changes in physical activity[77]. Taken together, this may suggest that FGF21 administration led to an increased energy expenditure by the induction of metabolically activated adipose tissue[77]. Interestingly, beige adipocyte formation and expression of thermogenic genes were seen in subcutaneous inguinal fat, but not epididymal WAT, demonstrating a depot-specific response of FGF21-induced browning. It has also been demonstrated that FGF21 expression is induced by BAT and inguinal WAT following cold exposure without any changes in liver and circulating levels of FGF21[69,76,78]. This suggests that FGF21 is not only released by the liver, but can also be induced by BAT and WAT and acts as an autocrine factor[79].

Atrial natriuretic peptide (ANP) and brain natriuretic peptide (BNP) are key hormones released by the heart for regulation of hemodynamic homeostasis, however; they have also been shown to promote lipolysis and beige adipocyte development within WAT[10,80]. Comparable to the response of adipocytes to catecholamines, natriuretic peptides activate the guanylyl-clyclase containing natriuretic peptide receptor-A that generates the second messenger cGMP which activates cGMP-dependent protein kinase in response to cold temperatures. Similar to PKA, PKG phosphorylates the same targets as β-agonists and thus

lipolysis increases. In human adipocytes, ANP treatment increased PGC-1α and UCP-1 expression, accompanied by an increased mitochondrial biogenesis and increased respiration. BNP infusion in mice robustly increased PGC-1α and UCP-1 expression in both BAT and WAT and correspondingly, resulted in an increase in respiration and energy expenditure[80].

Irisin, another factor secreted by skeletal muscle that regulates the browning of WAT will be discussed in further detail in a later section.

2.7.2. Molecular and physiological regulators of beige/brite fat

The "browning" process in which white adipocytes change to UCP-1 expressing beige/brite adipocytes occurs following thermogenic stimulus such as prolonged cold exposure or treatment with β3-agonists. Contrary to previous beliefs, it appears that classical brown adipocytes differ in cell lineage when compared to beige/brite adipocytes. Myf5+ progenitor cells give rise to skeletal muscles and brown adipocytes, while white and beige adipocytes derive from a Myf5- cellular lineage[10,54](Figure 6). This suggests that brown adipocytes are different from inducible beige adipocytes even at the precursor stage. The molecular mechanism that mediates the induction of beige adipocytes in WAT from the Myf5- precursor cell involves the up-regulation of PGC-1α and PRDM16. Similar to the differentiation process of classical BAT, PRDM16 also interacts with transcriptional factors such as PPARγ, PPARα, and C/EBPs, which are key regulators of adipogenesis, to activate the thermogenic program.

There is also evidence that white adipocytes have the capacity to convert into inducible brown/beige adipocytes through transdifferentiation (Figure 6). After 10 days of cold

acclimatization, it was found that the total number of adipocytes in adult female mice were not significantly different from mice kept at thermoneutrality. However, the number of brown adipocytes in cold-acclimatized mice increased significantly in proportion to the number of white adipocytes that were lost. In addition, there was no evidence of apoptosis or mitosis which suggests the direct transformation of white to brown adipocytes also known as transdifferentiation[81].

WAT and BAT have the ability to acquire metabolic features of one another depending on physiological stimulus. Whether this is caused by de novo recruitment of classical BAT or transdifferentiation of already mature adipocytes to thermogenic beige adipocytes remains unclear.

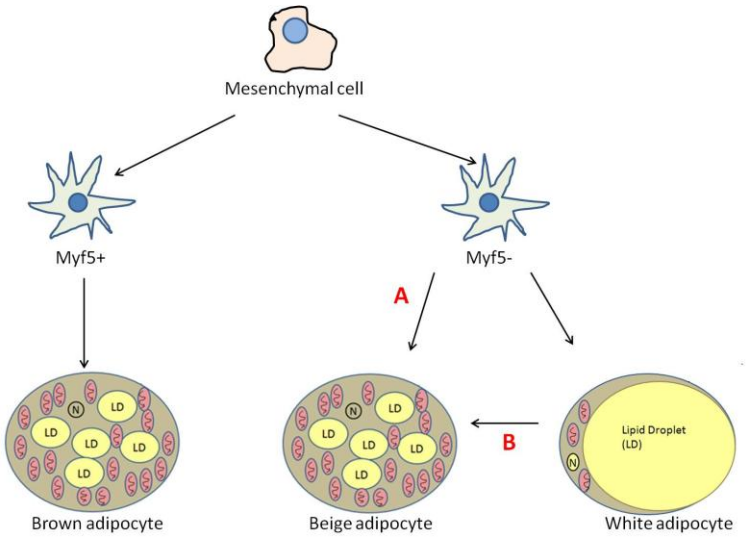

Figure 6: Schematic representation of the origin of fat cells. Brown adipocytes derive from Myf5+ cell lineage precursors and Myf5- precursors give rise to white and beige adipocytes (A). In addition, there is evidence of white adipocytes converting to beige adipocytes through transdifferentiation (B).

2.7.3. Effects of exercise on WAT and BAT plasticity

It is well documented that endurance training increases PGC-1α content in humans and rodents[52,82]. Human white adipocytes that overexpressed PGC-1α led to an increase in UCP-1 mRNA expression and FA oxidation[67]. However, exercise results in a large amount of heat production as a consequence of repeated muscle contractions and UCP-1 mRNA and thermogenic activity of BAT decrease in rats following exercise[83,84]. In fact, the oxidative capacity of isolated iBAT mitochondria was reduced as a result of endurance training marked by reduced levels of cytochrome oxidase activity[12]. Overall, the reduced thermogenic capacity of BAT in response to endurance exercise has been considered physiologically advantageous due to the increase in body temperature as a result of chronic exercise in the trained state.

Physiologically, SNS activity and circulating catecholamines strongly stimulate BAT activity through the activation of β3-AdR, which leads to an increase in the expression of thermogenic genes as well as lipolysis [8,9]. It is well known that SNS activity increases during exercise when compared before and after training under conditions of same relative intensity[7], however; thermogenic capacity of BAT following exercise is decreased regardless of the increased SNS activity. It has been previously demonstrated that prolonged exposure to β-AdR receptor agonist, Ro16-8714, selectively down-regulates β3-AdR, marked by a decreased in β3 mRNA and loss of receptor number in brown adipocytes[85]. This down-regulation by β-AdR agonists suggests the possibility that prolonged exposure to β-adrenergic stimulation through chronic endurance exercise can also down regulate β3-AdR expression in classical BAT. Interestingly, when mice were stimulated with a β3-agonist, CL316243, UCP-1 positive brown adipocytes

appeared within the Sc Ing fat pad but not in the visceral fat depot; this indicates a depot-specific response to browning[86].

Since adrenergic receptors in the WAT are also stimulated by exercise to increase lipolysis, it has been suggested that exercise may also induce the expression of thermogenic genes in the WAT. This mechanism has been proposed to be induced by a PGC-1α-dependent myokine called irisin. Irisin is cleaved from the ectodomain of fibronectin-domain containing protein 5 (FNDC5) produced in the skeletal muscle during exercise and is released into the circulation to signal white adipocytes in Sc tissues to undergo browning[11]. In humans, serum irisin levels were higher after submaximal exercise in comparison to maximal exercise, suggesting that endurance exercise as a more potent stimulator of irisin release following exercise[70]. However, the role of irisin in exercise-induced browning of Sc Ing fat has been challenged. As expected, *in vitro* contraction of human myotubes induced PGC-1α expression, however FNDC5 mRNA was not altered. In addition, muscle biopsies from human participants also showed no differences in FNDC5 expression in response to exercise[87]. Therefore, the discrepancy of findings across studies indicates a possible alternative mechanism behind the browning of Sc Ing fat. Interestingly, it has been reported that FNDC5 and irisin increase in Sc fat following exercise and consequently, irisin has also been proposed to behave as an adipokine[88,89].

In murine mammals and humans, classical BAT is highly vascularised and is found close to the heart so that the heat produced can be effectively distributed throughout the body. In response to chronic endurance exercise, body temperature rises as exercise is thermogenic in itself. As a consequence, it seems physiologically relevant for BAT thermogenesis to decrease to

avoid overheating. Importantly, Sc Ing fat is located peripherally and an increase in beige adipocytes within this fat depot may increase energy dissipation without increasing core body temperature. Therefore, the browning of Sc Ing fat may be important for the regulation of WAT metabolism and whole-body energy expenditure in response to chronic endurance exercise. It has been demonstrated that adipose-derived stromal/progenitor cells (hASCs) taken from human Sc WAT can efficiently be converted into beige adipocytes with functioning characteristics of typical brown adipocytes[90]. This exhibits the possibility that humans can convert WAT to beige adipocytes upon stimulation and is a potential target for alter whole-body energy expenditure.

2.8. Significance of WAT/BAT plasticity and its effect on whole-body energy expenditure

Up until a few decades ago, it was assumed that adult humans had too little brown fat to substantially affect body weight. However, recent imaging studies have revealed the presence of extensive depots of brown fat in adults[46,91]. Converting white into brown adipocytes gives rise to the possibility of dissipating energy beyond thermogenesis of classical BAT depots and holds tremendous promise for the treatment of obesity and its associated metabolic diseases.

Upon the discovery of UCP-1 and its energy dissipating capabilities, chemical mitochondrial uncoupling using 2,4-dinitrophenol (DNP) has been tried as a weight-loss therapy. Similar to activated UCP-1, DNP works as a chemical uncoupler that allows protons to leak across the mitochondrial membrane, utilizing FA and glucose and leaving less substrate for

storage in WAT. However, high doses of unregulated respiratory uncoupling causes deleterious side effects including hyperthermia and death[10]. Ideally, strategies should be developed to enhance respiratory uncoupling selectively in adipose tissue. Further studies are required to determine the molecular mechanisms that can increase BAT activity in a safe and effective manner.

The discovery of β3 agonists such as CL316243 have shown remarkable anti-obesity and anti-diabetic effects in rodents and has induced the BAT phenotype in WAT[86,92]. Despite of this, the physiological relevance to humans of β-agonists is limited. To date, the pharmaceutical industry has not been successful in developing a safe and effective β-agonist that is highly specific to adipose tissue, and the risk of side effects to other organs containing β-receptor subtypes is substantial. Poor pharmacokinetic properties and oral bioavailability are also obstacles[10] and the number of β3-AdRs in human WAT seems to be lower in humans and thus, the efficacy of a β3-AdR agonist is minimal[9,18].

Taken together, the data in this literature review suggests that both WAT and BAT are very plastic tissues with the ability of acquiring metabolic features of one another depending on the physiological stimulus, such as exercise, diet, and cold exposure. Further studies are required to determine the molecular mechanisms that affect WAT and BAT plasticity and holds tremendous possibilities in hopes to treat obesity.

3. OBJECTIVES AND HYPOTHESIS

Currently, there is no clear consensus regarding the effects of chronic endurance exercise on the thermogenic capacity of BAT and WAT. Therefore, the *objective* of this study was designed to determine the effects of chronic endurance exercise on thermogenesis in classical BAT and WAT and the impact on whole-body energy expenditure.

Based on the current concept that chronic endurance exercise decreases the oxidative capacity of isolated mitochondria from BAT, and that endurance training may promote browning of WAT, I *hypothesize* that chronic endurance exercise will decrease the overall thermogenic capacity of classical BAT and increase thermogenic capacity of WAT. Furthermore, I hypothesize that these adaptations will lead to an overall increased whole-body EE.

4. STATEMENT OF LABOUR

All experiments conducted in this study were carried out in equal contribution by Michelle Victoria Wu (MVW) and George Bikopoulos (GB). MVW's involvement included exercise training of animals, collection of food intake and body weight data, extraction of tissues, western blotting of adipose tissue samples, and palmitate oxidation. Due to the logistics of this experiment, the co-author of this manuscript is GB. Daily measurements of food intake and body weight, training of animals, extraction of tissues and palmitate oxidation experiments were equally shared responsibilities between GB and MVW. In addition, GB was also involved in the preparation of tissues for microscopy and determination of serum irisin levels. Validation of the PGC-1α antibody was also required by the reviewers of the manuscript and GB and MVW conducted additional experiments that are not included in the thesis. These experiments involved knock-down of PGC-1α in L6 muscle cells, which were conducted by GB. Also, western blots to probe for PGC-1α in tissues of PGC-1α knockout mice and PGC-1α overexpressing mice which were required by the reviewers, were conducted by MVW. Additional assistance was required from Steven Hung, who has completed his MSc. Degree in Dr. Ceddia's lab at York University. His contribution was essential in the collection of blood from animals under strict YUACC guidelines, and he also aided in western blotting experiments of muscle samples.

Dr. Rolando Ceddia is the primary investigator and supervisor of this project and this research was funded by the Natural Sciences and Engineering Research Council of Canada (NSERC) grant 311818-2011.

5. MATERIALS AND METHODS

5.1. Reagents – Fatty acid free bovine serum albumin (BSA), L-carnitine and CoA and palmitic acid were purchased from Sigma (St. Louis, MO). DTT, ATP, ADP and nicotinamide adenine dinucleotide phosphate (NADP) were obtained from Bioshop Canada Inc. (Burlington, ON). [1-14C] palmitic acid was purchased from GE Healthcare Radiochemicals (Quebec City, QC). The irisin kit was purchased from Pheonix Pharmaceuticals (Burlingame, CA). cOmplete ULTRA tablets and phosStop inhibitors were purchased from Roche Diagnostics (Mannheim). Specific antibodies against ATGL, AMPK, P-AMPKThr172, and β-actin were purchased from Cell Signalling Technology Inc. (Beverley, MA). The PGC-1α antibody was from Millipore (Temecula, CA) and the antibodies against UCP-1 and FNDC5 were purchased from abcam (Cabridge, MA).

5.2. Experimental Procedures – Male Wistar rats had ad libitum access to a low-fat (LF) diet or high-fat (HF) diet. Food intake (FI) and body weight (BW) measurements were taken on a daily basis, and blood was extracted every 2 weeks. Additionally, in vivo metabolic parameters such as energy expenditure (EE), respiratory exchange ratio (RER) and ambulatory activity was measured at the end of the 8 week protocol. By the end of the study, muscle and adipose tissue was extracted for further analysis and lean body mass was determined. Important proteins for thermogenesis (UCP-1, PGC1-α) were analyzed in adipose tissue, and oxidative capacity ex vivo was also measured. This experiment was designed to identify the thermogenic adaptations of adipose tissue in response to endurance training and the potential molecular mechanisms that alter whole-body energy homeostasis. All experimental procedures were approved by the York

University Animal Care Committee, permit number: 2011-14, and were carried out under strict YUACC guidelines. All surgery was performed under Ketamine/Xylazine anesthesia, and all efforts were made to minimize suffering.

5.3. Animals – Male albino rats of the Wistar strain from Charles River Laboratories, weighing ~200g (initial weight) were used for this experiment. Upon arrival, the animals were given 1 week to acclimatize to the new environment prior to initiating any of the experimental procedures. In order to assign each animal to an experimental group, the rats were subjected to an exercise protocol selection process to determine rats unwilling to exercise. The screening process consisted of 3 separate treadmill exercise sessions. Each session started with a 5-min warm-up period set at a constant 5% inclination and 10m/min speed. Following the warm-up, the inclination was raised to 10% and remained constant while the speed was increased by 2m/min every 2 min up to 30m/min. Any rats unwilling to run were excluded from this study. Only 10% of the animals did not meet the inclusion criteria. Animals that ran for the longest duration of time were then selected and randomly assigned to one of four experimental groups; Sedentary (Sed) LF, Exercise (Ex) LF, Sed HF, and Ex HF. The rats were kept in a constant 23°C temperature environment with a fixed 12-hour light(07:00-19:00)/12-hour dark cycle(19:00-07:00) with *ad libitum* access to water and either low-fat (LF) diet (10% fat, 70% CHO, and 20% protein) or high-fat (HF) diet (59.9% fat, 20.1% CHO, and 20% protein) obtained from Research Diets Inc. Animals were housed in individual cages so that FI and BW could be measured daily.

5.4. Exercise Protocol – In order to determine the initial training protocol, specialized treadmills connected to the Comprehensive Laboratory Animal Monitoring System (CLAMS) from Columbus Instruments were used to conduct maximal oxygen consumption (VO_2 max) tests at week 0, 2, 4, and 6 of the study. Animals were continuously monitored while running an incremental speed and inclination protocol until exhaustion was reached. Exhaustion was characterized by the rats remaining on the shock pad for longer than 5 consecutive seconds, or at which point oxygen consumption (VO_2) did not increase, or if the RER reached a value of 1. See Table 1 for the VO_2 max protocol. Animals in the exercise groups were subjected to 1 hour of treadmill running at 70-85% VO_2 max, 5 days a week for 8 weeks and the exercise protocol was adjusted accordingly to maintain exercise intensity throughout the study. At the beginning of the study, the average speed was 24m/min and progressed to 42m/min by week 8. Animals in the sedentary groups were also placed on the treadmills at a speed of 2m/min for 1 hour/day, 5 days a week for 8 weeks to ensure equal conditions.

Time (min)	Speed (m/min)	Incline (%)
0	0	0
5	10	0
7	12	5
9	14	10
11	16	10
13	18	10
15	20	10
17	22	10
19	24	10
21	26	10
23	28	10
25	30	10
27	32	10
29	34	10
30	36	10
32	38	10
34	40	10
36	42	10
38	44	10
40	46	10
42	48	10
44	50	10

Table 1. VO_2 max protocol

5.5. In vivo metabolic parameters – The CLAMS was also used to perform all in vivo measurements of VO_2, carbon dioxide production (VCO_2), spontaneous ambulatory activity and RER. Ambulatory activity was measured by a system of infrared beams that detect animal movement. Respiratory exchange ratio was calculated by the ratio of VCO_2 to VO_2 ($RER=VCO_2/VO_2$). A lower RER (0.7) indicated greater fat oxidation, while a higher RER (1.0) indicated greater carbohydrate oxidation. Energy expenditure (heat) was calculated by multiplying the calorific value ($CV= 3.815+1.232x$ RER) by VO_2. Measurements using the CLAMS were performed at week 8 of the diet and exercise protocol, 24 hours after the last exercise bout and animals were kept in the CLAMS for 25 hours. The first hour was discarded as the time required for the rats to acclimatize to the new cage environment and the remaining 24 hours were monitored encompassing the light (07:00-19:00 h) and dark cycle (19:00-07:00 h).

5.6. Tissue extraction and organ mass – Following the 8 week endurance exercise and diet protocol, animals were dissected 48 hours after the last bout of exercise to ensure that all results were a consequence of chronic endurance exercise and not from an acute exercise bout. Animals were weighed and anesthetized (Ketamine/Xylazine, 0.4mg and 8mg/100g BW). SC inguinal (Ing) WAT, epididymal (EPID), retroperitoneal (RETRO), iBAT and aBAT were carefully excised and weighed. A portion of each adipose tissue depot were used for palmitate oxidation and another portion immediately snap frozen for further analysis. A scalpel was used to detach the entire skin of the animal including the head and weighed separately. The abdominal and thoracic cavity was incised longitudinally which exposed internal organs that accounted for the

viscera. Lean body mass (LBM) was measured by weighing the remaining carcass consisting of skeletal muscle, bones, and the skinned head, liver, heart and kidneys.

5.7. Irisin determination in the serum – Blood was extracted immediately after exercise at week 6, and also during resting conditions at week 8 of the study. For resting irisin levels, blood was collected from the saphenous vein 24h after the last bout of exercise, in a fed state. For the determination of irisin immediately after exercise, blood was collected from the saphenous vein immediately after running for 1h at 70-85% VO_2 max for exercise trained animals, and after exposure to the treadmill for 1h at 2m/min for sedentary animals. Irisin was determined using the ELISA Kit from Pheonix Pharmaceuticals Inc.

5.8. Palmitate oxidation – After extraction, samples of soleus (Sol) and extensor digitorum longus (EDL) muscles (~100 mg), and iBAT and aBAT (~100 mg), and SC Ing fat (~300 mg) were thoroughly minced in ice cold SETH buffer (300 mM sucrose, 2 mM EDTA, and 10 mM Tris-HCL, pH 7.4). The solution was then homogenized in an ice-cold Potter-Elvehjen glass homogenizer and 400 μl of the tissue homogenate was transferred to plastic scintillation vials containing 1.6ml reaction mixture (150mM sucrose, 5mM $MgCl_2$, 30mM kcl, 30mM potassium phosphate buffer, 2mM EDTA, 2mM ADP, 15mM Tris-HCl, 1% BSA, 0.75mM palmitate, 1mM carnitine,.25mM CoA, pH7.4) containing 0.2 μCi/ml [1-^{14}C] palmitic acid. Cold and ^{14}C-labeled palmitate were complexed with fatty-acid free bovine serum albumin (BSA) before being added

to the reaction mixture. Within the plastic scintillation vial, an isolated eppendorf tube containing a loosely folded filter paper was moistened with 2-phenylethylamine/methanol (1:1 vol) to collect $^{14}CO_2$. After 1 hour of incubation at 37°C, the media was acidified with 200 μl of sulphuric acid (5N) to release $^{14}CO_2$. Scintillation vials remained sealed for another hour of incubation. Subsequently, the filter papers were transferred to scintillation vials for radioactivity counting of ^{14}C. Rates of palmitate oxidation were measured by the production of $^{14}CO_2$ from the [1-^{14}C] palmitic acid.

5.9. Adipose tissue morphology – Upon extraction of each fat pad, small samples (~50-100 mg) of each fat depot was removed for microscopy. Within Sc Ing WAT, two samples were collected; one from the upper portion of the tissue, and another from the middle portion of the tissue with a visible brown appearance. Samples were fixed in 4% paraformaldehyde, 0.1 M phosphate buffer solution (pH 7.4) and stored at room temperature for 24 hours. Tissues were then washed and stored in 70% ethanol and subsequently sent to the Toronto Centre for Phenogenomics for sectioning and hemotoxylin and eosin (H&E) staining. In order to prevent biased selection of cells and cell measurement for the determination of average adipocyte area, two independent investigators measured 3 randomly selected fields of view of 150 cells for each animal.

5.10. Western blot analysis – Upon extraction, adipose tissues were immediately snap frozen in liquid nitrogen and homogenized in lysis buffer [25 mM Tris-HCl, 25 mM NaCl, 1 mM $MgCl_2$, 2.7 KCl, 1% Nonidet P-40, and protease (cOmplete ULTRA tablets) and phosphatise (PhosStop) inhibitors (pH 7.4)]. Homogenates were centrifuged for 10min at 16,000 rpm at 4°C and the infranatant was collected. An aliquot of each sample was used to determine protein concentration using the Bradford method. Samples were diluted 1:1 with Laemmeli sample buffer [62.5mM Tris-HCl, pH 6.8; 2% (wt/vol) sodium dodecyl sulfate; 50mM DTT; 0.01% (wt/vol) bromophenol blue] and heated at 95°C for 5 min before loading onto sodium dodecyl sulfate-polyacrylamide gel (SDS-PAGE), and then transferred to polyvinyl difluoride (PVDF) membranes (Bio-Rad Laboratories). Aliquots of cell lysates containing 10-50μg of protein were used to determine the content of UCP-1 (33kDA), PGC-1α (113kDA), total AMPK, phospho-AMPK $_{Thr172}$ (62kDA), ATGL (54kDA), GAPDH (36kDA), FNDC5 (22kDA) and β-actin (45kDA). Blots were scanned and the density was determined using the ImageJ Program. The values (expressed as arbitrary units) were obtained by dividing the density of the band of interest by either β-actin or GAPDH from the same blot (as indicated by figure legends). Similarily, P-AMPK was normalized by total AMPK.

5.11. Statistical analyses – Graph Pad Prism 5 was used for all statistical analyses. The significance of differences between two groups was determined by a two-tailed Student's t-test, and by one-way or two-way ANOVA for multiple comparisons. A Bonferroni post-hoc test was used when differences were identified.

6. RESULTS

6.1. Effects of endurance training and high-fat diet on body mass, LBM, and adiposity – Body mass of Ex LF and Ex HF rats was ~12% lower than Sed LF and Sed HF controls (Table 2). LBM of Ex LF and Ex HF rats were also reduced by ~7% in comparison to Sed LF and Sed HF animals (Table 2). In Ex LF and Ex HF animals, the masses of Epid, SC Ing, and Retro fat pads were significantly reduced by 33% and 30%, 40% and 26% and by 42% and 37% respectively, when compared to Sed LF and Sed HF controls (Table 2). As expected, HF feeding significantly increased adiposity in all three fat pad masses by 1.73-. 1.3- and 1.86- times in Sed HF animals when compared to Sed LF controls (Table 2.) Endurance training prevented this increase in adiposity induced by HF feeding. Epid, Sc Ing, and Retro fat pads of the Ex HF animals were similar to Sed LF controls (Table 2).

	Sed LF	Ex LF	Sed HF	Ex HF
Body mass (g)	481.50 ± 8.54	428.43 ± 10.29[a]	524.20 ± 8.77	464.89 ± 9.73[a]
Fat pad mass (g)				
Epid	8.16 ± 0.55	5.49 ± 0.36[b]	14.09 ± 0.77[c]	9.83 ± 0.93[d]
SC Ing	11.41 ± 0.67	6.79 ± 0.32[b]	14.89 ± 0.87[c]	11.00 ± 0.85[d]
Retro	6.78 ± 0.78	3.94 ± 0.23[b]	12.61 ± 0.85[c]	7.95 ± 0.78[d]
LBM (g)	294.30 ± 6.14	271.60 ± 5.22[a]	295.20 ± 4.2	273.80 ± 5.6[a]

[a] $p < 0.05$ is *versus* Sed LF and Sed HF.
[b] $p < 0.05$ is *versus* Sed LF, Sed HF, and Ex HF.
[c] $p < 0.05$ is *versus* Sed LF, Ex LF, and Ex HF.
[d] $p < 0.05$ is *versus* Ex LF and Sed HF. Two-way ANOVA is $n = 18$.

Table 2. Effects of chronic endurance exercise training and high-fat diet on body mass, adiposity, and LBM. Measured at the end of the study.

6.2. iBAT mass and assessment of unilocular droplet area – iBAT mass significantly increased with HF feeding (1.84-fold) when comparing Sed HF animals to Sed LF animals (Figure 7A and C). Chronic endurance exercise reduced iBAT mass by 39% and 26% when comparing Sed LF to Ex LF, and Sed HF and Ex HF animals, respectively (Figure 7A and C). Microscopic analysis revealed that iBAT extracted from Sed LF and Sed HF animals displayed typical multilocular brown adipocytes, while Ex LF and Ex HF animals displayed larger unilocular lipid droplets resembling adipocytes normally found in white adipose tissue (Figure 7B). In fact, unilocular adipocyte area was 3-fold higher in iBAT taken from an Ex LF animal than a Sed LF animal, and 1.84-fold higher in Ex HF than Sed HF animals (Figure 7D).

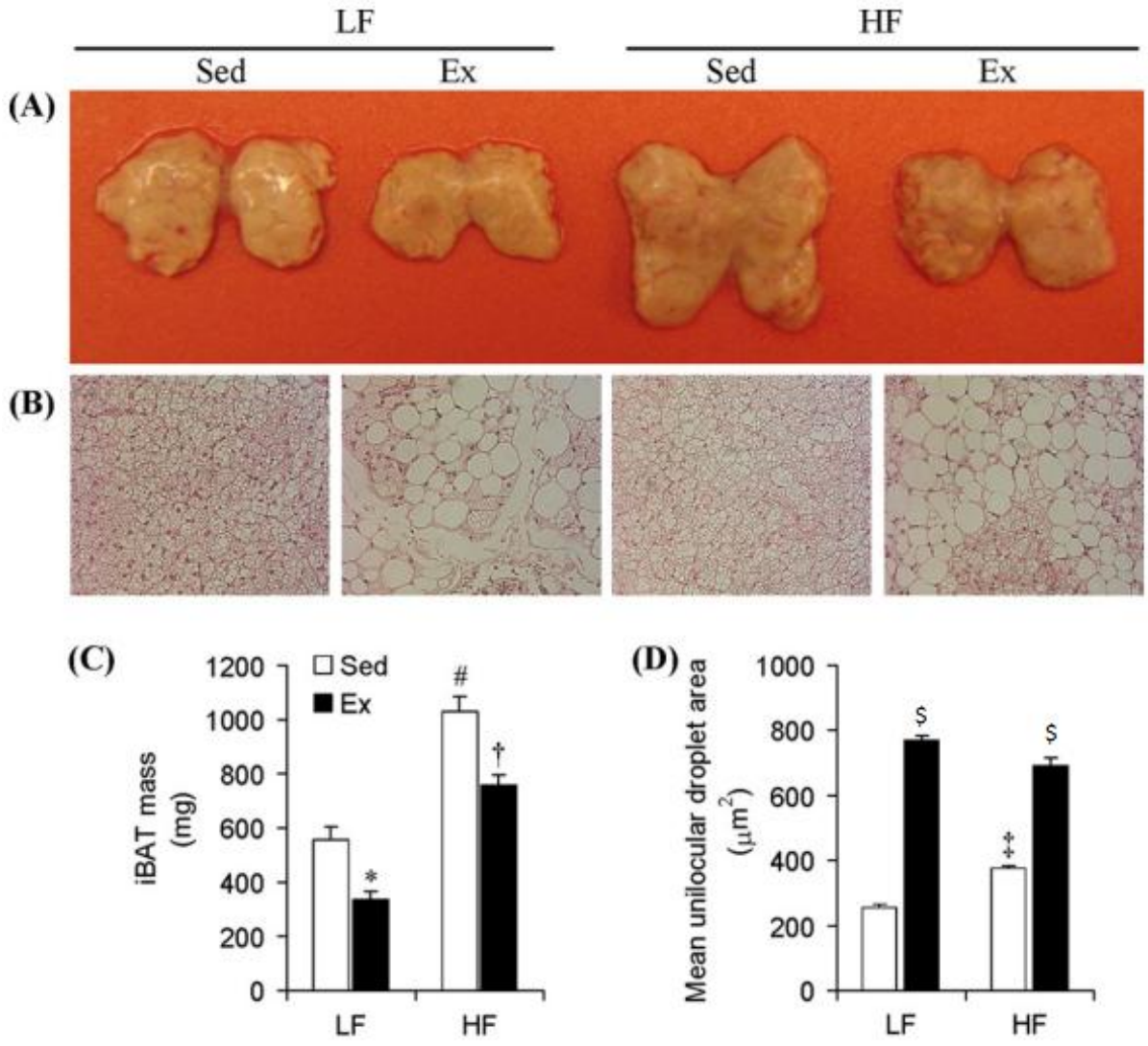

Figure 7. Chronic endurance training and high-fat (HF) diet exert antagonistic effects on mass and unilocular lipid content in the interscapular brown adipose tissue (iBAT). (A) iBATs dissected from sedentary (Sed) or endurance exercise trained (Ex) rats, fed either a low-fat (LF) or HF diet. (B) Microscopic images (20x magnification) of H&E staining of iBAT samples. (C) Average iBAT mass and (D) unilocular adipocyte area of all four groups. *$p<0.05$ vs. Sed LF; # $p<0.05$ vs. Sed LF, Ex LF, Ex HF; † $p<0.05$ vs. Ex LF; \$$p<0.05$ vs. Sed LF, Sed HF; ‡ $p<0.05$ vs. all other conditions. Two-way ANOVA (n=8).

6.3. PGC-1α and UCP-1 content and palmitate oxidation in iBAT and aBAT – PGC-1α and UCP-1 contents of iBAT and aBAT were increased by 3.5-fold and 2.55-fold, and by 3.38-fold and 2.21-fold when compared to Sed LF rats, respectively (Figure 8A-F). Conversely, animals in the Ex LF group revealed a reduction in PGC-1α and UCP-1 content by 69% and 63% and by 79% and 45%, respectively, when compared to Sed LF animals. Importantly, chronic endurance exercise completely attenuated the HF-diet induced effect of increased PGC-1α and UCP-1 in iBAT and aBAT (Figure 8A-F). A similar trend was found in palmitate oxidation of iBAT and aBAT. Palmitate oxidation decreased by 65% and 72%, and by 45% and 51% in iBAT and aBAT, respectively, when comparing Ex LF and Ex HF animals to Sed LF and Sed LF animals and increased in iBAT (2-fold) and aBAT (2.5-fold) of Sed HF rats when compared to Sed LF controls (Figure 8G and H). These results indicate that chronic endurance exercise reduces, and HF feeding increases thermogenic capacity of iBAT and aBAT.

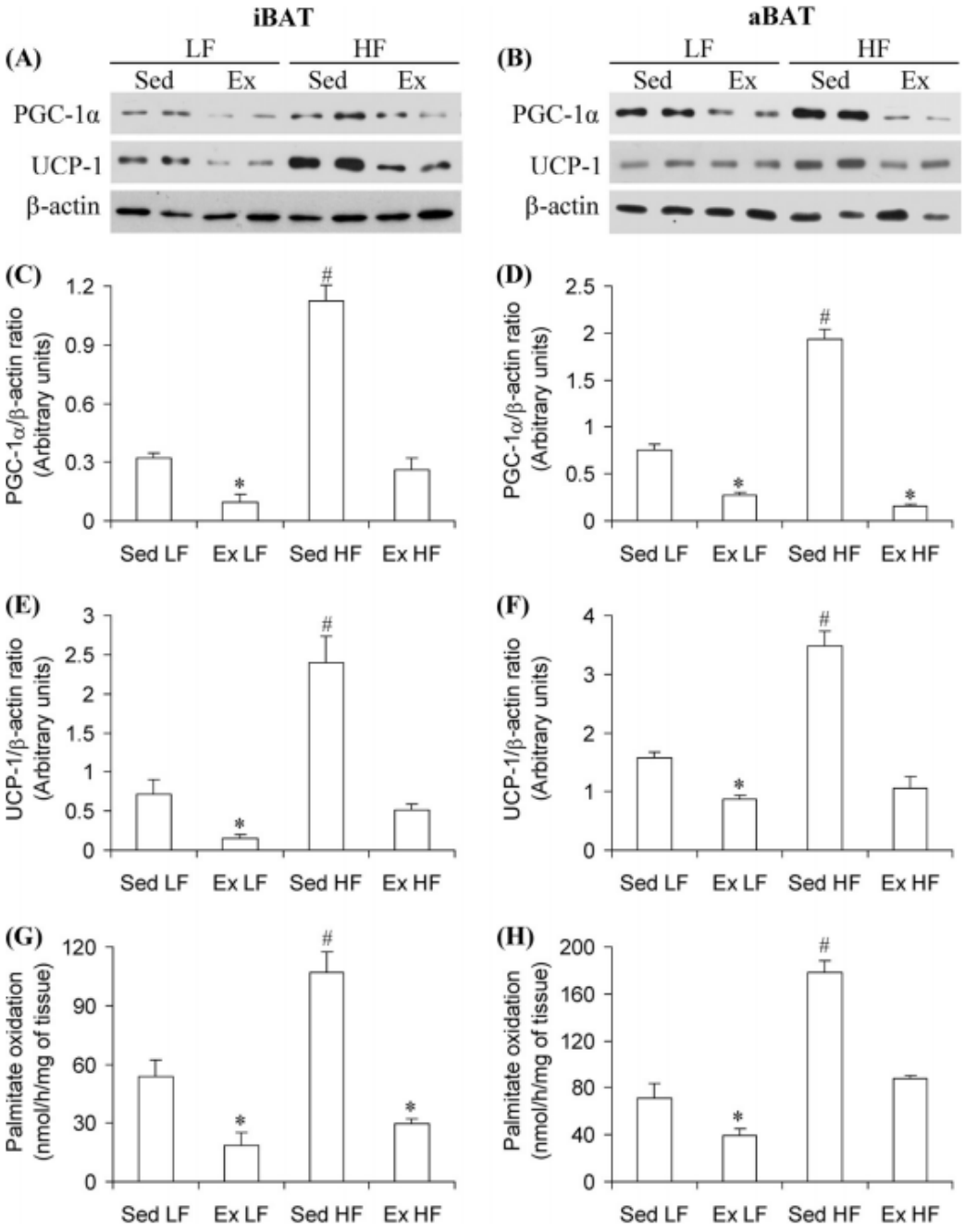

Figure 8. Interscapular and aortic brown adipose tissue (iBAT and aBAT, respectively) were extracted from sedentary (Sed) or endurance-trained (Ex) rats fed either a low-fat (LF) or high-fat (HF) diet. Ex and HF diet increases PGC-1α and UCP-1 content, as well as palmitate oxidation in iBAT and aBAT. Representative blots (A, B) and densitometric analysis of PGC-1α (C, D), UCP-1 (E,F) contents, and palmitate oxidation (G, H) in iBAT and aBAT. β-actin was used as loading control for all western blot experiments. *$p<0.05$ vs. Sed LF; # $p<0.05$ vs. all other conditions. One-way ANOVA (n=8).

6.4. Morphological analysis and mean adipocyte area of the Sc Ing fat depot – Upon visual analysis of the Sc Ing fat depot, the middle region of the tissue was browner in animals exposed to chronic endurance exercise than sedentary animals, although the upper extremity of the tissue remained white (Figure 9A and B, G and H). Samples of the upper and middle regions of the tissue were used for H&E staining, as indicated by the black circles (Figure 9A and B, G and H). It was found that the middle and upper regions of the Sc Ing fat from Sed LF (Figure 9C and D) and Sed HF Figure 9I and J) rats contained unilocular adipocytes, typical of WAT. The upper extremities of the Ex LF (Figure 9E) and Ex HF (Figure 9K) animals also contained typical white adipocytes, but interestingly, the middle region of the SC Ing fat depot taken from an Ex LF (Figure 9F) and the Ex HF (Figure 9L) animal showed the appearance of multilocular adipocytes, typical of what is seen in BAT. Furthermore, when comparing the middle regions of the SC Ing fat depot between Ex LF and Ex HF animals, the former contained a much larger area occupied by multilocular brown adipocytes (Figure 9F and L). These findings suggest that chronic endurance exercise induced the browning of SC Ing fat, and HF feeding attenuated this effect. It is also to be noted that the mean adipocyte area taken from the upper extremity of the SC Ing fat depot was significantly higher in the Sed HF animal than all other conditions (Figure 10A). Intriguingly, this robust increase in mean adipocyte area of Sed HF animals was not seen in the middle region of the Sc Ing fat (Figure 10B). Additionally, the mean adipocyte area in the middle region of the fat depot was also reduced by 30% in Ex LF rats and by 36% in Ex HF rats when compared to their SED LF and SED HF controls (Figure 10B). These findings suggest that the adipocytes located in the middle region of the Sc Ing fat pad are not only capable of inducing a brown-like phenotype, but are also resistant to HF feeding induced hypertrophy.

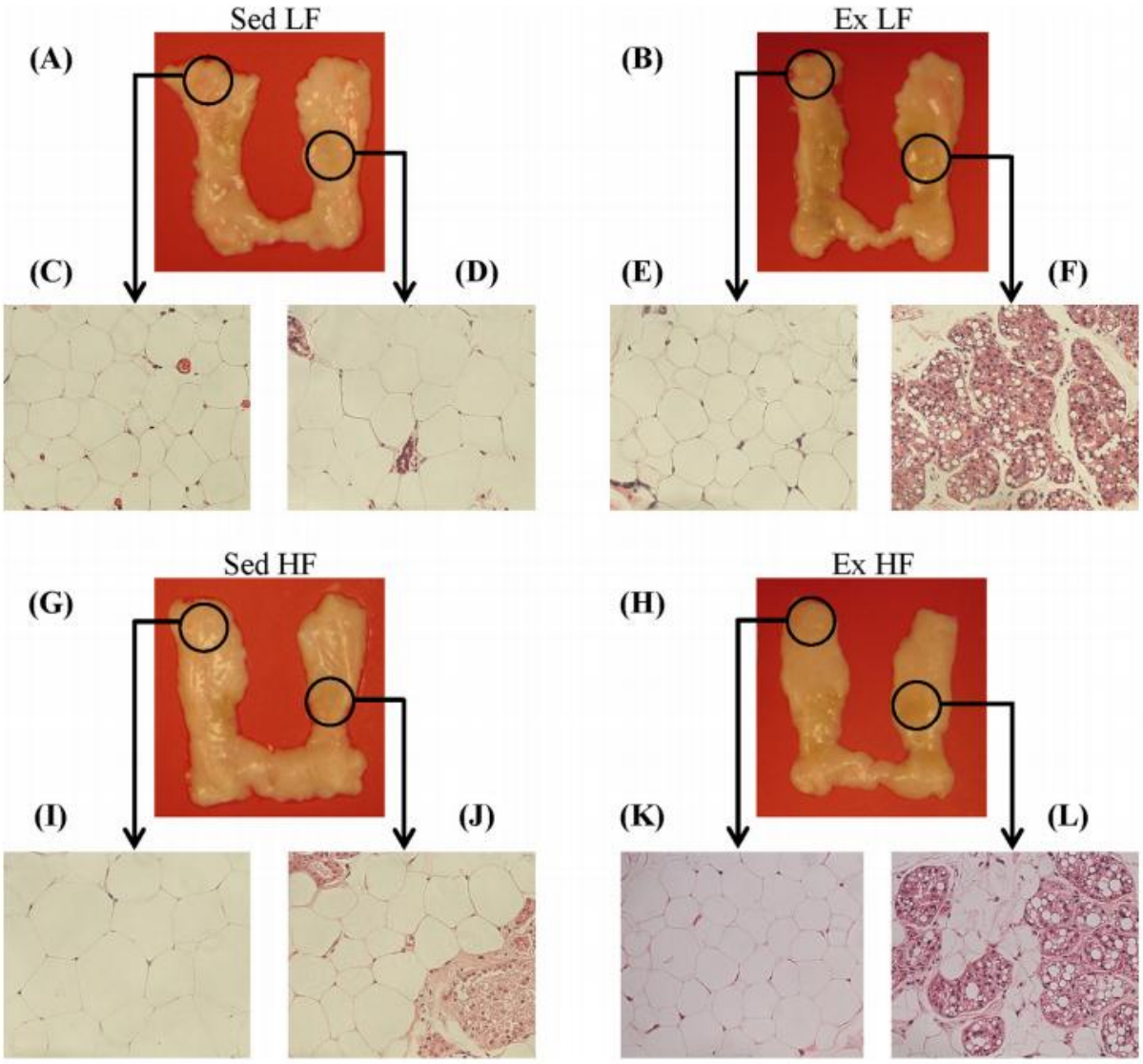

Figure 9. Chronic endurance training induces browning and the presence of multilocular adipocytes in the subcutaneous inguinal (SC Ing) fat depot of low-fat (LF) and high-fat (HF)-fed rats. Left and right SC Ing fat depots taken from sedentary (Sed) and endurance trained (Ex) rats fed either a LF (A, B) or HF (G, H) diet for 8 weeks. Samples from the upper extremity and middle region of the SC Ing fat depots, as indicated by the black circles, were used for H&E staining and microscopy analysis. Representative images (20x magnification) of adipocytes from Sed (C, D) and Ex (E, F) rats fed a LF diet and Sed (I, J) and Ex (K, L) rats fed a HF diet are shown.

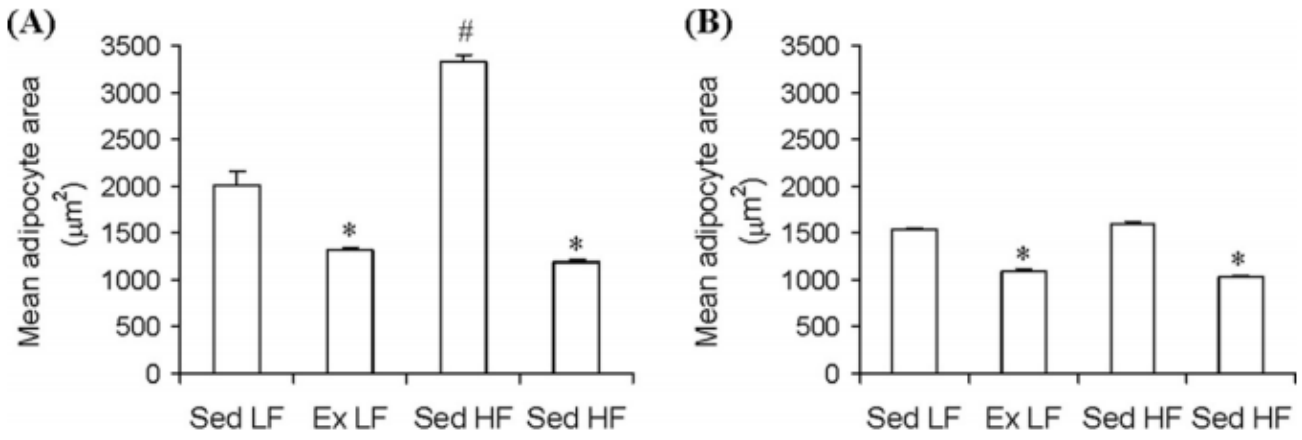

Figure 10. Chronic endurance training reduces mean adipocyte area in the upper (A) and middle (B) region of the subcutaneous inguinal (SC Ing) fat depot. High-fat (HF) feeding increases mean adipocyte area only in the upper region. Samples of the upper and middle regions of the SC Ing fat depot (as indicated in Figure 3) were taken from sedentary (Sed) or endurance trained (Ex) rats fed either a low-fat (LF) or high-fat (HF) diet. *$p<0.05$ vs. Sed LF; # $p<0.05$ vs. all other conditions. One-way ANOVA (n=8).

6.5. PGC-1α, UCP-1, and ATGL content, AMPK phosphorylation, and palmitate oxidation in the Sc Ing fat depot – In order to determine whether or not the middle region of the Sc Ing fat depot actually contained functional brown adipocytes, important proteins involved in thermogenesis and oxidative capacity of the tissue was measured. PGC-1α, UCP-1, and ATGL content, and AMPK phosphorylation were increased in Ex LF animals by 9.1-fold (Figure 11A and B), 6.13-fold (Figure 11A and C), 4.84-fold (Figure 11D and E), and 3.8-fold (Figure 11F and G), respectively, when compared to Sed LF animals. PGC-1α, UCP-1, and ATGL content, and AMPK phosphorylation also increased in Ex HF animals when compared to Sed LF controls, but to a much lesser extent than what was seen in Ex LF animals (Figure 11A-H). In Sed HF rats, PGC-1α was down-regulated by 78% and UCP-1 was almost undetectable. No alterations were

observed for ATGL content or AMPK phosphorylation in Sed HF rats when compared to Sed LF controls. These findings are compatible with palmitate oxidation results in which oxidative capacity of Ex LF animals was 3.35-fold higher than Sed LF controls, and no significant alterations were apparent between Sed HF rats and Sed LF animals. Taken together, these findings indicate that chronic endurance exercise induced the browning of Sc Ing fat and the appearance of these brown-like adipocytes was accompanied by functional thermogenic adaptive responses. Conversely, HF feeding attenuated these effects.

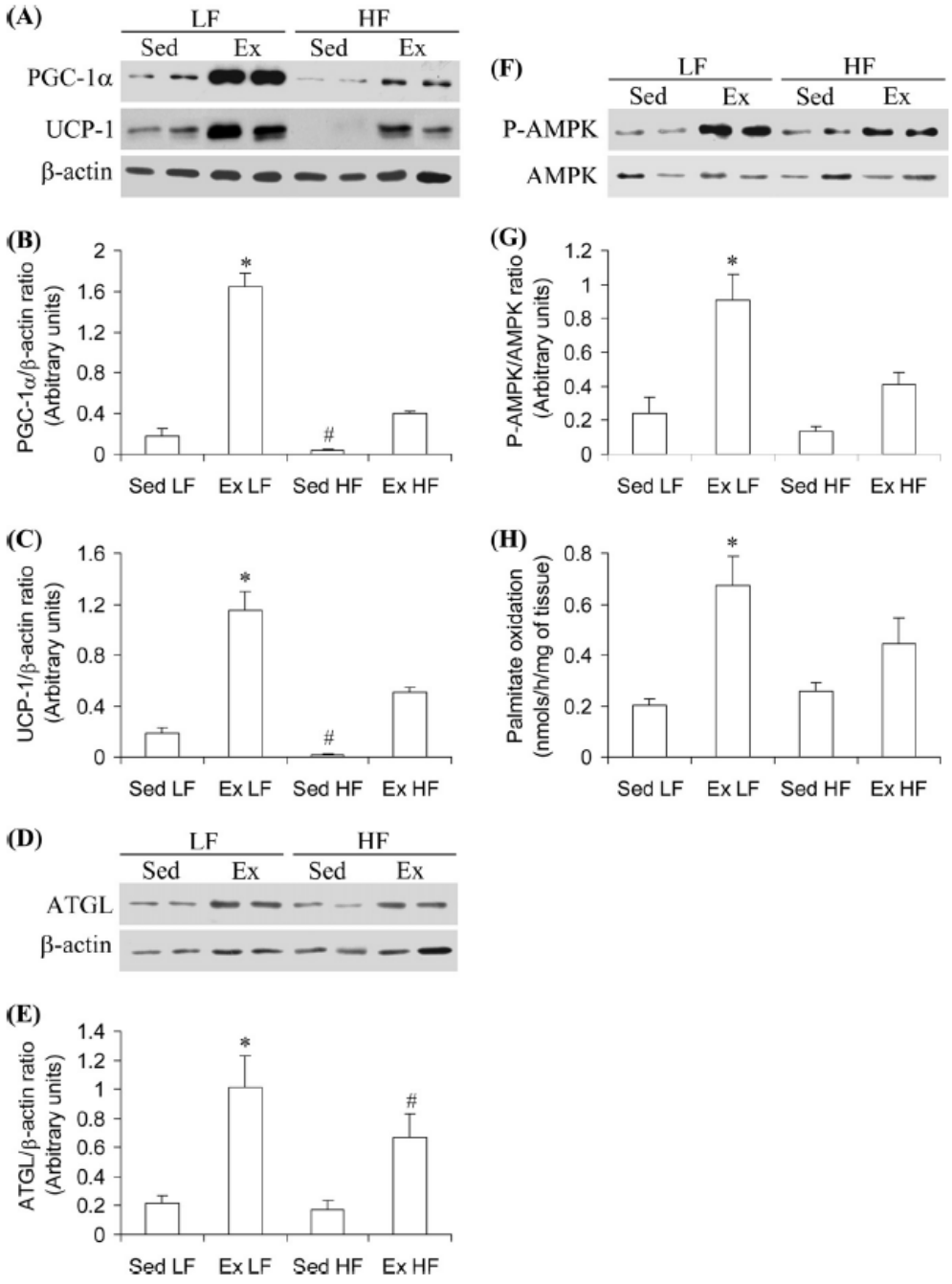

Figure 11. The middle region of subcutaneous inguinal (SC Ing) fat was extracted from sedentary (Sed) or endurance trained (Ex) rats fed either a low-fat (LF) or high-fat (HF) diet. Chronic endurance training and high-fat (HF) diet reduces PGC-1α (A,B), UCP-1 (A,C), and ATGL (D,E), contents, as well as AMPK phosphorylation (F,G), and palmitate oxidation (H) of the SC Ing fat depot. β-actin was used as loading control for all western blot experiments. *$p<0.05$ vs. Sed LF; # $p<0.05$ vs. all other conditions. One-way ANOVA (n=8).

6.6. UCP-1 content in visceral fat depots – We also wanted to test whether exercise also induced the browning of visceral fat depots. Upon visual inspection, there was no browning that occurred in neither Epid, nor Retro fat pads. We also we measured UCP-1 content in both fat pads (Figure 12). UCP-1 was not detected under any of the experimental conditions indicating that Sc Ing fat was the only WAT depot that underwent browning under chronic endurance exercise conditions.

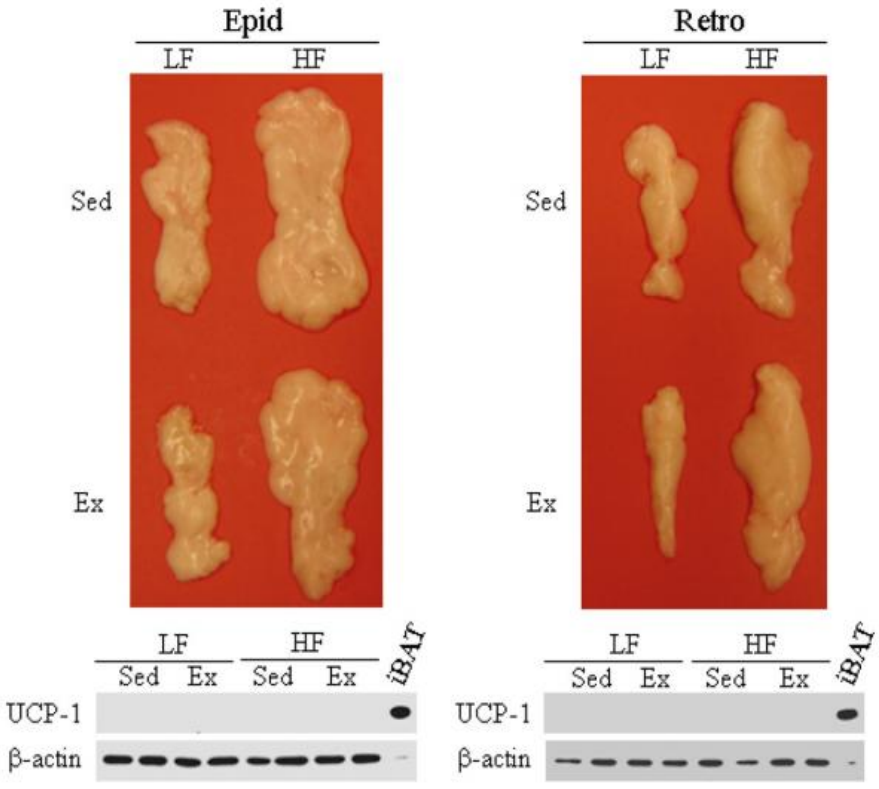

Figure 12. Neither endurance exercise (Ex) nor high-fat (HF) diet affected UCP-1 content in both the epididymal (Epid) and retroperitoneal (Retro) fat depots. The Epid and Retro fat pads were extracted sedentary (Sed) or Ex rats fed either a low-fat (LF) or HF diet. β-actin was used as loading control for all western blot experiments. A sample of interscapular brown adipose tissue (iBAT) containing 10μg of protein was used as a positive control for UCP-1. Samples of Epid and Retro fat pads contained 50μg of protein.

6.7. PGC-1α and FNDC5 content and palmitate oxidation in soleus muscles – PGC-1α content increased by 2.5-, 3.45-, and 3.58- fold in soleus muscles from Ex LF, Sed HF, and Ex HF rats when compared to Sed LF rats (Figure 13A and B). No significant differences were found in FNDC5 content in soleus muscles across all experimental conditions (Figure 13A and C). Palmitate oxidation results showed a 2.4-, 2.1-, 2.45- fold increase in Ex LF, Sed HF, and Ex HF rats respectively, when compared to Sed LF rats (Figure 13D). Similar findings for PGC-1α, FNDC5, and palmitate oxidation were found for EDL muscles (data not shown). Together, these findings indicated that chronic endurance exercise caused a robust training effect in skeletal muscle; however, it did not affect FNDC5 content in these tissues.

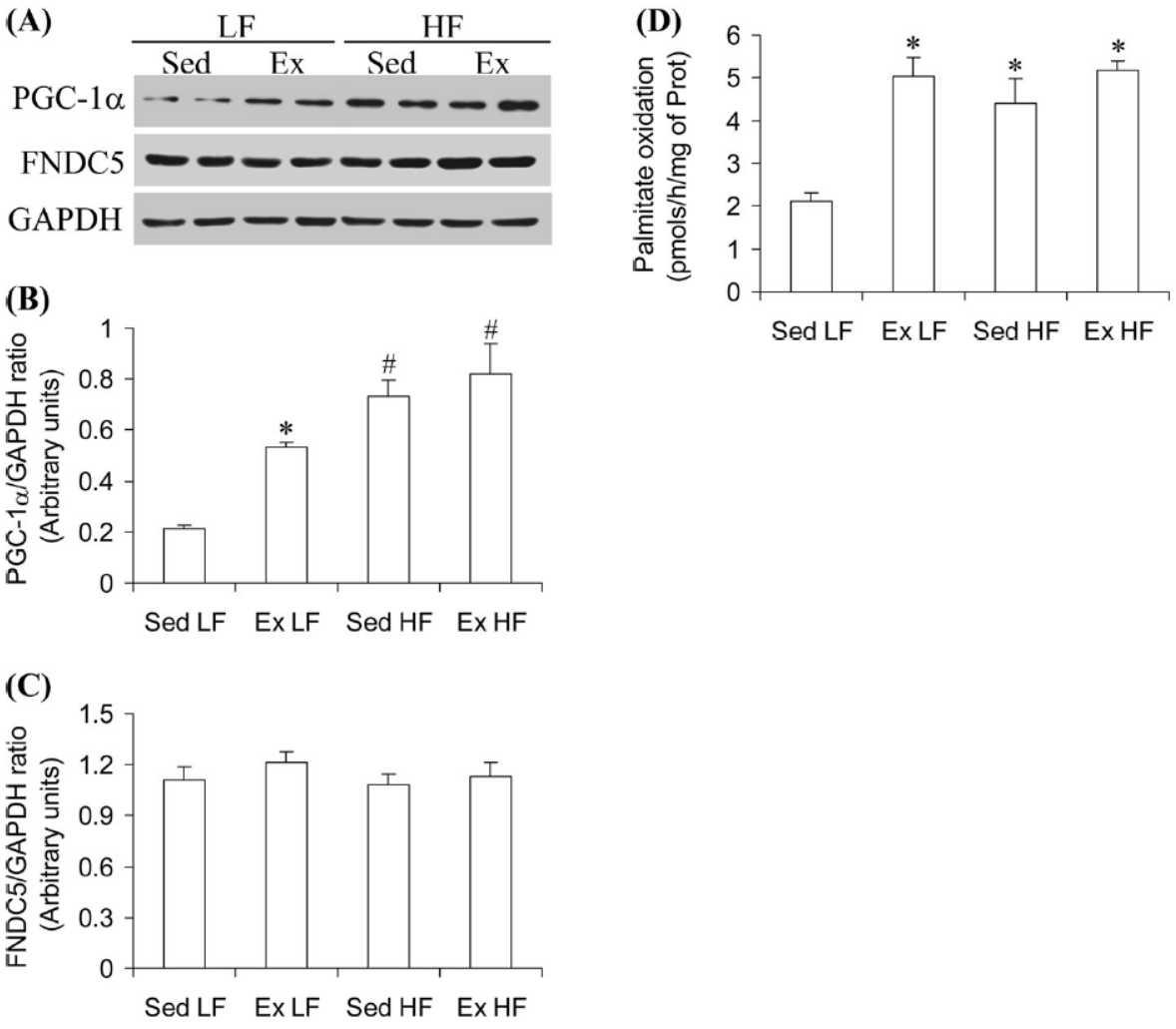

Figure 13. Soleus muscles extracted from sedentary (Sed) or 8-week endurance-trained (Ex) rats fed either a high-fat (HF) or low-fat (LF) diet were assayed for PGC-1α content (A and B), FNDC5 content (A, C), as well as palmitate oxidation (D). GAPDH was used as loading control. *$p<0.05$ vs. Sed LF; # $p<0.05$ vs. all other conditions. One-way ANOVA (n=8).

6.8. Circulating irisin and FNDC5 content in Sc Ing fat – Circulating irisin levels did not differ among the four experimental groups under resting conditions at week 8 (Figure 14A), nor immediately after exercise at week 6 (Figure 14B). Following the 8 week chronic endurance exercise and HF diet protocol, animals fed a HF diet seemed to have lower levels of circulating

irisin when compared to those on a LF diet. However, these values did not reach statistical significance. FNDC5 content of Sc Ing fat from Ex LF animals significantly increased, while the content in Sed HF animals was markedly reduced (Figure 14C and D). Exercise seemed to attenuate the affect of HF diet and raised FNDC5 content of Ex HF animals to levels similar to the SED LF controls (Figure 14C and D).

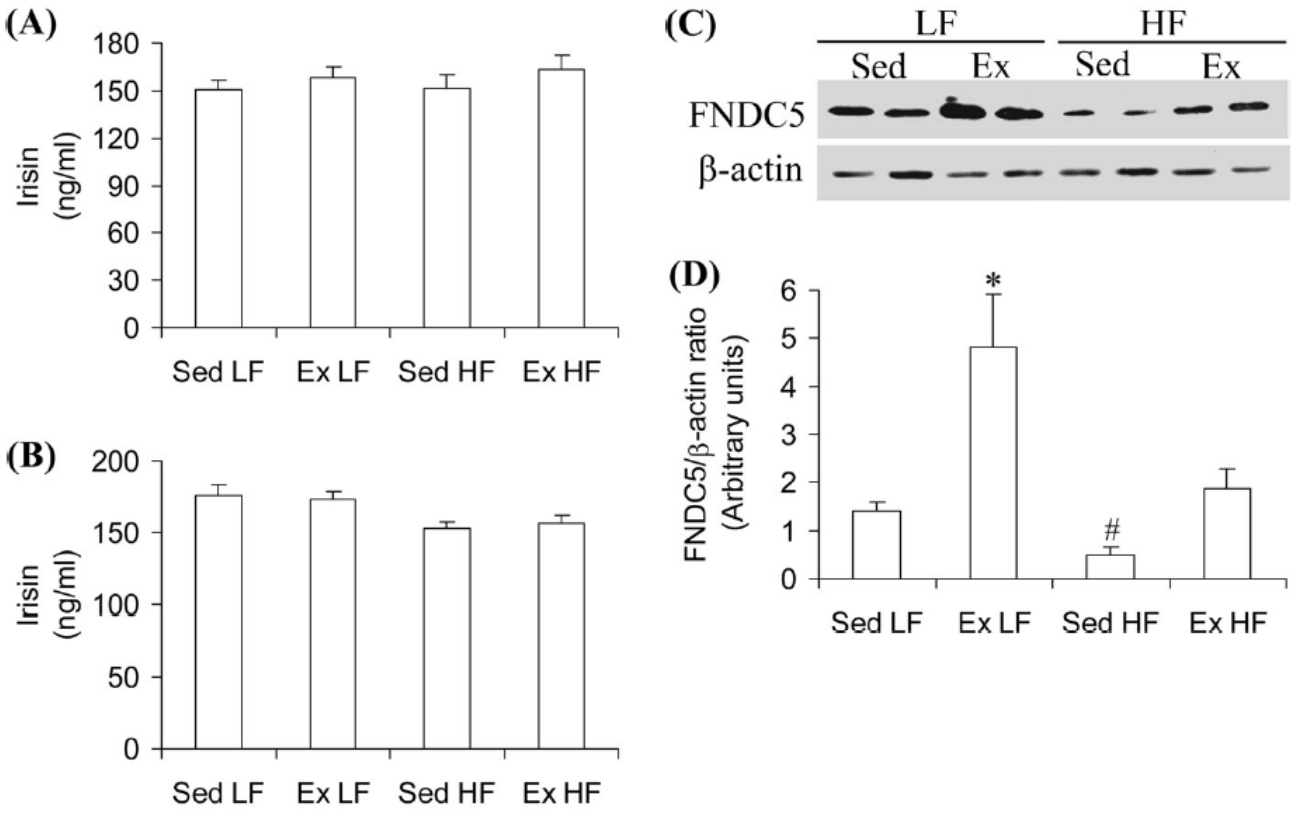

Figure 14. Serum irisin levels measured under resting conditions 24h after the last bout of exercise at week 8 (A), and immediately after exercise at week 6 (B). Chronic endurance exercise increases FNDC5 content in subcutaneous inguinal (SC Ing) fat (C and D). The middle region of the SC Ing fat depot was used for the determination of FNDC5 content. β-actin was used as loading control. *$p<0.05$ vs. Sed LF; # $p<0.05$ vs. all other conditions. One-way ANOVA (n=8).

6.9. 24-hr ambulatory activity and energy expenditure – There were no significant differences in ambulatory activity and energy expenditure across all four groups during the light cycle (Figure 15A-D) However, there was a significant decrease (23%, 29%, and 35%) in ambulatory activity of Sed HF animals when compared to Sed LF, Ex LF, and Ex HF animals, respectively, during the dark cycle (Figure 15A and B). In addition, energy expenditure analysis revealed a

significant increase of 14.2% in Ex LF rats, and 17.8% in Ex HF rats when compared to Sed LF animals during the dark cycle (Figure 15C and D). The increase in energy expenditure of Ex LF and Ex HF animals is not due to alterations in ambulatory activity as this variable was not changed during the dark cycle.

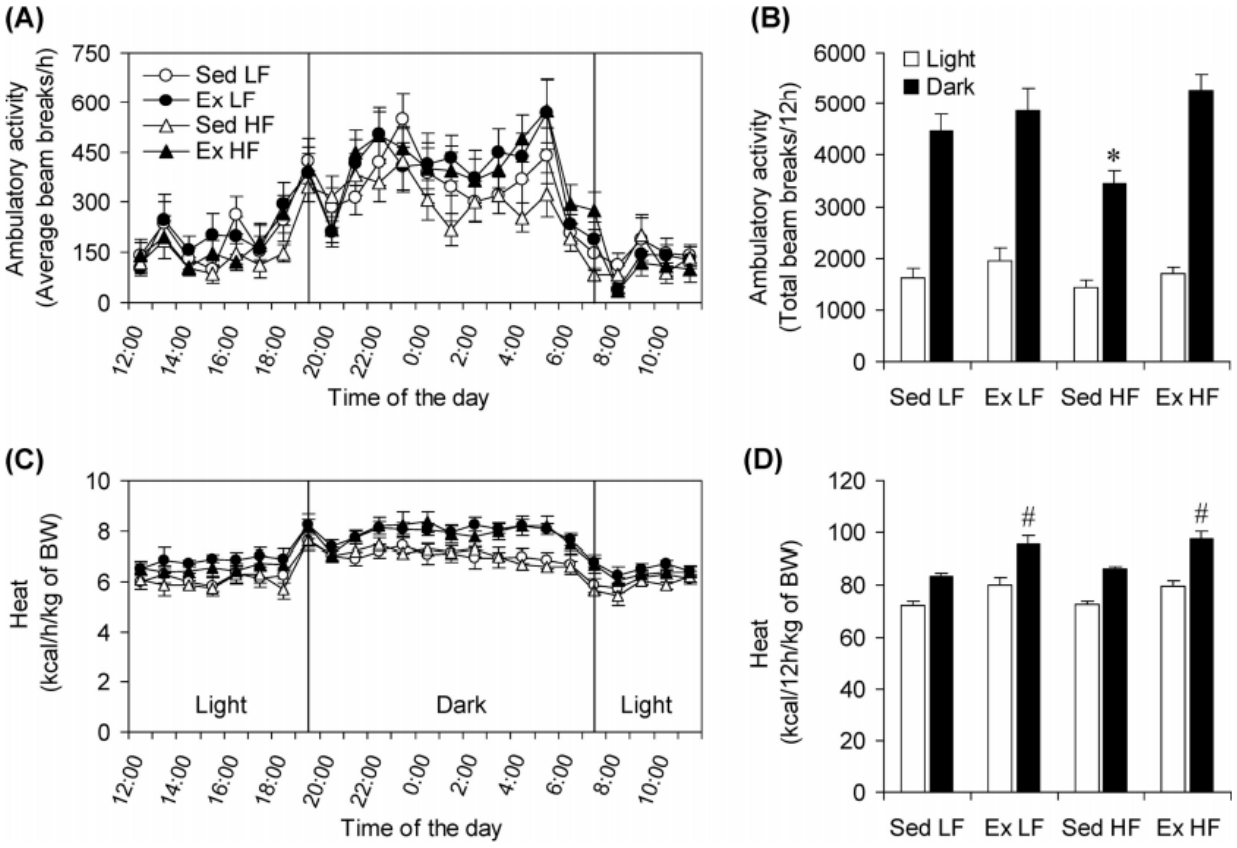

Figure 15. Effects of chronic endurance training (Ex) and high-fat (HF) diet on spontaneous physical activity and whole-body energy expenditure. 24 hour measurement of ambulatory activity (A, B) and energy expenditure (C, D) at the end of the 8 week endurance exercise protocol. The rats were allowed to rest for 24hrs prior to being placed in the Comprehensive Laboratory Animal Monitoring System (CLAMS) from Columbus instruments. *$p<0.05$ vs. Sed LF; # $p<0.05$ vs. all other conditions. Two-way ANOVA (n=8).

7. DISCUSSION

The findings of this study revealed that thermogenesis is antagonistically regulated under conditions of chronic endurance exercise and HF feeding in classical BAT and SC Ing WAT which is important for the regulation of whole-body energy expenditure. Energy surplus through a HF diet increased the mass, PGC-1α and UCP-1 contents and palmitate oxidation in iBAT and aBAT, while in Ex LF animals, these variables were markedly reduced. These results are compatible with our findings that endurance training caused an accumulation of unilocular adipocytes in iBAT and aBAT, indicating reduced thermogenic capacity in these tissues. Conversely, the middle portion of the Sc Ing fat depot of Ex LF animals displayed higher levels of PGC-1α, UCP-1, and ATGL content, along with increased AMPK phosphorylation and palmitate oxidation, and HF feeding attenuated these effects. These molecular changes in combination with the observed presence of UCP-1-positive multilocular adipocytes in the Sc Ing tissue of Ex LF animals indicated an increased thermogenic capacity. These findings are in agreement with previous studies in which exercise induced the browning of WAT[11,92]. In addition, the middle region of the Sc Ing fat depot was more responsive to browning induced by exercise than the upper region. In fact, the middle region of the Sc Ing tissue displayed an increase in multilocular adipocytes, UCP-1 content, and rate of oxidation when exposed to chronic endurance training. These observations were not found at the proximal or distal extremities of this fat depot. Furthermore, the mean adipocyte area in the extremities of the Sc Ing fat increased in Sed HF animals, whereas the middle region of the fat depot remained unchanged. This indicates that the middle portion of the Sc Ing fat is not only capable of browning induced by exercise, but it is

also resistant to adipocyte hypertrophy induced by HF feeding. These results are compatible with the site-specific differences in thermogenic capacity we found in the Sc Ing fat depot in rats. Previous studies in mice have reported major depot- and strain-specific differences in UCP-1 expression, indicating that the Sc Ing fat depot is more prone to acquiring a brown-like phenotype than visceral fat depots [10,11,81,86]. In this study, we demonstrated that exercise-induced browning of WAT in rats is also depot-specific, since we found an increased UCP-1 content and the presence of multilocular adipocytes in Sc Ing WAT but not in Epid or Retro WAT in response to exercise.

Previous studies have shown that moderate to high intensity endurance training increases SNS activity and circulating catecholamines[7] and importantly, BAT activity is strongly stimulated by catecholamines [8,93]. In our study, VO_2 max tests were conducted every two weeks and training intensity for endurance exercise animals was kept at a constant 70-85% throughout the study, so circulating catecholamines were expected to increase during exercise. Despite of this, thermogenic capacity of BAT and WAT were antagonistically regulated. Chronic heat exposure from exercise seemed to override the catecholamine-induced BAT activity normally observed in centrally located fat depots by decreasing thermogenic capacity of iBAT and aBAT, but not in peripheral body regions such as the Sc Ing fat depot. It is unclear whether these antagonistic effects are due to a different distribution of α- and β-adrenergic receptors and catecholamine response, or by other exercise-induced factors independent of catecholamines.

In this context, previous studies have suggested that exercise induces the browning of Sc Ing WAT by stimulating the release of a PGC-1α-dependent myokine called irisin. Irisin has been proposed to derive from the cleavage of the FNDC5 receptor under exercising conditions and results in the browning and increased UCP1 expression in subcutaneous adipose tissue[11] . In order to assess whether circulating irisin could mediate the exercise-induced browning effect found in this study, we measured circulating irisin levels and FNDC5 content. We found that chronic endurance exercise and HF diet both caused robust increases in PGC-1α content and palmitate oxidation in Sol and EDL muscles. However, we did not detect any significant alterations in FNDC5 content. Furthermore, circulating irisin levels under resting conditions were unaffected by endurance exercise and HF feeding. It is possible that irisin increased transiently after exercise and values obtained under resting conditions may have missed such an effect. Therefore, we also measured circulating irisin levels immediately after exercise at week 6 of the study. We found no significant differences across all four groups of animals. Our findings are compatible with other studies reporting lack of muscle FNDC5 and irisin release after exercise [87,94]. It has also been reported that FNDC5 and irisin can be released by adipocytes [89], therefore, we also measured FNDC5 content within the Sc Ing fat depot. Similar to PGC-1α and UCP-1 content, chronic endurance exercise significantly increased FNDC5 content, while HF diet markedly reduced it. These findings suggest that locally produced FNDC5 in the adipose tissue rather than circulating irisin could have mediated the browning effect seen in the Sc Ing fat depot following exposure to chronic endurance exercise.

Exercise is thermogenic in itself and a large amount of heat is produced as a consequence of repeated muscle contractions. Thus, a reduction in BAT activity is expected and has been demonstrated in previous studies[84]. Our findings were consistent with this since iBAT and aBAT had reduced UCP-1 content and oxidative capacity as a consequence of chronic endurance exercise. This result can be explained by the adaptive response to down-regulate thermogenesis in response to chronic exercise-induced heat production. Besides exercise and cold temperature, structural and functional alterations in BAT are also regulated by diet-induced thermogenesis (DIT) [47,95,96]. In mice, UCP-1 ablation eliminated DIT and the animals developed obesity when living at thermoneutrality [50]. In addition, it has been reported that glucose uptake in BAT increases after a meal in humans [65]. These studies indicate the role of BAT in reducing metabolic efficiency and increasing energy expenditure. In our study, the increased thermogenic capacity of iBAT and aBAT in sedentary animals exposed to HF diet is also compatible with the adaptive response of increased DIT under conditions of energy surplus.

Regular exercise is often prescribed to facilitate and maintain weight loss[2,97]. This study confirms that chronic endurance exercise reduces body weight through a reduction in adiposity and LBM. In the final week of training, ambulatory activity and EE were measured. There were no significant alterations in spontaneous ambulatory activity, yet energy expenditure of Ex LF and Ex HF animals was 14.2% and 16.8% higher, respectively, when compared to Sed LF controls during the dark cycle. Despite having a decreased iBAT and aBAT thermogenic capacity, the resting EE of endurance trained animals was significantly higher than controls. It appears

that the browning of Sc Ing fat could have contributed to this increase in EE as demonstrated by the increase in UCP-1 content and palmitate oxidation found in the endurance-exercised animals. However, it seems paraxodical for the body to facilitate the browning of Sc Ing fat and increase thermogenesis when chronic endurance exercise is already thermogenic in itself. It has been proposed that exercise-induced browning of Sc Ing fat could have evolved from shivering-related muscle contractions in response to cold stress. When shivering occurs, muscle contractions lead to the release of myokines that allow the browning of white fat, and in this context, muscle contractions due to exercise could also lead to the release of hormones that activate adipose thermogenesis[11,70]. In our study, the rats lived in thermoneutral environments and were not exposed to cold stress. Typically thermogenic tissues such as iBAT and aBAT displayed a decrease in mass, UCP-1 content, and oxidative capacity when exposed to chronic endurance exercise. Therefore, it seems unlikely that the browning of the Sc Ing fat depot occurred in order to enhance non-shivering thermogenesis and increase heat production. Instead, this response suggests a compensatory mechanism in which the body induces browning of Sc Ing fat depots to regulate whole-body energy expenditure in response to the decreased BAT mass and activity in core regions.

8. CONCLUSIONS

When comparing the thermogenic capacity of classical BAT and WAT fat depots, the effects of exercise are paradoxical. In fact, the opposite responses seen in BAT and WAT to chronic endurance exercise and HF diet prove to play a very important role in regulating whole-body energy expenditure. Our results demonstrated that the thermogenic capacity of WAT and BAT is antagonistically regulated by chronic endurance exercise and HF diet, and the alterations seen in these animals may reflect a compensatory mechanism in which the browning of Sc Ing fat occurs to allow the organism to regulate whole-body energy homeostasis in response to the decreased thermogenic capacity of BAT located in the central core area. This is characterized by a reduction in thermogenic capacity of classical BAT, accompanied by the browning of Sc Ing fat in response to chronic endurance exercise. This shift of thermogenic capacity from core regions to peripherally located tissues may allow the organism to adjust whole-body energy expenditure by activating thermogenesis when required, while simultaneously coping with the chronic heat production induced by exercise. These novel findings also raised the following question: How does the antagonistic effect of exercise on classical WAT and BAT affect whole-body energy expenditure? Our i*n vivo* findings demonstrated that there were no differences in ambulatory activity, however; the energy expenditure of exercised animals were significantly higher than the sedentary controls. Not only this, but the animals in the chronic endurance exercise groups showed smaller BAT mass and lower thermogenic capacity. Therefore, the higher energy expenditure seen in these animals could be explained by the browning of Sc Ing fat observed in animals exposed to exercise. Therefore, even though the metabolic alterations

to classical BAT and WAT in response to exercise seem paradoxical, they may be of great physiological relevance in regards to whole-body energy expenditure. Collectively, our results provide novel evidence that the browning of Sc WAT may play an important role in regulating whole-body energy expenditure and could potentially be used as a therapeutic approach to treat obesity and its related metabolic disorders.

9. FUTURE DIRECTIONS

In our study, we observed that exercise exerts an antagonistic effect on thermogenic capacity of brown and white adipose tissue. The mechanisms that lead to this paradoxical effect remain to be determined. It is well understood that lipolysis is controlled by the activation of β-receptors during exercise-induced increases in catecholamine release, and the rate of lipolysis is regulated in two ways; 1.) the variation in the regulating signal and 2.) the variation in responsiveness to the regulating signal. The density of receptors found in each adipose tissue depot vary to a great extent[20]. Obesity is associated with a decreased lipolytic effect in response to catecholamine stimulation due to alterations in adrenergic signaling pathways[21]. Our results could be conferred by similar adaptive responses that affect the distribution of α- or β-receptors and catecholamine release within each fat depot in response to exercise and HF diet. Therefore, the aim of my future studies is to determine whether chronic endurance exercise changes the distribution of adrenergic receptors or NE release in classical BAT and Sc Ing WAT.

9.1. Distribution of adrenoreceptors in different fat depots

Adrenoreceptors play a crucial role in the regulation of TG storage within adipocytes. The combination of α- and β-Ad receptors mediate the lipolytic response of adipose tissue to catecholamines. When the body requires increased energy or rate of heat production, a signal is transmitted via the SNS and NE is released from local nerve endings. NE binds to β-AdR that

are coupled to a G-stimulatory protein that activates AC which will then catalyze the conversion of ATP to cAMP. Increased cAMP levels lead to the activation of PKA which then initiates two processes; the phosphorylation and activation of HSL and the phosphorylation, and thus deactivation, of PLIN. These two steps are vital for the breakdown of TG to free FA which are used as acute substrate for thermogenesis, and importantly to regulate UCP-1 activity. Conversely, α-AdR are coupled with G-inhibitory protein, which inhibits AC activity and decreases cAMP levels and thus reduces the rate of lipolysis downstream [9,27]. The balance between adrenoreceptor subtypes regulates lipolytic drive and thus, is an essential factor for thermogenesis. There are species-and depot-specific differences in the expression of adrenoreceptor subtypes that modulate to fat cell function [23]. In this context, one major objective I wish to address in my future studies is to examine any distribution differences of α- and β-Ad receptors in the BAT and WAT, and importantly within the different regions of Sc Ing fat. The exercise-induced browning response was only seen in the middle portion of the Sc Ing fat, indicating a possible variance of adrenergic receptor distribution in comparison to the upper extremity. A higher expression of β-AdR found in the middle portion of the Sc Ing fat could theoretically have resulted in an increased rate of lipolysis which could have allowed for the increased thermogenesis seen in our results. Thus, it is important to investigate the combination of α- and β-AdR that mediate the lipolytic effect of catecholamines, and consequently alter the thermogenic capacity of different fat depots. In order to confirm our hypotheses, we will assess the distribution of α- and β-receptors in each type of tissue by measuring their protein content through western blot analysis.

9.2. Catecholamine release in different fat depots

In addition to the various adrenoreceptors expression in each type of fat, the amount of catecholamines released at nerve endings is also an important determinant of lipolytic activity and thermogenic capacity. Catecholamines such as NE, attach to binding sites on fat cells according to the affinity of each adrenoreceptor subtype. It has been proposed that α-AdR inhibit lipolysis at rest with low levels of catecholamines, whereas β-AdR modulate lipolysis when exposed to high levels of catecholamines such as physical exercise. During exercise, high NE concentrations maximally stimulate β-AdR which mask the inhibitory actions of α-AdR [98]. This supports the idea that NE may exert dual actions in the cell depending on the concentration of NE available at the adipocyte level [23]. In fact, it has been demonstrated that catecholamines play different roles in lipolysis at rest and during exercise in human subcutaneous fat tissue [98]. Therefore, it would be interesting to investigate the amount of catecholamines, specifically NE, released by nerve endings in both types of tissue.

It is well known that exercise transiently increases SNS activity, and catecholamine release stimulates BAT thermogenesis [8,9]. Surprisingly, in the present study, we see that exercise reduces thermogenic capacity of BAT and increases it in specific portions of the WAT. It could be possible that chronic exercise mediates the amount NE released in the BAT versus the WAT. To confirm our hypothesis, we will assess the capacity of NE release in each fat depot by measuring Tyrosine hydroxylase (TyrH) and dopamie-β-hydroxylase (dβH), which are essential enzymes for catecholamine synthesis. Low levels of TyrH or dβH will signify a decreased capacity to synthesize NE. This information will further elucidate the regulation of thermogenesis in classical BAT and WAT in response to exercise.

10. REFERENCES

1 OECD. Obesity Update. 2014.

2 Laddu D, Dow C, Hingle M, Thomson C, Going S. A review of evidence-based strategies to treat obesity in adults. *Nutr Clin Pract* 2011; **26**: 512–25.

3 Kumar A, Nayak BP. Obesity: single house for many evils. *Minerva Endocrinol* 2015.http://www.ncbi.nlm.nih.gov/pubmed/26006699 (accessed 27 May2015).

4 Kopelman PG. Obesity as a medical problem. *Nature* 2000; **404**: 635–643.

5 Rosenbaum M, Goldsmith R, Bloomfield D, Magnano A, Weimer L, Heymsfield S *et al.* Low-dose leptin reverses skeletal muscle , autonomic , and neuroendocrine adaptations to maintenance of reduced weight. *J Clin Invest* 2005; **115**: 3579–3586.

6 Yao X, Shan S, Zhang Y, Ying H. Recent progress in the study of brown adipose tissue. *Cell Biosci* 2011; **1**: 35.

7 Péronnet F, Cléroux J, Perrault H, Cousineau D, de Champlain J, Nadeau R. Plasma norepinephrine response to exercise before and after training in humans. *J Appl Physiol* 1981; **51**: 812–5.

8 Lowell BB, Bachman ES. Beta-Adrenergic receptors, diet-induced thermogenesis, and obesity. *J Biol Chem* 2003; **278**: 29385–8.

9 Cannon B, Nedergaard J. Brown adipose tissue: function and physiological significance. *Physiol Rev* 2004; **84**: 277–359.

10 Harms M, Seale P. Brown and beige fat: development, function and therapeutic potential. *Nat Med* 2013; **19**: 1252–63.

11 Boström P, Wu J, Jedrychowski MP, Korde A, Ye L, Lo JC *et al.* A PGC1α-dependent myokine that drives browning of white fat and thermogenesis. *Nature* 2012; **481**: 463–468.

12 Terblanche SE, Gohil K, Packer L, Henderson S, Brooks GA. The effects of endurance training and exhaustive exercise on mitochondrial enzymes in tissues of the rat ž Rattus nor ¨ egicus /. 2001.

13 Levine J a. Non-Exercise Activity Thermogenesis (NEAT). *Nutr Rev* 2004; **62**: 82–97.

14 Rolfe D, Brown G. Cellular Energy Utilization of Standard Metabolic and Molecular Origin Rate in Mammals. *Physiol Rev* 1997; **77**: 731–758.

15 Leibel RL, Rosebaum M, Hirsch J. CHANGES IN ENERGY EXPENDITURE RESULTING FROM ALTERED BODY WEIGHT. *N Engl J Med* 1995; **332**: 621–628.

16 Moitra J, Mason MM, Olive M, Krylov D, Gavrilova O, Marcus-Samuels B *et al.* Life without white fat: a transgenic mouse. *Genes Dev* 1998; **12**: 3168–3181.

17 Trujillo ME, Scherer PE. Adipose tissue-derived factors: impact on health and disease. *Endocr Rev* 2006; **27**: 762–78.

18 Frayn KN, Karpe F, Fielding B a, Macdonald I a, Coppack SW. Integrative physiology of human adipose tissue. *Int J Obes Relat Metab Disord* 2003; **27**: 875–88.

19 Casteilla L, Pénicaud L, Cousin B, Calise D. Choosing an Adipose Tissue Depot for Sampling Factors in Selection and Depot Specificity. *Adipose Tissue Protoc*; **456**: 23–38.

20 Stich V, Berlan M. Physiological regulation of NEFA availability: lipolysis pathway. *Proc Nutr Soc* 2004; **63**: 369–74.

21 Duncan RE, Ahmadian M, Jaworski K, Sarkadi-Nagy E, Sul HS. Regulation of lipolysis in adipocytes. *Annu Rev Nutr* 2007; **27**: 79–101.

22 Coppack SW, Jensen MD, Miles JM. In vivo regulation of lipolysis in humans. *J Lipid Res* 1994; **35**: 177–193.

23 Lafontan M, Berlan M. Fat cell adrenergic receptors and the control of white and brown fat cell function. *J Lipid Res* 1993; **34**: 1057–1091.

24 Tansey JT, Sztalryd C, Hlavin EM, Kimmel AR, Londos C. The central role of perilipin a in lipid metabolism and adipocyte lipolysis. *IUBMB Life* 2004; **56**: 379–85.

25 Macpherson REK, Peters SJ. Piecing together the puzzle of perilipin proteins and skeletal muscle lipolysis. *Appl Physiol Nutr Metab* 2015; **40**: 1–11.

26 DiPilato LM, Ahmad F, Harms M, Seale P, Manganiello V, Birnbaum MJ. The role of PDE3B phosphorylation in the inhibition of lipolysis by insulin. *Mol Cell Biol* 2015. doi:10.1128/MCB.00422-15.

27 Polak J, Bajzova M, Stich V. Effect of exercise on lipolysis in adipose tissue. *Future Lipidol* 2008; **5**.

28 Jaworski K, Sarkadi-Nagy E, Duncan RE, Ahmadian M, Sul HS. Regulation of triglyceride metabolism. IV. Hormonal regulation of lipolysis in adipose tissue. *Am J Physiol Gastrointest Liver Physiol* 2007; **293**: G1–4.

29 Haemmerle G, Lass A, Zimmermann R, Gorkiewicz G, Meyer C, Rozman J *et al.* Defective Lipolysis and Altered Energy Metabolism in Mice Lacking Adipose Triglyceride Lipase. *Science (80-)* 2006; **312**: 734–737.

30 Kiens B, Alsted TJ, Jeppesen J. Factors regulating fat oxidation in human skeletal muscle. *Obes Rev* 2011; **12**: 852–8.

31 Fischer J, Lefèvre C, Morava E, Mussini J-M, Laforêt P, Negre-Salvayre A *et al.* The gene encoding adipose triglyceride lipase (PNPLA2) is mutated in neutral lipid storage disease with myopathy. *Nat Genet* 2007; **39**: 28–30.

32 Lebeck J. Metabolic impact of the glycerol channels AQP7 and AQP9 in adipose tissue and liver. *J Mol Endocrinol* 2014; **52**: R165–78.

33 Madeira A, Moura TF, Soveral G. Aquaglyceroporins: implications in adipose biology and obesity. *Cell Mol Life Sci* 2015; **72**: 759–71.

34 Maeda N, Funahashi T, Hibuse T, Nagasawa A, Kishida K, Kuriyama H *et al.* Adaptation to fasting by glycerol transport through aquaporin 7 in adipose tissue. *Proc Natl Acad Sci U S A* 2004; **101**: 17801–6.

35 Horowitz JF. Fatty acid mobilization from adipose tissue during exercise. *Trends Endocrinol Metab* 2003; **14**: 386–392.

36 Winder WW, Thomson DM. Cellular energy sensing and signaling by AMP-activated protein kinase. *Cell Biochem Biophys* 2007; **47**: 332–347.

37 Nolan CJ, Madiraju MSR, Delghingaro-Augusto V, Peyot M-L, Prentki M. Fatty Acid Signaling in the -Cell and Insulin Secretion. *Diabetes* 2006; **55**: S16–S23.

38 Eaton S, Bartlett K, Pourfarzam M, James S, Infirmary RV, Ne N. Mammalian mitochondrial β -oxidation. *Biochem J* 1996; **320**: 345–357.

39 Park H, Kaushik VK, Constant S, Prentki M, Przybytkowski E, Ruderman NB *et al.* Coordinate regulation of malonyl-CoA decarboxylase, sn-glycerol-3-phosphate acyltransferase, and acetyl-CoA carboxylase by AMP-activated protein kinase in rat tissues in response to exercise. *J Biol Chem* 2002; **277**: 32571–32577.

40 Lin J, Handschin C, Spiegelman BM. Metabolic control through the PGC-1 family of transcription coactivators. *Cell Metab* 2005; **1**: 361–70.

41 Gaidhu MP, Ceddia RB. The role of adenosine monophosphate kinase in remodeling white adipose tissue metabolism. *Exerc Sport Sci Rev* 2011; **39**: 102–8.

42 Anthony NM, Gaidhu MP, Ceddia RB. Regulation of visceral and subcutaneous adipocyte lipolysis by acute AICAR-induced AMPK activation. *Obesity* 2009; **17**: 1312–7.

43 Daval M, Foufelle F, Ferré P. Functions of AMP-activated protein kinase in adipose tissue. *J Physiol* 2006; **574**: 55–62.

44 Gaidhu MP, Fediuc S, Anthony NM, So M, Mirpourian M, Perry RLS *et al.* Prolonged AICAR-induced AMP-kinase activation promotes energy dissipation in white adipocytes: novel mechanisms integrating HSL and ATGL. *J Lipid Res* 2009; **50**: 704–15.

45 Wu J, Cohen P, Spiegelman BM. Adaptive thermogenesis in adipocytes: is beige the new brown? *Genes Dev* 2013; **27**: 234–50.

46 Enerbäck S. Human brown adipose tissue. *Cell Metab* 2010; **11**: 248–52.

47 Rothwell NJ, Stock MJ. Luxuskonsumption, diet-induced thermogenesis and brown fat: The case in favour. *Clin Sci* 1983; **64**: 19–23.

48 Van Marken Lichtenbelt WD, Vanhommerig JW, Smulders NM, Drossaerts JM a FL, Kemerink GJ, Bouvy ND *et al.* Cold-activated brown adipose tissue in healthy men. *N Engl J Med* 2009; **360**: 1500–8.

49 Saito M, Okamatsu-Ogura Y, Matsushita M, Watanabe K, Yongeshiro T, Nio-Kobayashi J *et al.* High incidence of metabolically active brown adipose tissue in healthy adult humans effects of cold exposure and adiposity.pdf. *Diabetes* 2009; **58**: 1526–1531.

50 Feldmann HM, Golozoubova V, Cannon B, Nedergaard J. UCP1 ablation induces obesity and abolishes diet-induced thermogenesis in mice exempt from thermal stress by living at thermoneutrality. *Cell Metab* 2009; **9**: 203–9.

51 Matthias A, Ohlson KB, Fredriksson JM, Jacobsson A, Nedergaard J, Cannon B. Thermogenic responses in brown fat cells are fully UCP1-dependent. UCP2 or UCP3 do not substitute for UCP1 in adrenergically or fatty scid-induced thermogenesis. *J Biol Chem* 2000; **275**: 25073–81.

52 Slocum N, Durrant JR, Bailey D, Yoon L, Jordan H, Barton J *et al.* Responses of brown adipose tissue to diet-induced obesity, exercise, dietary restriction and ephedrine treatment. *Exp Toxicol Pathol* 2013; **65**: 549–57.

53 Virtanen KA, Lidell ME, Orava J, Heglind M, Westergren R, Niemi T *et al.* Functional brown adipose tissue in healthy adults. *N Engl J Med* 2009; **360**: 1518–25.

54 Giralt M, Villarroya F. White, brown, beige/brite: different adipose cells for different functions? *Endocrinology* 2013; **154**: 2992–3000.

55 Sharma BK, Patil M, Satyanarayana A. Negative regulators of brown adipose tissue (BAT)-mediated thermogenesis. *J Cell Physiol* 2014; **229**: 1901–7.

56 Kajimura S, Seale P, Spiegelman BM. Transcriptional control of brown fat development. *Cell Metab* 2010; **11**: 257–62.

57 Qi Z, Ding S. Transcriptional Regulation by Nuclear Corepressors and PGC-1α: Implications for Mitochondrial Quality Control and Insulin Sensitivity. *PPAR Res* 2012; **2012**: 348245.

58 Birerdinc A, Jarrar M, Stotish T, Randhawa M, Baranova A. Manipulating molecular switches in brown adipocytes and their precursors: a therapeutic potential. *Prog Lipid Res* 2013; **52**: 51–61.

59 Bachman ES, Dhillon H, Zhang C, Cinti S, Bianco AC, Kobilka BK *et al.* BAR Signaling Required for Diet-Induced Thermogenesis and Obesity Resistance. *Science (80-)* 2002; **297**: 843–845.

60 Fedorenko A, Lishko P V, Kirichok Y. Mechanism of fatty-acid dependent UCP1 uncoupling in brown fat mitochondria. *Cell* 2012; **151**: 400–413.

61 Divakaruni AS, Humphrey DM, Brand MD. Fatty acids change the conformation of uncoupling protein 1 (UCP1). *J Biol Chem* 2012; **287**: 36845–53.

62 Rothwell N, Stock M. A role for brown adipose tissue in diet-induced thermogenesis. *Nature* 1979; **281**: 31–35.

63 Glick Z, Teague R, Bray G, Lee M. Compositional and metabolic changes in brown adipose tissue following a single test meal. *Metabolism* 1983; **32**: 1146–1150.

64 Glick Z, Wickler S, Stern J, Horwitz B. Regional blood flow in rats after a single low-protein , high-carbohydrate test meal. *Am J Physiol* 1984; **247**: 160–166.

65 Vosselman MJ, Brans B, van der Lans AAJJ, Wierts R, van Baak MA, Mottaghy FM *et al.* Brown adipose tissue activity after a high-calorie meal in humans. *Am J Clin Nutr* 2013; **98**: 57–64.

66 Cinti S. Transdifferentiation properties of adipocytes in the adipose organ. *Am J Physiol Endocrinol Metab* 2009; **297**: E977–86.

67 Tiraby C, Tavernier G, Lefort C, Larrouy D, Bouillaud F, Ricquier D *et al.* Acquirement of brown fat cell features by human white adipocytes. *J Biol Chem* 2003; **278**: 33370–6.

68 Cohen P, Levy JD, Zhang Y, Frontini A, Kolodin DP, Svensson KJ *et al.* Ablation of PRDM16 and beige adipose causes metabolic dysfunction and a subcutaneous to visceral fat switch. *Cell* 2014; **156**: 304–16.

69 Fisher FM, Kleiner S, Douris N, Fox EC, Mepani RJ, Verdeguer F *et al.* FGF21 regulates PGC-1 and browning of white adipose tissues in adaptive thermogenesis. *Genes Dev* 2012; **26**: 271–281.

70 Lee P, Linderman JD, Smith S, Brychta RJ, Wang J, Idelson C *et al.* Irisin and FGF21 are cold-induced endocrine activators of brown fat function in humans. *Cell Metab* 2014; **19**: 302–9.

71 Tseng Y, Kokkotou E, Schulz TJ, Huang TL, Winnay JN, Taniguchi CM *et al.* New role of bone morphogenetic protein 7 in brown adipogenesis and energy expenditure. *Nature* 2008; **454**: 1000–1004.

72 Seo J a, Kim NH. Fibroblast growth factor 21: a novel metabolic regulator. *Diabetes Metab J* 2012; **36**: 26–8.

73 Li H, Zhang J, Jia W. Fibroblast growth factor 21: a novel metabolic regulator from pharmacology to physiology. *Front Med* 2013; **7**: 25–30.

74 Mai K, Schwarz F, Bobbert T, Andres J, Assmann A, Pfeiffer AFH *et al.* Relation between fibroblast growth factor-21, adiposity, metabolism, and weight reduction. *Metabolism* 2011; **60**: 306–11.

75 Dostálová I, Haluzíková D, Haluzík M. Fibroblast Growth Factor 21 : A Novel Metabolic Regulator With Potential Therapeutic Properties in Obesity / Type 2 Diabetes Mellitus. *Physiol Res* 2009; **58**: 1–7.

76 Chartoumpekis D V, Habeos IG, Ziros PG, Psyrogiannis AI, Kyriazopoulou VE, Papavassiliou AG. Brown adipose tissue responds to cold and adrenergic stimulation by induction of FGF21. *Mol Med* 2011; **17**: 736–40.

77 Coskun T, Bina H a, Schneider M a, Dunbar JD, Hu CC, Chen Y *et al.* Fibroblast growth factor 21 corrects obesity in mice. *Endocrinology* 2008; **149**: 6018–27.

78 Hondares E, Iglesias R, Giralt A, Gonzalez FJ, Giralt M, Mampel T *et al.* Thermogenic activation induces FGF21 expression and release in brown adipose tissue. *J Biol Chem* 2011; **286**: 12983–90.

79 Zhang X, Yeung DCY, Karpisek M, Stejskal D, Zhou Z, Liu F *et al.* Serum FGF21 Levels Are Increased in Obesity and Are in Humans. *Diabetes* 2008; **57**: 1246–1253.

80 Bordicchia M, Liu D, Amri E, Ailhaud G, Dessì-fulgheri P, Zhang C *et al.* Cardiac natriuretic peptides act via p38 MAPK to induce the brown fat thermogenic program in mouse and human adipocytes. *J Clin Invest* 2012; **122**: 1022–1036.

81 Vitali A, Murano I, Zingaretti MC, Frontini A, Ricquier D, Cinti S. The adipose organ of obesity-prone C57BL/6J mice is composed of mixed white and brown adipocytes. *J Lipid Res* 2012; **53**: 619–29.

82 Liang H, Ward WF. PGC-1alpha: a key regulator of energy metabolism. *Adv Physiol Educ* 2006; **30**: 145–51.

83 Yamashita H, Yamamoto M, Sato Y, Izawa T, Komabayashi T, Saito D *et al.* Effect of running training on uncoupling protein mRNA expression in rat brown adipose tissue. *Int J Biometeorol* 1993; **37**: 61–4.

84 Larue-Achagiotis C, Rieth N, Goubern M, Laury MC, Louis-Sylvestre J. Exercise-Training Reduces BAT Thermogenesis in Rats. *Physiol Behav* 1995; **57**: 1013–1017.

85 Revelli J, Muzzin P, Giacobino J. Modulation in vivo of f-adrenergic-receptor subtypes in rat brown adipose tissue by the thermogenic agonist Ro 16-8714. *Biochem J* 1992; **286**: 743–746.

86 Barbatelli G, Murano I, Madsen L, Hao Q, Jimenez M, Kristiansen K *et al.* The emergence of cold-induced brown adipocytes in mouse white fat depots is determined predominantly by white to brown adipocyte transdifferentiation. *Am J Physiol Endocrinol Metab* 2010; **298**: E1244–53.

87 Raschke S, Elsen M, Gassenhuber H, Sommerfeld M, Schwahn U, Brockmann B *et al.* Evidence against a beneficial effect of irisin in humans. *PLoS One* 2013; **8**: e73680.

88 Moreno-Navarrete JM, Ortega F, Serrano M, Guerra E, Pardo G, Tinahones F *et al.* Irisin is expressed and produced by human muscle and adipose tissue in association with obesity and insulin resistance. *J Clin Endocrinol Metab* 2013; **98**: E769–78.

89 Roca-Rivada A, Castelao C, Senin LL, Landrove MO, Baltar J, Belén Crujeiras A *et al.* FNDC5/irisin is not only a myokine but also an adipokine. *PLoS One* 2013; **8**: e60563.

90 Bartesaghi S, Hallen S, Huang L, Svensson P-A, Momo RA, Wallin S *et al.* Thermogenic activity of UCP1 in human white fat-derived beige adipocytes. *Mol Endocrinol* 2015; **29**: 130–9.

91 Van der Lans A a JJ, Wierts R, Vosselman MJ, Schrauwen P, Brans B, van Marken Lichtenbelt WD. Cold-activated brown adipose tissue in human adults: methodological issues. *Am J Physiol Regul Integr Comp Physiol* 2014; **307**: R103–13.

92 Wu J, Boström P, Sparks LM, Ye L, Choi JH, Giang A-H *et al.* Beige adipocytes are a distinct type of thermogenic fat cell in mouse and human. *Cell* 2012; **150**: 366–76.

93 Nedergaard J, Cannon B. The changed metabolic world with human brown adipose tissue: therapeutic visions. *Cell Metab* 2010; **11**: 268–72.

94 Norheim F, Langleite TM, Hjorth M, Holen T, Kielland A, Stadheim HK *et al.* The effects of acute and chronic exercise on PGC-1α, irisin and browning of subcutaneous adipose tissue in humans. *FEBS J* 2014; **281**: 739–49.

95 Bonet ML, Oliver P, Palou A. Pharmacological and nutritional agents promoting browning of white adipose tissue. *Biochim Biophys Acta* 2013; **1831**: 969–85.

96 Young JB, Saville E, Rothwell NJ, Stock MJ, Landsberg L. Effect of diet and cold exposure on norepinephrine turnover in brown adipose tissue of the rat. *J Clin Invest* 1982; **69**: 1061–71.

97 Conn VS, Hafdahl A, Phillips LJ, Ruppar TM, Chase J-AD. Impact of physical activity interventions on anthropometric outcomes: systematic review and meta-analysis. *J Prim Prev* 2014; **35**: 203–215.

98 Arner P, Kriegholm E, Engfeldt P, Bolinder J. Adrenergic Regulation of Lipolysis In Situ at Rest and during Exercise. *J Clin Invest* 1990; **85**: 893–898.

11. APPENDICES

11.1. Appendix A: Detailed Experimental Methods

11.1.1. Determination of irisin in the serum using ELISA kit from Pheonix Pharmaceuticals (CAT#EK-067-29)

This Enzyme Immnoassay Kit contains an immunoplate pre-coated with a secondary antibody and the non-specific binding sites are blocked. The secondary antibody can bind to the primary peptide antibody that is also bound with biotinylated peptide and peptide standard. The biotinylated peptide interacts with streptavidin-horseradish peroxidise (SA-HRP) that catalyzes the substrate solution (containing 3,3',5,5'-te-tramethylbenzidine, TMB) and hydrogen peroxide that produces a blue solution. Adding hydrochloric acid (HCl) stops the enzyme-substrate reaction and the solution turns yellow. The intensity of the yellow colouring is directly proportional to the SA-HRP amount and inversely proportional to the amount of peptide in the samples. A standard curve of known concentration is established first and the unknown concentration of the samples can be determined by extrapolation of the standard curve.

Kit Reagents

1. 20x assay buffer concentrate
2. 96 well immunoplate
3. Acetate plate sealer (APS)
4. Primary antibody
5. Standard peptide
6. Positive control
7. Biotinylated peptide
8. Streptavidin-horseradish peroxidise (SA-HRP)
9. Substrate solution (TMB)
10. 2N HCl

Note: Kit components must be equilibrated to room temperature before starting the assay. After rehydration, use solutions as soon as possible.

Preparation of peptide standard solutions

Standard #	Standard Vol.	1x Assay Buffer	Concentrations
Stock	0	1000 µl	1000ng/ml
#1	100 µl of Stock	900 µl	100ng/ml
#2	100 µl of #1	900 µl	10ng/ml
#3	100 µl of #2	900 µl	1ng/ml
#4	100 µl of #3	900 µl	0.1ng/ml

Protocol

1. Dilute 20x assay buffer concentrate (50mL) with 950ml of ddH_20. This will make it a 1x assay buffer solution. Use this solution to dilute or dissolve all other reagents.
2. Centrifuge and rehydrate the standard peptide with 1ml of 1x assay buffer. Vortex. Now, the concentration of this stock solution is 1000ng/ml. Allow solution to sit at room temperature to be completely dissolved. Vortex and centrifuge immediately before use.
3. Centrifuge and dilute samples with 1x assay buffer. Different samples may require different dilution factors to ensure samples are within dynamic range of the standard curve.
4. Centrifuge and rehydrate positive control with 200µl of 1x assay buffer, primary antibody with 5mL of 1x assay buffer, and biotinylated peptide with 4ml of 1x assay buffer. Allow solutions to sit for 5 mins to completely dissolve and mix well.
5. Leave A1 and A2 empty as blanks.
6. Pipette 50µl of 1x assay buffer into B1 and B2 as total binding.
7. Add 50µl of prepared peptide standards into wells in duplicates.
8. Add 50µl of positive controls in duplicates.
9. Add 50µl of samples into designated wells in duplicates.
10. Add 25µl of primary antibody into each well EXCEPT the blank well
11. Add 25µl of bitinylated peptide into each well, EXCEPT the blank well
12. Seal the immunoplate with APS. Incubate for 2 hours at room temperature on an orbital shaker.
13. Centrifuge SA-HRP vial and pipette 12µl into 12mL of 1x assay buffer to make SA-HRP solution. Vortex vigorously.
14. Remove APS from immunoplate, discard contents of the wells.
15. Wash each well with 1x asay buffer, discard the buffer, invert and blot dry. Repeat 4 times
16. Add 100µl SA-HRP solution into each well.
17. Reseal immunoplate with APS. Incubate for 1 hour at room temperature on orbital shaker.

18. Remove APS from immunoplate, discard contents of the wells. Wash and blot dry immunoplate 4 times again.
19. Add 100µl TMB substrate solution into each well. Reseal plate with APS. Incubate for 1 hour at room temperature on orbital shaker. Protect immunoplate from light at this point.
20. Remove APS from immunoplate, add 100µl 2N Hcl into each well to stop the reaction. The colour should change from blue to yellow and gently tap plate to ensure thorough mixing.
21. Load immunoplate onto Microplate reader and read absorbance O.D. at 45nm.

Results

Standard curve should show a reverse sigmoidal shape and is constructed by plotting the known concentrations on the X-axis and cooresponding O.D. reading on the Y-axis.
The standard curve shows an inverse relationship between O.D. absorbance and peptide concentration. As standard concentration increases, the yellow colour intensity should decrease which results in a reduced O.D. absorbance.

The concentration of the peptide in each sample is determined by locating the O.D. of each sample on the Y-axis and the a horizontal line should intersect with the standard curve. At this point, a vertical line will intersect the X-axis to show corresponding peptide concentration of the sample.
Note: if the samples were diluted prior to the assay, the concentration calculated must be multipled by the dilution factor.

The final results are expressed as irisin (ng/ml)

11.1.2. Complexation of Palmitate

1. Prepare 30mL of SETH Buffer (Recipe found in palmitate oxidation buffers section)
2. Add 3.75g FA-free BSA (Sigma Cat# A3803) to get a 12.5% solution
3. Heat to 50°C in water bath
4. Take 1600mg palmitic acid (Sigma Cat# P-5585) to put into a 2mL eppendorf
5. Dissolve palmitic acid with 100µl NaOH (10N) and vortex vigorously
6. Add palmitic acid into preheated medium while stirring. (note; it will precipitate)
7. Pour into falcon tube, protected from light
8. Incubate in 50°C water bath for 4+ hours while shaking at 150-200rpm
9. After the incubation period, filter solution to get chunks out using a 10mL syringe and sterile strainer
10. pH to 7.4
11. Aliquot solution and store at -20°C

11.1.3. Determination of FFA using Wako Pure Chemicals HR Series NEFA –HR Kit

1. Dissolve Reagent A into Solvent A
    - 4.1mg of Reagent A per 1mL of solvent A (calculate total volume you need for samples and standards)
2. Add 0.5mL of Reagent A solution into each cuvette and incubate for 5 min at 37°C
3. Dissolve Reagent B into Solvent B
    - 10.6mg of Reagent B per 1mL of solvent B
4. Add 0.25mL of Reagent B solution into each cuvette and incubate for 5 min at 37°C
5. Read at OD 550nm

Cuvette	1mEq/L NEFA Std (µL)	H_20 (µL)	Reagent A Sol. (mL)	I N C U B A T E	Reagent B Sol. (mL)	I N C U B A T E	Optical Density 550nm	NEFA Conc. (mEq/L)
Blank	-	12.5	0.5		0.25		0 (Ref)	0
0	-	12.5	0.5		0.25		0	0
Low Std	6.25	6.25	0.5		0.25		read	0.5
Mid Std	12.5	-	0.5		0.25		read	1.0
High Std	25	-	0.5		0.25		read	1.97
Sample	12.5	-	0.5		0.25		read	TBD

11.1.4. Palmitate Oxidation Buffers

Seth Buffer (pH-7.4)

300mM	Sucrose
2mM	EDTA
10mM	Tris-HCL

Reaction Mixture (pH-7.4)

150mM	Sucrose
5mM	MgCl2
30mM	KCl
30mM	Potassium phosphate buffer
2mM	EDTA
2mM	ADP
15mM	Tris-HCL
1%	BSA
0.75mM	Palmitate
1mM	Carnitine
0.025mM	CoA
0.2µCi/ml	[1-^{14}C] Palmitic acid

11.1.5. Palmitate Oxidation Protocol

1. Following extraction, weigh tissues (~100mg muscle, ~100mg BAT, ~300mg WAT) and place into 200µl of ice-cold SETH buffer
2. Depending on weight of tissue, add additional SETH buffer to yield a 20-fold (wt/vol) dilution
3. Homogenize solution in an ice-cold Potter-Elvehjen glass homogenizer for approx. 30 seconds
4. Take 400µl of tissue homogenate and pipette into plastic scintillation vial containing 1.6mL of reaction mixture
5. Place isolated well containing loosely folded piece of filter paper inside of scintillation vial and cap using rubber stopper
6. Include 2 blanks and 2 totals
7. Gasify each scintillation vial for approx 1 minute, and incubate for 1 hour at 37°C
8. After 1 hour, add 200µl (1:1, vol/vol) 2-phenylethylamine/methanol onto loosely folded filter paper in the center of the well, and 200µl of H_2SO_4 (5N) to acidify media.
9. Incubate for 1 hour at 37°C
10. Collect filter papers and transfer to corresponding scintillation vial containing 10mL of ECOLITE+ liquid scintillation cocktail (MP Biomedicals Cat #01882475) and place in scintillation counter for radioactivity counting

11.1.6. Western Blotting Buffers

10x Running Buffer (pH- 8.3)
30.34g Tris base
144g Glycine
10g SDS
Dissolve contents in 1L of ddH_20 and store at room temperature.

1x Running Buffer (pH- 8.3)
10% 10x Running buffer
90% ddH_20
Mix solutions and store at room temperature.

10x Transfer Buffer (pH- 8.3)
30.3g Tris base
144g Glycine
Dissolve contents in 1L of ddH_20 and store at room temperature.

1x Transfer Buffer (pH- 8.3)
10% 10x Transfer buffer
20% Methanol
70% ddH_20
Mix solutions and store at -20°C prior to use.

10x Wash Buffer
60.57g Tris base
87.66g Sodium Chloride (NaCl)
Dissolve contents in 1L of ddH_20, store at room temperature.

1x Wash Buffer
10% 10x Wash buffer
90% ddH_20
Add 500µl/L of Tween-20 and NP-40.
Mix solutions and store at room temperature.

Blocking Buffer
3% BSA (w/v: 1.5g/50mL)
Dissolve in 1x Wash buffer, store at 4°C.

Antibody (Ab) Buffer
1° Ab- 1part blocking buffer + 2 parts wash buffer + 0.02% NaAzide (stock in ddH_20)
2°Ab- 1part blocking buffer + 2 parts wash buffer (NO NaAzide).

Typically 1:1000-1:5000 dilution is appropriate for an Ab, may vary depending on how good the signal is.

Resolving gl Tris Buffer (1.5M) (pH-8.8)
90.86g/500mL ddH_20

Stacking gel Tris Buffer (0.5M) (pH-6.8)
30.3g/500mL ddH_20

10% APS Solution
10% (w/v) Ammoniumperoxide Sulfate in ddH_20.
Use 0.1g/mL
Store at -20°C.

10% SDS Solution
10% (w/v) Sodium dodecylsulfate in ddH_20
Use 1g/10mL
Store at room temperature.

Lysis Buffer for Protein Determination prior to Western blot

Reagent	Concentration/MW
NaCl	135mmol/L (MW=58.44)
$MgCl_2$	1mmol/L (MW=203.3)
KCl	2.7mmol/L (MW=74.55)
Tris (pH 8)	20mmol/L (MW=121.14)
Triton 1%	
Glycerol 10%	

Prepare lysis buffer stock and store at -20°C. Aliquot desired volumes and add protease(cOmplete ULTRA Tablets) and phosphatise (PhoStop) inhibitors just prior to use.

Laemmli Sample Buffer (2x)- (Bio-Rad, Cat#161-0737)
Per 1mL: 950µl of 2x Laemmli sample buffer
50µl β-Mercaptoethanol
Store at room temperature. Dilute the sample (1 in 2) with sample buffer and boil for 5min.

11.1.7. Preparation of tissue lysates:

1. After extraction, tissues are snap frozen and stored at -80°C.
2. Weigh tissues and add to 250µl lysis buffer. (~20mg skeletal muscle, ~70mg BAT, ~200mg WAT).
3. Homogenize tissue. Keep on ice as much as possible to avoid heating up the sample.
4. Centrifuge homogenate for 5min at 13,000rpm at 4°C.
5. Remove middle aqueous protein-rich layer and place in a fresh microtube.
6. Add 100µl lysis buffer to residual fat cake and pellet for additional extraction if necessary. If so, repeat steps 3-5.
7. Centrifuge extracted sample for 1min at 13,000rpm at 4°C and transfer to a fresh microtube. Discard any residual cell debris.
8. Take an aliquot from each sample for protein determination by the Bradford method.
9. Dilute sample with 2x Laemmli sample buffer (1:1 v/v), vortex well and boil samples for 5min.
10. Samples can be used immediately for western blots or stored at -80°C.

11.1.8. Western Blotting Protocol

Preparing the Gel/Gel Recipes

Note: Use low % acrylamide gel when probing for large proteins, and a higher % acrylamide gel for smaller proteins.

Resolving Gel

RESOLVING GEL	2 gels (8%)	2 gels (10%)
ddH_20	9.4 mL	8.2 mL
30% Acrylamide (37:5:1)	5.4 mL	6.6 mL
Tris-HCL (0.5M, pH 6.8)	5 mL	5 mL
10% SDS	0.2 mL	0.2 mL
Temed	20 µL	20 µL
10% APS	100 µL	100 µL

Add APS and Temed immediately prior to pouring the gel into plates. Pipette a thin layer of Isopropanol over the top of the gel to prevent resolving gel from drying out. Allow gel to set (approx. 20min).

Stacking Gel

STACKING GEL (4%)	2 gels (10mL)
ddH_20	6.1 mL
30% Acrylamide (37:5:1)	1.3 mL
Tris-HCL (0.5M, pH 6.8)	2.5 mL
10% SDS	0.1 mL
Temed	10 µL
10% APS	50 µL

Once the resolving gel is set, pour out Isopropanol and carefully blot excess with filter paper. Pour stacking gel on top of resolving gel. Put combs in place. Allow gel to set (approx. 20min).

Running the Gel

1. Take samples out of -80° freezer and place on ice.
2. Place gels into tanks, and add 1x running buffer to fill the tank.
3. Once samples have thawed, spin in centrifuge for a few seconds.
4. Take out combs and pipette 7µL Bio-Rad protein ladder.
5. Add samples into each well accordingly.
6. Top up running buffer to make sure tank is full.
7. Match electrodes up-black to black and red to red.
8. Turn on the voltage for 60V for 2min, then turn it up to 110V for approx. 1.5hours until dye runs off the gel.
9. At this point, you can prepare 1x transfer buffer. Once transfer buffer is well mixed, cover with parafilm and place in the -20°C freezer until ready for transfer.

Transferring the Gel onto a membrane

1. Fill Pyrex dish with cold transfer buffer.
2. Cut out equal sized membranes and dip in methanol to activate. Also cut out equal sized filter papers and prepare the appropriate number of foam pads.
3. Place membranes in transfer buffer after activation.
4. Once dye has run off the gel, remove the gels from tank and soak in transfer buffer. Carefully remove glass plates. Cut off and discard combs of the gel. Loosen gel from the glass plate with scraper. Allow to sit in transfer buffer.
5. In the pyrex dish, place the black side of the cassette on the bottom, and place two foam pads and 3 filter papers on top. Ensure there are no bubbles.
6. Carefully place gel on top of filter paper and use the roller to get any air bubbles out. Make sure gel is in the correct orientation so that the ladder will end up on the left side of the membrane when removed.
   Note: transfer runs from negative (black) to positive (red). Always ensure proteins will run from gel to the membrane.
7. Carefully place the membrane on top of the gel and roll out any bubbles.
8. Place 3 more filter papers on top and roll out any bubbles.
9. Add one more foam pad and roll out any bubbles.
10. Carefully close sandwich and place into transfer tank. Make sure black matches black and red matches red.
11. Place iced pack in tank to keep buffer cold. Attach lid by matching electrodes- black to black, and red to red. Surround transfer tank with ice to keep cold.
12. Turn on transfer at 120V for 2.5 hours or at 60V overnight.
13. Check on temperature throughout transfer time to ensure no overheating.

Probing the membrane

1. Prepare containers to hold blocking buffer for each membrane, approx. 10mL.
2. Once transfer has finished, open cassettes and quickly place membranes in containers with blocking buffer.
3. Allow the membranes to surf in the blocking buffer for 1hr at room temperature.
4. Pour out blocking buffer and add 1°Ab.
5. Incubate overnight at 4°C. Ensure containers are fully sealed to avoid evaporation.
6. The next day, remove 1°Ab and wash membranes 5x for 10min each with 10mL 1x wash buffer to rid the membrane of any unbound Ab.
7. Add 2° Ab and allow membranes to surf for 1hr at room temperature.
8. Remove 2°Ab and wash membranes 5x for 10min each with 10mL 1x wash buffer to rid the membrane of any unbound 2°Ab.
9. Membranes are ready for developing

Developing the membrane

1. For each membrane, use 3mL chemiluminescence (Millipore Luminata Forte Western HRP Substrate, Cat # WBLUF0500) per membrane and incubate for 3 minutes.
2. Dip membranes into ddH_20 to rinse and place on transparency inside cassette.
3. In the darkroom, expose film for desired time.
4. Place film in developer for a few seconds until signal appears. Dip into water and to stop the reaction, place in fixer solution. Ensure ample fixing time.
5. Rinse with water and allow to dry.

11.2. Appendix B: Published Work

11.2.1. Copyright Permission

The Journal of Biological Chemistry is a part of the American Society of Biochemistry and Molecular Biology (ASMBM). The ASMBM automatically grants original authors the use without requiring copyright permission request to do the following:

- reuse an article in a thesis and/or dissertation
- reproduce an article, reuse a figure, photo and/or table
- present the work orally in its entirety

Further information can be obtained from the ASMBM copyright permission policy online at: http://www.jbc.org/site/misc/Copyright_Permission.xhtml

11.2.2. Publication

THE JOURNAL OF BIOLOGICAL CHEMISTRY VOL. 289, NO. 49, pp. 34129–34140, December 5, 2014
© 2014 by The American Society for Biochemistry and Molecular Biology, Inc. Published in the U.S.A.

Thermogenic Capacity Is Antagonistically Regulated in Classical Brown and White Subcutaneous Fat Depots by High Fat Diet and Endurance Training in Rats

*IMPACT ON WHOLE-BODY ENERGY EXPENDITURE**

Received for publication, June 21, 2014, and in revised form, October 22, 2014 Published, JBC Papers in Press, October 25, 2014, DOI 10.1074/jbc.M114.591008

Michelle V. Wu[1], **George Bikopoulos**[1], **Steven Hung, and Rolando B. Ceddia**[2]

From the Muscle Health Research Center, School of Kinesiology and Health Science, York University, Toronto, Ontario M3J 1P3, Canada

Background: Brown adipose tissue (BAT) is important for cold- and diet-induced thermogenesis.
Results: Obesity and chronic exercise antagonistically regulate thermogenic capacity of BAT and subcutaneous white fat (SC WAT).
Conclusion: Endurance exercise reduces thermogenic capacity in classical BAT while increasing it in the SC WAT.
Significance: Browning of the SC WAT may be potentially used to treat obesity.

This study investigated the regulation of thermogenic capacity in classical brown adipose tissue (BAT) and subcutaneous inguinal (SC Ing) white adipose tissue (WAT) and how it affects whole-body energy expenditure in sedentary and endurance-trained rats fed *ad libitum* either low fat or high fat (HF) diets. Analysis of tissue mass, PGC-1α and UCP-1 content, the presence of multilocular adipocytes, and palmitate oxidation revealed that a HF diet increased the thermogenic capacity of the interscapular and aortic brown adipose tissues, whereas exercise markedly suppressed it. Conversely, exercise induced browning of the SC Ing WAT. This effect was attenuated by a HF diet. Endurance training neither affected skeletal muscle FNDC5 content nor circulating irisin, but it increased FNDC5 content in SC Ing WAT. This suggests that locally produced FNDC5 rather than circulating irisin mediated the exercise-induced browning effect on this fat tissue. Importantly, despite reducing the thermogenic capacity of classical BAT, exercise increased whole-body energy expenditure during the dark cycle. Therefore, browning of subcutaneous WAT likely exerted a compensatory effect and raised whole-body energy expenditure in endurance-trained rats. Based on these novel findings, we propose that exercise-induced browning of the subcutaneous WAT provides an alternative mechanism that reduces thermogenic capacity in core areas and increases it in peripheral body regions. This could allow the organism to adjust its metabolic rate to accommodate diet-induced thermogenesis while simultaneously coping with the stress of chronically increased heat production through exercise.

Adipose tissue can be broadly classified into white and brown (1). Although WAT[3] is specialized to store energy, BAT has a great capacity to dissipate energy in the form of heat (2). In its activated state, BAT utilizes glucose and fatty acids for heat production via the mitochondrial uncoupling protein-1 (UCP-1), thereby reducing the availability of substrate for storage in WAT. It is now recognized that adult humans have significant amounts of inducible BAT (3–6). In fact, two populations of these inducible brown fat cells have been identified as follows: classical brown and "beige" adipocytes (7, 8). The former displays all the features of the typical brown fat cell found in rodents and is activated upon cold exposure. The latter does not seem to have the same developmental origin as classical BAT, but it can be induced to acquire a "brown-like" thermogenic phenotype and potentially increase whole-body energy expenditure (8).

It has been suggested that humans have a population of quiescent beige adipocytes dispersed within the WAT (particularly in the SC WAT) that can be recruited to promote energy dissipation (8) and therefore can be targeted for the treatment of major metabolic disorders such as obesity and type 2 diabetes. In this context, it has been reported that chronic endurance exercise (9, 10) has the ability to promote the expression of thermogenic genes in white adipocytes ("browning" of the WAT) and increase whole-body energy expenditure. Such effects have been proposed to be induced by a myokine released during exercise (irisin) derived from the cleavage of fibronectin domain-containing protein 5 (FNDC5) that promotes browning of the SC WAT (9). These findings established a direct novel relationship between endurance exercise and browning of WAT with important potential implications for the regulation of whole-body energy homeostasis. However, the contribution of exercise-induced WAT browning to whole-body energy expenditure has been questioned. Particularly, because exercise is thermogenic in itself, it seems counterintuitive that it would

* This work was supported by Natural Sciences and Engineering Research Council of Canada Grant 311818-2011 (to R. B. C.).
[1] Both authors contributed equally to this work.
[2] To whom correspondence should be addressed: Muscle Health Research Center, School of Kinesiology and Health Science, York University, 4700 Keele St., North York, Ontario M3J 1P3, Canada. Tel.: 416-736-2100 (Ext. 77204); Fax: 416-736-5774; E-mail: roceddia@yorku.ca.
[3] The abbreviations used are: WAT, white adipose tissue; AMPK, AMP-activated protein kinase; ATGL, adipose triglyceride lipase; CLAMS, comprehensive laboratory animal monitoring system; DIT, diet-induced thermogenesis; BAT, brown adipose tissue; aBAT, aortic BAT; SC WAT, subcutaneous WAT; Sed, sedentary; Ex, endurance-trained; HF, high fat; LF, low fat; SC Ing, subcutaneous inguinal; Epid, epididymal; Retro, retroperitoneal; ANOVA, analysis of variance; iBAT, interscapular BAT; LBM, lean body mass; Sol, soleus; EDL, extensor digitorum longus.

Downloaded from http://www.jbc.org/ at York University - OCUL on December 8, 2014

augment heat production by conferring brown-like features to WAT. Also, it has been reported that oxidation of pyruvate, α-ketoglutarate, palmitoylcarnitine, and succinate were reduced by at least 50% in mitochondria isolated from interscapular BAT (iBAT) of rats subjected to treadmill running for 5–6 weeks when compared with sedentary counterparts (11, 12).

These studies provide evidence that chronic endurance exercise actually reduces thermogenic activity in classical BAT. Based on these findings, it seems that chronic endurance exercise exerts antagonistic effects on thermogenesis in classical BAT *versus* SC WAT. Currently, limited information is available with regard to the thermogenic capacity of classical BAT in comparison with SC WAT under conditions of chronic endurance exercise. Additionally, even though the extent and mechanisms by which exercise-induced browning of WAT affects whole-body energy expenditure are of great interest, they remain largely undetermined. Therefore, the aim of this study was to determine the effects of chronic endurance exercise on thermogenic capacity in classical BAT and SC WAT and the impact on whole-body energy expenditure. To accomplish this, we assessed alterations in major molecular determinants of thermogenesis in classical brown and SC Ing WAT, as well as circulating irisin and FNDC5 content in skeletal muscle and SC WAT. Because classical BAT plays an important role in diet-induced thermogenesis (DIT) and regulation of whole-body energy homeostasis (13–15), we also assessed molecular markers of thermogenesis (PGC-1α and UCP-1 content) and palmitate oxidation in iBAT and aortic BAT (aBAT), as well as in SC WAT from sedentary and chronically endurance-trained rats fed either LF or HF diets. Here, we provide a detailed analysis of the physiological and molecular mechanisms by which thermogenic capacity is regulated in classical BAT and SC WAT and at the whole-body level under diet-induced obesity and chronic endurance exercise conditions.

EXPERIMENTAL PROCEDURES

Reagents—Fatty acid-free bovine serum albumin (BSA), L-carnitine, CoA, and palmitic acid were obtained from Sigma. DTT, ATP, ADP, and nicotinamide adenine dinucleotide phosphate (NADP) were obtained from BioShop Canada Inc. (Burlington, Ontario, Canada). [1-^{14}C]Palmitic acid was from GE Healthcare. The irisin kit (catalog no. 067-29) was from Phoenix Pharmaceuticals, Inc. (Burlingame, CA). Protease (cOmplete ULTRA Tablets) and phosphatase (PhosStop) inhibitors were from Roche Diagnostics. Specific antibodies against ATGL, AMPK, P-AMPKα (Thr-172), and β-actin were purchased from Cell Signaling Technology Inc. (Beverly, MA). The PGC-1α antibody was from Millipore (Temecula, CA), and the antibodies against UCP-1, FNDC5, and GAPDH were purchased from Abcam (Cambridge, MA).

Animals, Selection Protocol, and Diet—Male albino rats from the Wistar strain (Charles River Laboratories, Montreal, Quebec, Canada) weighing ~200 g (initial weight) were maintained at a constant temperature (23 °C), with a fixed 12-h light/12-h dark cycle. The protocol containing all animal procedures described in this study was specifically approved by the Committee on the Ethics of Animal Experiments of York University (York University Animal Care Committee, permit number 2011-14) and performed strictly in accordance with the York University Animal Care Committee guidelines. All surgery was performed under ketamine/xylazine anesthesia, and all efforts were made to minimize suffering. Prior to assigning animals to each experimental group, each rat was subjected to a screening exercise protocol to determine the ones unwilling to exercise. The screening protocol consisted of three separate treadmill exercise sessions, each starting with a 5-min warm-up period with constant inclination and speed set at 5% and 10 m/min, respectively. Subsequently, the inclination was increased to 10% and maintained constant, although the speed was increased by 2 m/min every 2 min up to 30 m/min. Rats that did not run beyond the speed of 20 m/min for at least 20 min all 3 days of the selection period were excluded from the study. Only 10% of the animals did not meet the inclusion criteria. The selected animals were then randomly divided into four groups as follows: 1) sedentary fed a LF diet (Sed LF); 2) endurance-trained fed a LF diet (Ex LF); 3) sedentary fed a HF diet (Sed HF); and 4) endurance-trained fed a HF diet (Ex HF). The animals were fed *ad libitum* purified ingredient diets from Research Diets Inc. Rats on the LF diet groups were provided with food containing 10, 70, and 20% of the total calories from fat, carbohydrate (sucrose levels matching the HF diet), and protein, respectively (catalog no. D12450J). The HF diet groups were provided with food containing 59.9, 20.1, and 20% of the total calories from fat, carbohydrate, and protein, respectively (catalog no. D12492).

Determination of Organ Mass and Lean Body Mass (LBM)—Body composition was assessed as described previously (16). Briefly, at the end of the study, Sed and Ex rats were weighed, anesthetized (ketamine/xylazine 0.4 and 8 mg per 100 g of body weight), decapitated, and exsanguinated. A longitudinal anterior skin incision from neck to tail was then made. A scalpel was used to detach the entire skin consisting of fur and SC WAT from the carcass of each animal. At this point, the SC Ing fat depot was carefully excised and weighed. A similar procedure was carried out to remove the skin from the head. The head and body skins were weighed separately. The iBAT was removed, thoroughly trimmed of any visual white adipose tissue present, and weighed. The abdominal and thoracic cavities were then incised longitudinally, and the internal organs were exposed. The aBAT was excised along with the liver, kidneys, and heart and individually weighed. The remaining abdominal organs as well as the lungs were all accounted for as viscera. Next, the epididymal and retroperitoneal fat depots were removed and weighed. The mass of the remaining carcass consisting of skeletal muscle and bones combined with the skinned head, liver, heart, and kidneys was used as LBM (16).

Determination of Irisin in the Serum—Irisin was determined by using ELISA kits from Phoenix Pharmaceuticals, Inc. Blood was extracted under resting conditions at week 8 of the study and also immediately after exercise at week 6 of the study. For the determination of resting irisin, blood was collected from the saphenous vein 24 h after the last bout of exercise in the fed state. For the determination of irisin immediately after exercise, blood was collected at week 6 with all animals (including the sedentary groups) immediately after running for 1 h at 70–85% of peak VO_2.

Downloaded from http://www.jbc.org/ at York University - OCUL on December 8, 2014

Peak Oxygen Consumption (Peak VO_2) and Training Protocol—To set the initial training intensity and to adjust it as the animals improved their running ability, peak VO_2 tests were conducted at weeks 0, 2, 4, and 6 of the study. Specially designed treadmills connected to the comprehensive laboratory animal monitoring system (CLAMS) from Columbus Instruments (Columbus, OH) were used to apply an exercise protocol of incremental workloads to determine peak VO_2 in rats. To accomplish that, all rats were placed on the treadmill, and VO_2 was continuously monitored under resting (after 15–20 min of being in the treadmill chamber) and exercising conditions. After recording resting VO_2 values, the rats were exposed to a 5-min warm-up period (10 m/min, 0% inclination). Subsequently, treadmill speed was progressively increased (2 m/min every 2 min) until exhaustion was reached (characterized by the rats remaining on the shocking grid for 5 consecutive seconds) or at the point at which increments in speed were not accompanied by increases in VO_2, and respiratory exchange ratio approached the value of 1. Treadmill inclination was increased to 5% in stage 1 and to 10% in stage 2 and then maintained constant until the end of the test. Rats in the endurance training groups were exposed to treadmill running at 75–85% of peak VO_2, 1 h/day, 5 days/week for 8 weeks. To ensure equal conditions between the sedentary and endurance-trained groups, all rats were placed on the treadmill simultaneously. The treadmill speed for sedentary animals was kept at 1–2 m/min during the entire duration (1 h) of the training session. Treadmill speed was adjusted every 2 weeks to maintain the exercise intensity between 75 and 85% of peak VO_2 throughout the study. For weeks 1 and 2, the training sessions started with a warm-up period (3 min at 12 m/min, 0% inclination, followed by 2 min at 14 m/min, 5% inclination). Treadmill inclination was then increased to 10% and maintained constant, and the speed was progressively increased in a manner that by the 20th min all animals had reached the 75–85% peak VO_2 training range and were then exercised at that intensity for the remaining 40 min. The animals quickly adapted to the training protocol. Thus, for weeks 3–8 the warm-up lasted only 2 min and started at 24 m/min and 10% inclination with the speed being progressively increased every 2 min. This was done in a manner that the training range was reached within 10 min of the start and then maintained for the remaining 50 min of each training session. The average treadmill speed required to maintain the training intensity also increased from 24 m/min (week 1) to 38 m/min (week 4) and then to 42 m/min at week 8. With this training regimen, the total weekly mileage increased from 6.57 km at week 1 to 11.09 km at week 4, reaching 11.98 km at week 8. The intensity, frequency, and volume of exercise chosen here have been previously demonstrated to significantly increase peak VO_2 in rats (17). This training protocol is also compatible with exercise prescriptions used in humans to improve cardiovascular fitness (18).

Adipose Tissue Morphology—Morphological analysis was performed using light microscopy as described previously (19) with a few modifications. Briefly, upon extraction of the fat pads, small samples (~50–100 mg) of iBAT and aBAT, as well as of SC Ing and epididymal (Epid) white adipose tissues, were removed. For the SC Ing fat depot, two samples were collected as follows: one with a visible brownish appearance localized within the central portion of the tissue, and another clearly white in appearance localized to the proximal (upper) and distal (lower) extremities of the SC Ing fat depot. All fat samples were fixed in 4% paraformaldehyde, 0.1 M phosphate buffer solution, pH 7.4, for 24 h at room temperature. After fixation, tissue samples were washed (three times) and stored in 70% ethanol. Samples were subsequently sent to the Toronto Centre for Phenogenomics (Toronto, Ontario, Canada) where they were embedded in paraffin blocks, sectioned, and processed for hematoxylin and eosin staining. Stained samples were viewed using a Nikon Eclipse TiE inverted microscope (Nikon Canada, Mississauga, Ontario, Canada) under ×10 and ×20 magnification. Average adipocyte area was determined by two independent investigators who measured the area of 150 cells in three randomly selected fields of view for each animal. This was done to prevent the biased selection of cells for measurement. Area was determined by NIS-elements basic research imaging software (Nikon Canada, Mississauga, Ontario, Canada), and images were captured with a digital Nikon DS-QI1Mc camera (Nikon Canada, Mississauga, Ontario, Canada).

Western Blot Determination of UCP-1, PGC-1α, AMPK, Phospho-AMPK, ATGL, FNDC5, GAPDH, and β-Actin—Immediately after extraction, tissues were snap-frozen in liquid nitrogen and homogenized in buffer containing 25 mM Tris-HCl, 25 mM NaCl, 1 mM $MgCl_2$, 2.7 mM KCl, 1% Nonidet P-40, and protease (cOmplete ULTRA Tablets) and phosphatase (PhosStop) inhibitors, pH 7.4. Sample homogenates were then transferred to microtubes and centrifuged (16,000 × *g* for 10 min at 4 °C), and the infranatant was collected. An aliquot of the tissue lysates was used to determine the concentration of protein in each sample by the Bradford method. Before loading onto SDS-polyacrylamide gels, the samples were diluted 1:1 (v/v) with Laemmli sample buffer (62.5 mM Tris-HCl, pH 6.8, 2% (w/v) SDS, 50 mM DTT, 0.01% (w/v) bromphenol blue). To determine the total and phosphorylated (Thr-172) forms of AMPK (62 kDa), aliquots containing 80 μg of protein were subjected to SDS-PAGE and then transferred to polyvinyldifluoride (PVDF) membranes (Bio-Rad). To determine ATGL (54 kDa) and UCP-1 (33 kDa) contents in SC Ing fat, aliquots containing 50 μg of protein were loaded onto the gels. Aliquots containing 25 μg of protein were used to probe for UCP-1 content in lysates from iBAT and aBAT. All primary antibodies were at 1:1000 dilution. The blots were scanned, and the density of each band of interest was determined using the ImageJ program. Western blot data for ATGL, FNDC5 (22 kDa), PGC-1α (~113 kDa), and UCP-1 were expressed as arbitrary units. The values were obtained by dividing the density of the band of interest by that of either β-actin (45 kDa) or GAPDH (36 kDa) (as indicated in the figure legends) from the same blot. Similarly, P-AMPK data were normalized by total AMPK.

Palmitate Oxidation—Samples of soleus (Sol) and extensor digitorum longus (EDL) muscles (100 mg), iBAT and aBAT (100 mg), and SC Ing fat (300 mg) were extracted and thoroughly minced in 200 μl of ice-cold SETH buffer (300 mM sucrose, 2 mM EDTA, and 10 mM Tris-HCl, pH 7.4). Additional SETH buffer was added to yield a 20-fold (w/v) diluted minced tissue sample. The solution was then homogenized in an ice-

Downloaded from http://www.jbc.org/ at York University - OCUL on December 8, 2014

cold Potter-Elvehjem glass homogenizer (10–12 passes across ~30 s). Subsequently, 400 μl of tissue homogenates were transferred to plastic scintillation vials containing 1.6 ml of the reaction mixture (150 mM sucrose, 5 mM $MgCl_2$, 30 mM KCl, 30 mM potassium phosphate buffer, 2 mM EDTA, 2 mM ADP, 15 mM Tris-HCl, 1% BSA, 0.75 mM palmitate, 1 mM carnitine, 0.025 mM CoA, pH 7.4) containing 0.2 μCi/ml [1-^{14}C]palmitic acid. Cold and labeled palmitate were complexed with fatty acid-free BSA prior to adding to the reaction mixture. The rates of palmitate oxidation by Sol and EDL muscles, iBAT, aBAT, and SC Ing fat homogenates were measured by the production of $^{14}CO_2$ from [1-^{14}C]palmitic acid. The flasks where tissue homogenates were incubated had a centered isolated well containing a loosely folded piece of filter paper moistened with 0.2 ml of 2-phenylethylamine/methanol (1:1, v/v). After the 1-h incubation period, the media were acidified with 0.2 ml of H_2SO_4 (5 N), and the flasks were maintained sealed at 37 °C for an additional 1 h for collection of the released $^{14}CO_2$. Subsequently, the filter papers were carefully removed and transferred to scintillation vials for radioactivity counting (20).

Determination of in Vivo Metabolic Parameters—The CLAMS was used to perform all automated *in vivo* determinations as described previously (16). Briefly, the CLAMS measures oxygen consumption (VO_2), carbon dioxide production (VCO_2), and respiratory exchange ratio. Each cage is also equipped with a system of infrared beams that detects animal movement in the *x* and *z* axes, which was used to determine spontaneous ambulatory activity. Energy expenditure (heat) was calculated by multiplying the calorific value (CV = 3.815 + 1.232 × respiratory exchange ratio) by VO_2. Measurements using the CLAMS were performed after 8 weeks of diet and exercise interventions. The animals were placed in the CLAMS at 11:00 a.m. and 24 h after the last exercise training session. The 1st h of data collected in the CLAMS was discarded, because it is the time required for the rats to acclimatize to the cage environment (16). The rats were monitored for a 24-h period encompassing the light (07:00–19:00 h) and dark (19:00–07:00 h) cycles.

Statistical Analyses—The significance of differences between two groups was determined by two-tailed Student's unpaired or paired *t* tests and for multiple comparisons by either one-way or two-way analysis of variance (ANOVA) as indicated. The Bonferroni post hoc multiple comparison test was used when differences were identified. The Graph Pad Prism 5 software was used for all statistical analyses.

RESULTS

Body Mass, LBM, and Adiposity—Body mass of the Ex LF and Ex HF rats was ~12% lower than the Sed LF and Sed HF controls (Table 1). Body mass of Sed HF rats was 8% higher than that of Sed LF rats, although this did not reach statistical significance (Table 1). LBM of Ex LF and Ex HF rats was also reduced by ~7% when compared with Sed LF and Sed HF controls (Table 1). In Ex LF and Ex HF animals, the masses of the Epid, SC Ing, and Retro fat pads were significantly reduced by 33 and 30%, 40 and 26%, and by 42 and 37%, respectively, when compared with Sed LF and Sed HF controls (Table 1). As expected, adiposity was significantly increased by HF feeding, which was demonstrated by 1.73-, 1.3-, and 1.86-fold increases in the masses of the Epid, Sc Ing, and Retro fat pads of Sed HF when compared with Sed LF rats (Table 1). Conversely, endurance training prevented the increase in adiposity induced by HF feeding. In fact, the masses of the Epid, Sc Ing, and Retro fat pads of Ex HF rats were similar to those of Sed LF rats (Table 1).

TABLE 1

Effects of chronic endurance training on body mass, adiposity, and LBM

Total body mass, Epid, SC Ing, and Retro fat masses and LBM were measured at the end of the study.

	Sed LF	Ex LF	Sed HF	Ex HF
Body mass (g)	481.50 ± 8.54	428.43 ± 10.29[a]	524.20 ± 8.77	464.89 ± 9.73[a]
Fat pad mass (g)				
Epid	8.16 ± 0.55	5.49 ± 0.36[b]	14.09 ± 0.77[c]	9.83 ± 0.93[d]
SC Ing	11.41 ± 0.67	6.79 ± 0.32[b]	14.89 ± 0.87[c]	11.00 ± 0.85[d]
Retro	6.78 ± 0.78	3.94 ± 0.23[b]	12.61 ± 0.85[c]	7.95 ± 0.78[d]
LBM (g)	294.30 ± 6.14	271.60 ± 5.22[a]	295.20 ± 4.2	273.80 ± 5.6[a]

[a] $p < 0.05$ is *versus* Sed LF and Sed HF.
[b] $p < 0.05$ is *versus* Sed LF, Sed HF, and Ex HF.
[c] $p < 0.05$ is *versus* Sed LF, Ex LF, and Ex HF.
[d] $p < 0.05$ is *versus* Ex LF and Sed HF. Two-way ANOVA is $n = 18$.

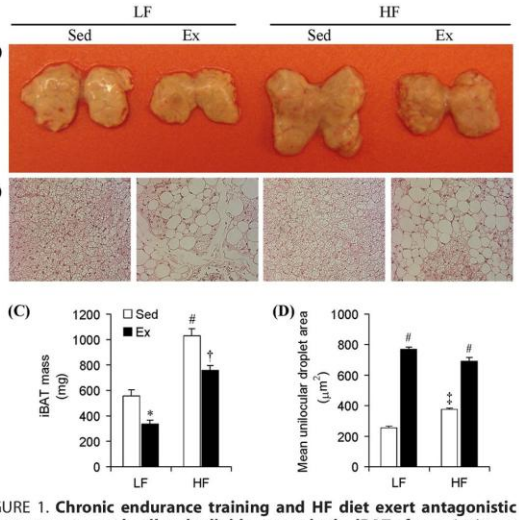

FIGURE 1. **Chronic endurance training and HF diet exert antagonistic effects on mass and unilocular lipid content in the iBAT of rats.** *A*, picture of iBATs dissected from Sed and Ex rats fed either LF or HF diets at week 8. *B*, respective microscopic images (×20 magnification) of H&E staining of iBAT samples from all groups of animals. Average iBAT mass (*C*) and unilocular adipocyte area (*D*) are present within the iBAT of all four groups of animals. *, $p < 0.05$ *versus* Sed LF; #, $p < 0.05$ *versus* Sed LF, Ex LF, and Ex HF; †, $p < 0.05$ *versus* Ex LF and Sed HF; ‡, $p < 0.05$ *versus* all other conditions. Two-way ANOVA ($n = 8$).

iBAT Mass and Assessment of Unilocular Droplet Area—iBAT mass significantly increased (1.84-fold) in Sed HF when compared with Sed LF rats (Fig. 1, *A* and *C*). Chronic endurance exercise significantly reduced iBAT mass by 39% when comparing Sed LF and Ex LF (558.26 ± 47.34 *versus* 338.23 ± 27.12 mg) and by 26% when comparing Sed HF and Ex HF (1028.39 ± 58.55 *versus* 756.66 ± 39.84 mg) rats (Fig. 1, *A* and *C*). Microscopic analysis revealed that iBAT of Sed LF and Sed HF rats contained essentially multilocular brown adipocytes (Fig. 1*B*), although the area of unilocular adipocytes was ~47% higher in the latter than the former (Fig. 1*D*). Interestingly, the iBAT of Ex LF and Ex HF rats was occupied by much larger unilocular lipid droplets resembling white adipocytes (Fig. 1*B*). In fact, it

Downloaded from http://www.jbc.org/ at York University - OCUL on December 8, 2014

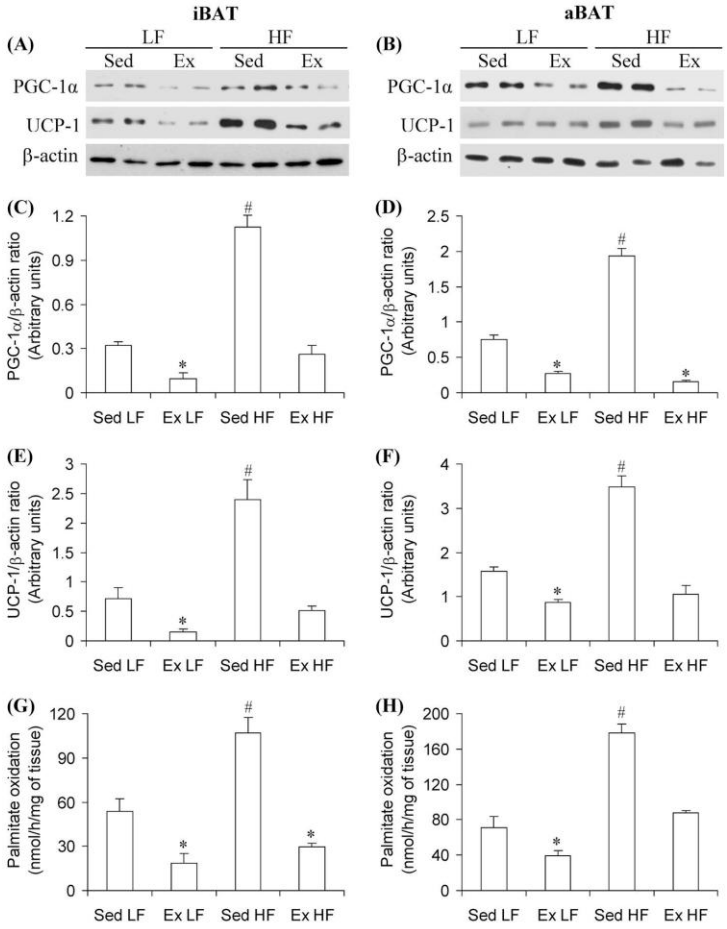

FIGURE 2. **Chronic endurance training reduces and HF diet increases PGC-1α and UCP-1 content, as well as palmitate oxidation in the iBAT and aBAT, respectively, brown adipose tissues.** iBAT and aBAT were extracted from Sed or 8-week Ex rats fed either a LF or a HF diet. Representative blots (*A* and *B*) and densitometric analysis of PGC-1α (*C* and *D*) and UCP-1 (*E* and *F*) contents and the assessment of palmitate oxidation (*G* and *H*) in iBAT and aBAT, respectively, are shown. β-Actin was used as loading control. *, $p < 0.05$ *versus* Sed LF; #, $p < 0.05$ *versus* all other conditions. One-way ANOVA ($n = 8$).

was found that the area of unilocular adipocytes present in iBAT was 3-fold higher in the Ex LF than Sed LF rats (768.6 ± 15.08 *versus* 256.1 ± 10.69 μm^2) and 1.84-fold higher in Ex HF than Sed HF (689.8 ± 27.04 *versus* 375.5 ± 8.99 μm^2) rats (Fig. 1*D*).

PGC-1α and UCP-1 Content and Palmitate Oxidation in iBAT and aBAT—Western blotting analysis revealed that in iBAT and aBAT of Sed HF rats, the contents of PGC-1α and UCP-1 were significantly increased by 3.5- and 2.55-fold and by 3.38- and 2.21-fold when compared with Sed LF rats, respectively (Fig. 2, *A–F*). Conversely, PGC-1α content was reduced by 69 and 63% and UCP-1 by 79 and 45% in the iBAT and aBAT of Ex LF rats, respectively, when compared with Sed LF controls. Furthermore, chronic endurance exercise completely prevented the HF diet-induced increase in PGC-1α and UCP-1 in iBAT and aBAT (Fig. 2, *A–F*). These effects were accompanied by increased palmitate oxidation in iBAT (2-fold) and aBAT (2.5-fold) of Sed HF rats when compared with Sed LF controls, whereas marked reductions were found in palmitate oxidation in iBAT (65 and 72%) and aBAT (45 and 51%) of Ex LF and Ex HF when compared with Sed LF and Sed HF, respectively (Fig. 2, *G* and *H*). These findings indicate that HF feeding increases and chronic endurance exercise reduces thermogenic capacity in iBAT and aBAT.

Morphological Analysis and Mean Adipocyte Area of the SC Ing Fat Depot—The initial visual impression of the SC Ing fat depot indicated that the middle region of the tissue was browner in animals exposed to chronic endurance training than in sedentary controls, although the upper and lower extremities conserved their white appearance (Fig. 3, *A* and *B* and *G* and *H*). To determine whether this was because the SC Ing fat depot was acquiring a brown-like phenotype, samples of the upper extremities and the middle regions of the tissue were used for H&E staining (Fig. 3, *A* and *B* and *G* and *H*). It was found that

Downloaded from http://www.jbc.org/ at York University - OCUL on December 8, 2014

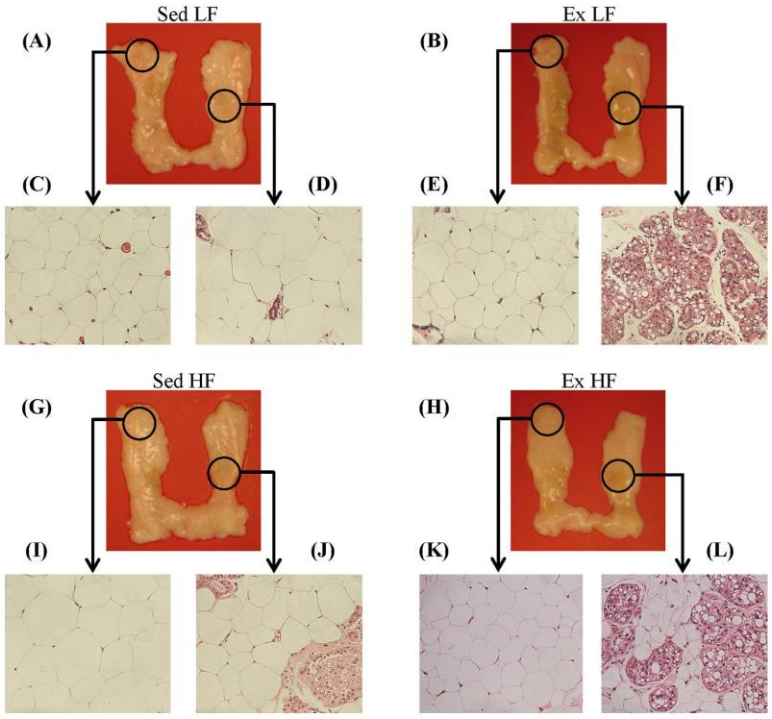

FIGURE 3. **Chronic endurance training induces browning and increases the number of multilocular adipocytes in the SC Ing fat depot of LF- and HF-fed rats.** Pictures of left and right SC Ing fat depots from Sed and Ex rats fed either a LF (*A* and *B*) or a HF (*G* and *H*) diet for 8 weeks. Samples of the upper extremities and middle regions of the SC Ing fat depots, as indicated by the *black circles*, were used for H&E staining and microscopy analyses. Representative images (×20 magnification) of adipocytes from Sed (*C* and *D*) and Ex (*E* and *F*) rats fed a LF diet or from Sed (*I* and *J*) and Ex (*K* and *L*) rats fed a HF diet are shown.

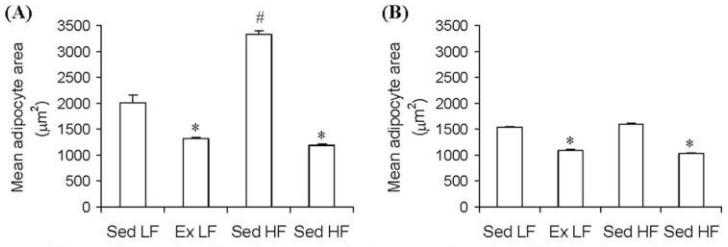

FIGURE 4. **Chronic endurance training reduces unilocular adipocyte area in the upper (*A*) and middle (*B*) regions of the SC Ing fat depots, whereas a HF diet increases unilocular adipocyte area only in the upper region.** Samples of the upper and middle regions of the SC Ing fat depot (as indicated in Fig. 3) from Sed and Ex rats fed either a LF or a HF diet for 8 weeks were extracted for microscopic analysis and determination of mean unilocular adipocyte area. *, $p < 0.05$ *versus* Sed LF; #, $p < 0.05$ *versus* all other conditions, One-way ANOVA ($n = 8$).

the middle and the upper extremity regions of the SC Ing fat from Sed LF (Fig. 3, *C* and *D*) and Sed HF (Fig. 3, *I* and *J*) rats contained essentially unilocular adipocytes typical of WAT. Interestingly, the middle region of the SC Ing fat depot from Ex LF (Fig. 3, *E* and *F*) and Ex HF (Fig. 3, *K* and *L*) rats were occupied by a large number of multilocular adipocytes typical of BAT, although the upper extremities of this tissue in Ex LF and Ex HF rats were occupied by unilocular adipocytes. Furthermore, when comparing the middle regions of the SC Ing fat depot between Ex LF and Ex HF, it was found that the former contained a much larger area occupied by multilocular brown-like adipocytes than the latter (Fig. 3, *F* and *L*). These findings suggested that although chronic endurance training induced browning of the SC Ing fat, HF feeding attenuated this effect. It was also found that the mean adipocyte area of the upper extremity of the SC Ing fat pad was significantly increased (1.66-fold) in Sed HF compared with Sed LF controls. Also, this variable was significantly reduced by 35% in Ex LF rats and by 65% in Ex HF when compared with Sed LF and Sed HF, respectively (Fig. 4*A*). In the middle region of the SC Ing fat depot, the mean adipocyte area was also reduced by 30% in Ex LF rats and by 36% in Ex HF when compared with Sed LF and Sed HF, respectively (Fig. 4*B*). However, this variable did not differ between Sed HF and Sed LF rats (Fig. 4*B*). These findings indicated that adipocytes located in the

Downloaded from http://www.jbc.org/ at York University - OCUL on December 8, 2014

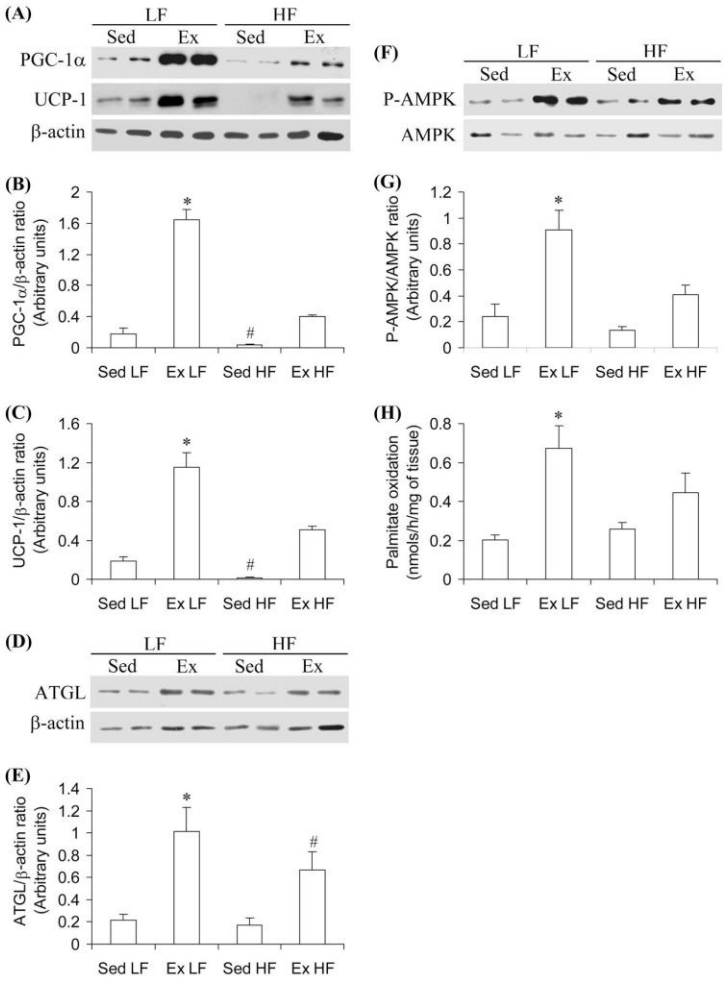

FIGURE 5. **Chronic endurance training increases and HF diet reduces PGC-1α (*A* and *B*), UCP-1 (*A* and *C*), and ATGL (*D* and *E*) contents, as well as AMPK phosphorylation (*F* and *G*) and palmitate oxidation (*H*) in the SC Ing fat depot.** The middle region of the SC Ing fat was extracted from Sed or 8-week Ex rats fed either an LF or a HF diet. β-Actin was used as loading control. *, $p < 0.05$ *versus* Sed LF; #, $p < 0.05$ *versus* all other conditions. One-way ANOVA ($n = 8$).

middle region of the SC Ing fat pad were resistant to HF-induced hypertrophy, which is compatible with the increased presence of multilocular brown-like adipocytes in this region.

PGC-1α, UCP-1, and ATGL Content, AMPK Phosphorylation, and Palmitate Oxidation in the SC Ing Fat Depot—To test whether or not the middle region of the SC Ing fat pad actually contained functional features of thermogenic brown adipocytes, we measured the content of proteins involved in thermogenesis and the oxidative capacity of the tissue. It was found that PGC-1α, UCP-1, and ATGL content, AMPK phosphorylation, and palmitate oxidation were increased by 9.1-fold (Fig. 5, *A* and *B*), 6.13-fold (Fig. 5, *A* and *C*), 4.84-fold (Fig. 5, *D* and *E*), 3.8-fold (Fig. 5, *F* and *G*), and 3.35-fold, respectively, in the middle region of the SC Ing fat pad of Ex LF when compared with Sed LF controls. In Sed HF rats, the content of PGC-1α was reduced by 78%, and UCP-1 was almost undetectable. No alterations were found for ATGL content, AMPK phosphorylation, and palmitate oxidation in the middle region of the SC Ing fat pad of Sed HF rats when compared with Sed LF controls. In Ex HF rats, PGC-1α, UCP-1, and ATGL content, AMPK phosphorylation, and palmitate oxidation also increased but to a much lower extent (2.28-, 2.9-, 3.18-, 1.71-, and 2.25-fold, respectively) than in Ex LF rats when compared with Sed LF controls (Fig. 5, *A–H*). These findings indicate that the exercise-induced appearance of multilocular brown-like adipocytes within the middle region of the SC Ing fat pad was also accompanied by functional thermogenic adaptive responses and that HF feeding attenuated these effects.

UCP-1 Content in Visceral Fat—To test whether exercise-induced browning effects were specific to the SC Ing fat depot

Downloaded from http://www.jbc.org/ at York University - OCUL on December 8, 2014

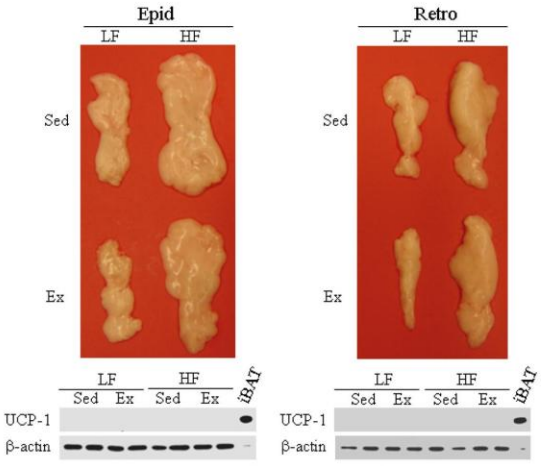

FIGURE 6. **Neither Ex nor HF diet affect UCP1 content in the Epid and Retro fat pads.** The Epid and Retro fat pads were excised from Sed and 8-week endurance-trained rats fed either a HF or a LF diet. The whole tissues were used for the determination by Western blot of UCP-1 content. β-Actin was used as loading control. A sample containing 10 μg of protein extracted from the iBAT was used as a positive control for UCP-1. All samples from Epid and Retro fat pads contained 50 μg of protein.

or also took place in other white fat depots, we measured UCP-1 content in the Epid and Retro (Fig. 6) fat pads. UCP-1 was not detected in these fat pads extracted from Sed LF, Ex LF, Sed HF, and Ex HF rats (Fig. 6). These findings indicated that the SC Ing fat was the only WAT depot that underwent browning under chronic exercise conditions.

PGC-1α and FNDC5 Content and Palmitate Oxidation in Soleus Muscles—PGC-1α content in soleus muscles from Ex LF, Sed HF, and Ex HF rats increased by 2.5-, 3.45-, and 3.85-fold, respectively, when compared with Sed LF rats (Fig. 7, *A* and *B*). No alterations in FNDC5 content were observed in Sol muscles from any of the HF and/or Ex conditions (Fig. 7, *A* and *B*). When compared with Sed LF, palmitate oxidation in Sol muscles increased by 2.4-fold in Ex LF, 2.1-fold in Sed HF, and 2.45-fold in Ex HF rats (Fig. 7*D*). Similar findings for PGC-1α, FNDC5 content, and for palmitate oxidation were also obtained with EDL muscles (data not shown). These findings indicate that chronic endurance exercise caused a very robust training effect in skeletal muscles; however, it did not alter FNDC5 content in this tissue.

Circulating Irisin and FNDC5 Content in Sc Ing Fat—After 8 weeks of the diet and exercise interventions, circulating levels of irisin under resting conditions were similar among all groups (Fig. 7*E*). When measured immediately after exercise at week 6, circulating irisin did not differ among the four groups of animals either (Fig. 7*F*). Irisin levels in the serum of HF-fed animals immediately after exercise were slightly lower than those rats fed a LF diet; however, this was not statistically significant. FNDC5 content was significantly increased (3.4-fold) in the SC Ing fat depot of Ex LF rats, and the content in Sed HF was markedly reduced (65%) (Fig. 7, *G* and *H*). Exercise attenuated the effect of HF diet and raised FNDC5 content in the SC Ing fat of Ex HF rats to values similar to those of Sed LF controls (Fig. 7, *G* and *H*).

Ambulatory Activity and Energy Expenditure—Ambulatory activity during the light cycle did not differ significantly among the groups; however, during the dark cycle this variable was 23, 29, and 35% lower in Sed HF rats than Sed LF, Ex LF, and Ex HF rats, respectively (Fig. 8, *A* and *B*). Analysis of energy expenditure expressed in kilocalories/kg of body weight revealed that this variable did not differ among the four groups during the light cycle, but it was significantly increased by 14.2% in Ex LF rats and by 16.8% during the dark cycle in Ex HF rats when compared with Sed LF controls (Fig. 8, *C* and *D*). Also, during the dark cycle, energy expenditure was 13.3% higher in Ex HF than Sed HF rats (Fig. 8, *C* and *D*).

DISCUSSION

Here, we provide novel evidence that thermogenesis is antagonistically regulated under conditions of chronic endurance exercise and energy surplus (HF diet) in classical brown fat depots and SC Ing WAT. This is supported by our observations that in Sed HF rats iBAT and aBAT tissue mass, PGC-1α and UCP-1 contents, and palmitate oxidation significantly increased, whereas in Ex LF rats these variables were markedly reduced. Conversely, in the SC Ing fat depot of Ex LF rats PGC-1α, UCP-1, and ATGL contents, AMPK phosphorylation as well as palmitate oxidation were robustly increased, whereas HF feeding attenuated these effects. These antagonistic effects of exercise and HF diet on thermogenesis in brown and WAT depots were also compatible with our findings that a large number of unilocular adipocytes typically found in WAT accumulated in iBAT and aBAT from Ex LF and Ex HF rats, although the SC Ing fat depot of Ex LF and Ex HF rats was enriched with brown-like UCP-1-positive multilocular adipocytes. Furthermore, specific areas within the SC Ing fat depot were more responsive to the browning effect of chronic endurance training than others. In fact, the exercise-induced increases in the number of multilocular adipocytes, UCP-1 content, and rate of palmitate oxidation were found in the middle region of the SC Ing fat but not at the proximal and distal extremities of this fat depot. Additionally, in Sed HF rats, the mean adipocyte area in the extremities of the SC Ing fat depot increased, whereas the middle region of this tissue remained unchanged. This indicates that the middle region of the SC Ing fat depot contains adipocytes that are resistant to hypertrophy under conditions of energy surplus, which is compatible with the site-specific differences in thermogenic capacity that we have found within the SC Ing fat depot in rats. Studies in mice have indeed reported major depot- and strain-specific differences in UCP-1 expression, indicating that the SC WAT is more prone to acquiring a brown-like phenotype through transdifferentiation than other visceral fat depots upon cold exposure (21). Here, we show that the exercise-induced browning of WAT is also depot-specific in rats, because increased UCP-1 content and the presence of multilocular adipocytes were found in the SC Ing fat pad but not in the Epid and Retro fat depots of these animals.

It has been reported that moderate to high intensity endurance training increases sympathetic nervous system activity

Downloaded from http://www.jbc.org/ at York University - OCUL on December 8, 2014

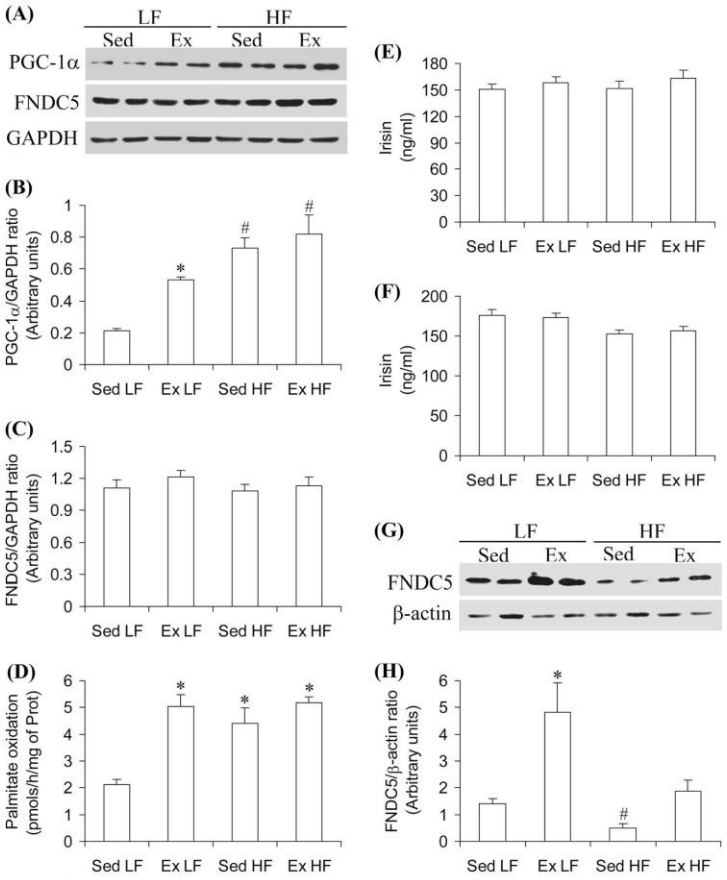

FIGURE 7. **Chronic endurance training increases PGC-1α and FNDC5 content in SC Ing fat, but neither affects soleus muscle FNDC5 content nor circulating irisin levels.** Soleus muscles were extracted from Sed and 8-week Ex rats fed either a LF or a HF diet and assayed for PGC-1α (*A* and *B*) and FNDC5 content (*A* and *C*), as well as palmitate oxidation (*D*). Irisin was measured in the plasma under resting conditions 24 h after the last bout of exercise (*E*) and immediately after exercise at week 6 (*F*). The middle region of the SC Ing fat depot was used for the determination of FNDC5 content (*G* and *H*). β-Actin and GAPDH were used as loading control. *, $p < 0.05$ *versus* Sed LF; #, $p < 0.05$ *versus* all other conditions. One-way ANOVA ($n = 8$).

and circulating catecholamines when compared before and after training under conditions of same relative intensity (22, 23). Importantly, catecholamines are well known for inducing BAT thermogenesis (24, 25). Throughout our study, training intensity was kept constant (70–85% VO_2 max), so circulating catecholamines are expected to have been consistently increased during exercise bouts in our endurance-trained rats. Despite that, thermogenic capacities in classical BAT and SC Ing fat were regulated in an opposite fashion. It appears that chronic exposure to increased heat production through exercise overrides catecholamine-induced nonshivering thermogenesis in core regions (iBAT and aBAT) but not in specific fat depots located peripherally. The mechanism underlying these effects is unknown. However, this could be conferred by adaptive responses that affect local catecholamine release and distribution of α- and β-adrenergic receptors, as well as by central nervous system-mediated regulatory responses that drive sympathetic activity in a tissue-specific manner. Also, it has been recently demonstrated that brown fat activation can occur via a nonadrenergic activation mechanism (26). Therefore, in our study, other exercise-induced factors could have promoted browning of the SC Ing fat independently of catecholamines.

In this context, previous studies have suggested that exercise-induced browning of the SC Ing fat depot is mediated by the release of a PGC-1α-dependent myokine named irisin, which is proposed to be derived from the cleavage of the ectodomain of the FNDC5 receptor under exercising conditions (9). Therefore, we tested whether this could also be the case in this study. We found that the exercise training protocol and HF diet both caused robust increases in PGC-1α content and palmitate oxidation in Sol and EDL muscles. However, we did not detect any significant alterations in FNDC5 content in these muscles. Furthermore, circulating levels of irisin under resting conditions were not affected by either chronic endurance training or HF feeding. It could be that irisin increased transiently after exercise, and values obtained under resting conditions 24 h

Downloaded from http://www.jbc.org/ at York University - OCUL on December 8, 2014

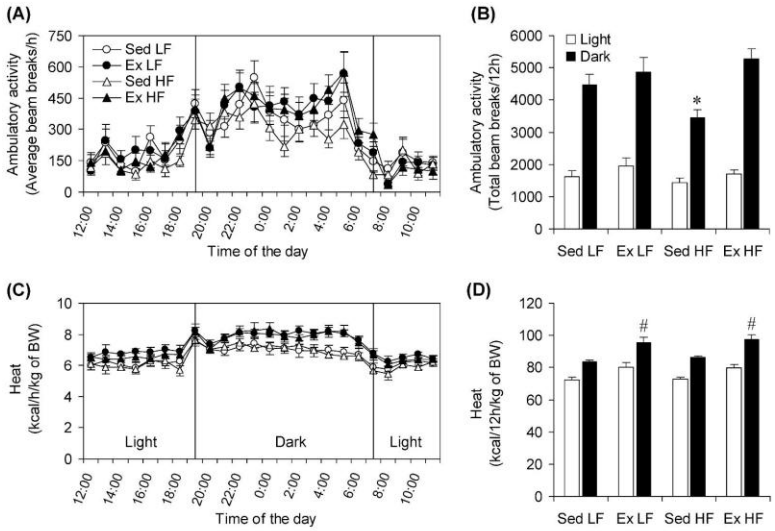

FIGURE 8. **Effects of chronic Ex and HF diet on spontaneous physical activity and whole-body energy expenditure.** Ambulatory activity (*A* and *B*) and energy expenditure (*C* and *D*) were measured after the last bout of exercise at the end of the 8-week endurance training period. The rats were allowed to rest for 24 h prior to being placed in the CLAMS. *, $p < 0.05$ *versus* Sed LF; #, $p < 0.05$ *versus* all other conditions. Two-way ANOVA ($n = 18$).

after the last bout of exercise could have missed such an effect. Therefore, we also measured circulating irisin immediately after exercise at week 6 of the study, but again, no significant differences were found among the four groups of animals. Our findings are consistent with other studies reporting a lack of muscle FNDC5 and irisin regulation under exercising conditions in humans (27–29). The discrepancy of our findings with those that do report an increase in circulating irisin with exercise in either humans or rodents (9, 30–34) could derive from methodological differences (rodent species, mode, intensity, and duration of exercise, as well as timing of blood sampling) that exist among the studies.

Because FNDC5 and irisin have been reported to be also expressed and released by adipocytes (35, 36), we measured FNDC5 content in the SC Ing fat depot. Similarly to what was found for PGC-1α and UCP-1, chronic endurance exercise caused a significant increase in FNDC5 content, whereas HF diet markedly reduced it in the SC Ing fat depot. These findings suggest that locally produced FNDC5 rather than circulating irisin could have mediated the browning effect of chronic endurance exercise on SC Ing fat. Recent crystal structure analysis and biochemical characterization studies have predicted that a tight dimerization of the FNDC5 ectodomain may form intra- and/or intercellular dimers at the cell surface, which could lead to autocrine or paracrine signaling independently of cleavage and release of irisin in the circulation (37). In this context, the increase and reduction in FNDC5 content found in the SC Ing fat depot of Ex LF and Sed HF rats, respectively, could provide a mechanism by which exercise induced a marked browning effect in LF-fed rats, whereas HF feeding attenuated this effect.

Exercise is thermogenic in itself, and a large amount of heat is actually produced as a consequence of muscle contractions. Thus, a reduction in BAT activity is expected to occur under conditions of repeated chronic endurance exercise. In fact, previous studies have reported that the tissue mass and *Ucp-1* mRNA levels of iBAT were markedly reduced in rodents exposed to chronic endurance training (38). Other studies have also demonstrated that chronic endurance exercise reduces the thermogenic activity of iBAT (11, 12, 39, 40). Besides cold-induced thermogenesis, previous studies in rats have consistently demonstrated that structural and functional alterations in iBAT are also directly related to DIT and the regulation of energy balance (13–15, 31, 41–44). In mice, UCP-1 ablation abolished DIT, and the animals developed obesity when living at thermoneutrality (44). In humans, it has also been reported that glucose uptake in BAT increases after a meal, which indicates a role for BAT in reducing metabolic efficiency (45). In this context, our findings that chronic endurance exercise reduces tissue mass and thermogenic capacity in iBAT and aBAT are compatible with a compensatory adaptive response that down-regulates thermogenesis in an animal that is regularly exposed to exercise-induced increased heat production. Also, our findings of increased iBAT and aBAT mass and thermogenic capacity in Sed HF rats are consistent with increased DIT in a sedentary animal that is chronically exposed to energy surplus and increased adiposity.

The question that arises is why does chronic endurance exercise induce browning of the SC Ing fat depot if heat production is already increased by muscle contractions? It has been proposed that exercise-induced browning of the SC WAT could have evolved from shivering-related muscle contractions, serving to augment brown fat thermogenesis under conditions of cold exposure (33). The rats in our study were not exposed to cold stress, and the typically thermogenic iBAT and aBAT had their masses, UCP-1 content, and rate of fatty acid oxidation

Downloaded from http://www.jbc.org/ at York University - OCUL on December 8, 2014

markedly reduced in animals exposed to chronic endurance training. Therefore, it seems unlikely that exercise-induced browning of the SC Ing fat depot took place to enhance BAT thermogenesis in these animals. Instead, it appears to be more compatible with an adaptive response to chronic endurance exercise that provides an alternative mechanism for the regulation of whole-body energy balance when DIT and cold-induced thermogenesis through classical BAT is impaired. This is consistent with our *in vivo* findings that whole-body dark-cycle energy expenditure was increased by 14.2% in Ex LF rats and by 16.8% in Ex HF rats when compared with Sed LF rats. This occurred despite the reductions in tissue mass, UCP-1 content, and palmitate oxidation in iBAT and aBAT in Ex LF and Ex HF rats. We cannot attribute these effects solely to browning of the SC Ing fat pad in these animals; however, it seems to have at least partially contributed to increase whole-body energy expenditure in chronically endurance-trained rats. This is supported by the fact that thermogenic capacity in iBAT and aBAT was markedly attenuated in Ex LF and Ex HF rats, yet whole-body energy expenditure was increased in these animals when compared with Sed LF rats. This suggests that an alternative mechanism, likely browning of SC WAT, exerted a compensatory effect and raised whole-body energy expenditure in these animals. Importantly, dark cycle spontaneous physical activity was 23–35% lower in Sed HF rats than in the other groups of animals, and endurance training completely reversed this effect. In fact, spontaneous physical activity of Ex HF rats in the dark cycle was the highest among the groups, although not statistically significant from those of Sed LF and Ex LF rats. Because energy expenditure did not differ between Sed LF and Sed HF rats despite lower ambulatory activity in the latter than the former, it appears that alterations in dark cycle spontaneous physical activity was not the major force driving the increase in energy expenditure found in chronically endurance-trained rats. This again provides support to a compensatory increase in thermogenesis through browning of SC Ing WAT.

In conclusion, this study provides novel evidence that thermogenic capacity is antagonistically regulated in classical brown and white adipose tissues by chronic endurance training and HF diet. These adaptive responses indicate that DIT, which normally depends on increased classical BAT activity in core areas, is shifted by chronic endurance exercise toward more superficial regions. This is characterized by a reduction in thermogenic capacity of classical BAT accompanied by browning of SC WAT. This may serve to allow the organism to make adjustments in whole-body energy expenditure by activating thermogenesis in peripheral tissues while simultaneously coping with the stress of exercise-induced heat production in core regions of the body. Our *in vivo* findings also provide evidence that the induction of browning in SC WAT may have an important impact on whole-body energy expenditure and be potentially used as a therapeutic approach to treat obesity and its related metabolic disorders.

Acknowledgment—We thank Diane Sepa-Kishi for helping with the organization of references.

REFERENCES

1. Cinti, S. (2009) Transdifferentiation properties of adipocytes in the adipose organ. *Am. J. Physiol. Endocrinol. Metab.* **297,** E977–E986
2. Cannon, B., and Nedergaard, J. (2004) Brown adipose tissue: function and physiological significance. *Physiol. Rev.* **84,** 277–359
3. van Marken Lichtenbelt, W. D., Vanhommerig, J. W., Smulders, N. M., Drossaerts, J. M., Kemerink, G. J., Bouvy, N. D., Schrauwen, P., and Teule, G. J. (2009) Cold-activated brown adipose tissue in healthy men. *N. Engl. J. Med.* **360,** 1500–1508
4. Virtanen, K. A., Lidell, M. E., Orava, J., Heglind, M., Westergren, R., Niemi, T., Taittonen, M., Laine, J., Savisto, N.-J., Enerbäck, S., and Nuutila, P. (2009) Functional brown adipose tissue in healthy adults. *N. Engl. J. Med.* **360,** 1518–1525
5. Ouellet, V., Labbé, S. M., Blondin, D. P., Phoenix, S., Guérin, B., Haman, F., Turcotte, E. E., Richard, D., and Carpentier, A. C. (2012) Brown adipose tissue oxidative metabolism contributes to energy expenditure during acute cold exposure in humans. *J. Clin. Invest.* **122,** 545–552
6. Cypess, A. M., White, A. P., Vernochet, C., Schulz, T. J., Xue, R., Sass, C. A., Huang, T. L., Roberts-Toler, C., Weiner, L. S., Sze, C., Chacko, A. T., Deschamps, L. N., Herder, L. M., Truchan, N., Glasgow, A. L., Holman, A. R., Gavrila, A., Hasselgren, P.-O., Mori, M. A., Molla, M., and Tseng, Y.-H. (2013) Anatomical localization, gene expression profiling and functional characterization of adult human neck brown fat. *Nat. Med.* **19,** 635–639
7. Lidell, M. E., Betz, M. J., Dahlqvist Leinhard, O., Heglind, M., Elander, L., Slawik, M., Mussack, T., Nilsson, D., Romu, T., Nuutila, P., Virtanen, K. A., Beuschlein, F., Persson, A., Borga, M., and Enerbäck, S. (2013) Evidence for two types of brown adipose tissue in humans. *Nat. Med.* **19,** 631–634
8. Wu, J., Cohen, P., and Spiegelman, B. M. (2013) Adaptive thermogenesis in adipocytes: is beige the new brown? *Genes Dev.* **27,** 234–250
9. Boström, P., Wu, J., Jedrychowski, M. P., Korde, A., Ye, L., Lo, J. C., Rasbach, K. A., Boström, E. A., Choi, J. H., Long, J. Z., Kajimura, S., Zingaretti, M. C., Vind, B. F., Tu, H., Cinti, S., Højlund, K., Gygi, S. P., and Spiegelman, B. M. (2012) A PGC1-α-dependent myokine that drives brown-fat-like development of white fat and thermogenesis. *Nature* **481,** 463–468
10. De Matteis, R., Lucertini, F., Guescini, M., Polidori, E., Zeppa, S., Stocchi, V., Cinti, S., and Cuppini, R. (2013) Exercise as a new physiological stimulus for brown adipose tissue activity. *Nutr. Metab. Cardiovasc. Dis.* **23,** 582–590
11. Gohil, K., Henderson, S., Terblanche, S. E., Brooks, G. A., and Packer, L. (1984) Effects of training and exhaustive exercise on the mitochondrial oxidative capacity of brown adipose tissue. *Biosci. Rep.* **4,** 987–993
12. Terblanche, S. E., Gohil, K., Packer, L., Henderson, S., and Brooks, G. A. (2001) The effects of endurance training and exhaustive exercise on mitochondrial enzymes in tissues of the rat (*Rattus norvegicus*). *Comp. Biochem. Physiol. A. Mol. Integr. Physiol.* **128,** 889–896
13. Rothwell, N. J., and Stock, M. J. (1979) A role for brown adipose tissue in diet-induced thermogenesis. *Nature* **281,** 31–35
14. Young, J. B., Saville, E., Rothwell, N. J., Stock, M. J., and Landsberg, L. (1982) Effect of diet and cold exposure on norepinephrine turnover in brown adipose tissue of the rat. *J. Clin. Invest.* **69,** 1061–1071
15. Schwartz, J. H., Young, J. B., and Landsberg, L. (1983) Effect of dietary fat on sympathetic nervous system activity in the rat. *J. Clin. Invest.* **72,** 361–370
16. Araujo, R. L., Andrade, B. M., Padrón, A. S., Gaidhu, M. P., Perry, R. L., Carvalho, D. P., and Ceddia, R. B. (2010) High-fat diet increases thyrotropin and oxygen consumption without altering circulating 3,5,3′-triiodothyronine (T3) and thyroxine in rats: the role of iodothyronine deiodinases, reverse T3 production, and whole-body fat oxidation. *Endocrinology* **151,** 3460–3469
17. Wisløff, U., Helgerud, J., Kemi, O. J., and Ellingsen, O. (2001) Intensity-controlled treadmill running in rats: VO(2 max) and cardiac hypertrophy. *Am. J. Physiol. Heart Circ. Physiol.* **280,** H1301–H1310
18. Pescatello, L., Arena, R., Riebe, D., and Thompson, P. D. (eds) (2014) *American College of Sports Medicine's Guideline for Exercise Testing and Prescription*, 9th Ed., pp. 162–193, Wolters Kluwer Health; Lippincott WIlliams & Wilkins

Downloaded from http://www.jbc.org/ at York University - OCUL on December 8, 2014

19. Gaidhu, M. P., Frontini, A., Hung, S., Pistor, K., Cinti, S., and Ceddia, R. B. (2011) Chronic AMP-kinase activation with AICAR reduces adiposity by remodeling adipocyte metabolism and increasing leptin sensitivity. *J. Lipid Res.* **52,** 1702–1711
20. Vitzel, K. F., Bikopoulos, G., Hung, S., Pistor, K. E., Patterson, J. D., Curi, R., and Ceddia, R. B. (2013) Chronic treatment with the AMP-kinase activator AICAR increases glycogen storage and fatty acid oxidation in skeletal muscles but does not reduce hyperglucagonemia and hyperglycemia in insulin deficient rats. *PLoS One* **8,** e62190
21. Barbatelli, G., Murano, I., Madsen, L., Hao, Q., Jimenez, M., Kristiansen, K., Giacobino, J. P., De Matteis, R., and Cinti, S. (2010) The emergence of cold-induced brown adipocytes in mouse white fat depots is determined predominantly by white to brown adipocyte transdifferentiation. *Am. J. Physiol. Endocrinol. Metab.* **298,** E1244–E1253
22. Winder, W. W., Hagberg, J. M., Hickson, R. C., Ehsani, A. A., and McLane, J. A. (1978) Time course of sympathoadrenal adaptation to endurance exercise training in man. *J. Appl. Physiol.* **45,** 370–374
23. Péronnet, F., Cléroux, J., Perrault, H., Cousineau, D., de Champlain, J., and Nadeau, R. (1981) Plasma norepinephrine response to exercise before and after training in humans. *J. Appl. Physiol.* **51,** 812–815
24. Bachman, E. S., Dhillon, H., Zhang, C.-Y., Cinti, S., Bianco, A. C., Kobilka, B. K., and Lowell, B. B. (2002) βAR signaling required for diet-induced thermogenesis and obesity resistance. *Science* **297,** 843–845
25. Lowell, B. B., and Bachman, E. S. (2003) β-Adrenergic receptors, diet-induced thermogenesis, and obesity. *J. Biol. Chem.* **278,** 29385–29388
26. Zhang, Y., Guo, H., Deis, J. A., Mashek, M. G., Zhao, M., Ariyakumar, D., Armien, A. G., Bernlohr, D. A., Mashek, D. G., and Chen, X. (2014) Lipocalin 2 regulates brown fat activation via a nonadrenergic activation mechanism. *J. Biol. Chem.* **289,** 22063–22077
27. Pekkala, S., Wiklund, P. K., Hulmi, J. J., Ahtiainen, J. P., Horttanainen, M., Pöllänen, E., Mäkelä, K. A., Kainulainen, H., Häkkinen, K., Nyman, K., Alén, M., Herzig, K.-H., and Cheng, S. (2013) Are skeletal muscle FNDC5 gene expression and irisin release regulated by exercise and related to health? *J. Physiol.* **591,** 5393–5400
28. Raschke, S., Elsen, M., Gassenhuber, H., Sommerfeld, M., Schwahn, U., Brockmann, B., Jung, R., Wisløff, U., Tjønna, A. E., Raastad, T., Hallén, J., Norheim, F., Drevon, C. A., Romacho, T., Eckardt, K., and Eckel, J. (2013) Evidence against a beneficial effect of irisin in humans. *PLoS One* **8,** e73680
29. Norheim, F., Langleite, T. M., Hjorth, M., Holen, T., Kielland, A., Stadheim, H. K., Gulseth, H. L., Birkeland, K. I., Jensen, J., and Drevon, C. A. (2014) The effects of acute and chronic exercise on PGC-1α, irisin and browning of subcutaneous adipose tissue in humans. *FEBS J.* **281,** 739–749
30. Huh, J. Y., Panagiotou, G., Mougios, V., Brinkoetter, M., Vamvini, M. T., Schneider, B. E., and Mantzoros, C. S. (2012) FNDC5 and irisin in humans: I. Predictors of circulating concentrations in serum and plasma and II. mRNA expression and circulating concentrations in response to weight loss and exercise. *Metabolism* **61,** 1725–1738
31. Aydin, S., Kuloglu, T., Aydin, S., Eren, M. N., Celik, A., Yilmaz, M., Kalayci, M., Sahin, İ., Gungor, O., Gurel, A., Ogeturk, M., and Dabak, O. (2014) Cardiac, skeletal muscle and serum irisin responses to with or without water exercise in young and old male rats: cardiac muscle produces more irisin than skeletal muscle. *Peptides* **52,** 68–73
32. Kraemer, R. R., Shockett, P., Webb, N. D., Shah, U., and Castracane, V. D. (2014) A transient elevated irisin blood concentration in response to prolonged, moderate aerobic exercise in young men and women. *Horm. Metab. Res.* **46,** 150–154
33. Lee, P., Linderman, J. D., Smith, S., Brychta, R. J., Wang, J., Idelson, C., Perron, R. M., Werner, C. D., Phan, G. Q., Kammula, U. S., Kebebew, E., Pacak, K., Chen, K. Y., and Celi, F. S. (2014) Irisin and FGF21 are cold-induced endocrine activators of brown fat function in humans. *Cell Metab.* **19,** 302–309
34. Brenmoehl, J., Albrecht, E., Komolka, K., Schering, L., Langhammer, M., Hoeflich, A., and Maak, S. (2014) Irisin is elevated in skeletal muscle and serum of mice immediately after acute exercise. *Int. J. Biol. Sci.* **10,** 338–349
35. Roca-Rivada, A., Castelao, C., Senin, L. L., Landrove, M. O., Baltar, J., Belén Crujeiras, A., Seoane, L. M., Casanueva, F. F., and Pardo, M. (2013) FNDC5/irisin is not only a myokine but also an adipokine. *PLoS One* **8,** e60563
36. Moreno-Navarrete, J. M., Ortega, F., Serrano, M., Guerra, E., Pardo, G., Tinahones, F., Ricart, W., and Fernández-Real, J. M. (2013) Irisin is expressed and produced by human muscle and adipose tissue in association with obesity and insulin resistance. *J. Clin. Endocrinol. Metab.* **98,** E769–E778
37. Schumacher, M. A., Chinnam, N., Ohashi, T., Shah, R. S., and Erickson, H. P. (2013) The structure of irisin reveals a novel intersubunit β-sheet fibronectin type III (FNIII) dimer: implications for receptor activation. *J. Biol. Chem.* **288,** 33738–33744
38. Yamashita, H., Yamamoto, M., Sato, Y., Izawa, T., Komabayashi, T., Saito, D., and Ohno, H. (1993) Effect of running training on uncoupling protein mRNA expression in rat brown adipose tissue. *Int. J. Biometeorol.* **37,** 61–64
39. Larue-Achagiotis, C., Rieth, N., Goubern, M., Laury, M. C., and Louis-Sylvestre, J. (1995) Exercise-training reduces BAT thermogenesis in rats. *Physiol. Behav.* **57,** 1013–1017
40. Arnold, J., and Richard, D. (1987) Exercise during intermittent cold exposure prevents acclimation to cold rats. *J. Physiol.* **390,** 45–54
41. Young, J. B., and Landsberg, L. (1983) Diminished sympathetic nervous system activity in genetically obese (ob/ob) mouse. *Am. J. Physiol.* **245,** E148–E154
42. Landsberg, L., and Young, J. B. (1981) Diet-induced changes in sympathoadrenal activity: implications for thermogenesis. *Life Sci.* **28,** 1801–1819
43. Rappaport, E. B., Young, J. B., and Landsberg, L. (1982) Initiation, duration and dissipation of diet-induced changes in sympathetic nervous system activity in the rat. *Metabolism* **31,** 143–146
44. Feldmann, H. M., Golozoubova, V., Cannon, B., and Nedergaard, J. (2009) UCP1 ablation induces obesity and abolishes diet-induced thermogenesis in mice exempt from thermal stress by living at thermoneutrality. *Cell Metab.* **9,** 203–209
45. Vosselman, M. J., Brans, B., van der Lans, A. A., Wierts, R., van Baak, M. A., Mottaghy, F. M., Schrauwen, P., and van Marken Lichtenbelt, W. D. (2013) Brown adipose tissue activity after a high-calorie meal in humans. *Am. J. Clin. Nutr.* **98,** 57–64

Downloaded from http://www.jbc.org/ at York University - OCUL on December 8, 2014